

Towards the use of (pseudo) nucleobase substituted amphiphiles as DNA nucleotide mimics and antimicrobial agents†

Kendrick K. L. Ng,^a Milan Dimitrovski,^a Jessica E. Boles,^{a/b} Rebecca J. Ellaby,^a Lisa J. White^a and Jennifer R. Hiscock*^a

**School of Physical Sciences, University of Kent, Canterbury, UK, CT2 7NH; Email: J.R.Hiscock@kent.ac.uk; Tel: +44(0)1227 816467*

Electronic Supplementary information

Contents

General remarks.....	2
Tensiometry studies.....	2
DLS studies.....	3
Zeta potential studies.....	3
High-resolution mass spectrometry studies.....	3
Self-association and association constant calculation.....	4
Single-crystal X-ray studies.....	4
Low level computational modelling.....	4
Biological experiments ⁷	4
Chemical structures.....	6
Chemical synthesis.....	6
Characterisation NMR.....	9
Single crystal X-ray structures.....	21
Mass spectrum data.....	25
¹ H NMR quantitative studies.....	30
¹ H NMR DOSY studies.....	35
¹ H NMR self-association studies.....	39
¹ H NMR titration study data.....	47
DLS data.....	53
Zeta potential data.....	62
Critical micelle concentration.....	64
Low level in-silico modelling.....	67
References.....	70

General remarks

A positive pressure of nitrogen and oven dried glassware were used for all reactions. All solvents and starting materials were purchased from known chemical suppliers or available stores and used without any further purification unless specifically stipulated. The NMR spectra were obtained using a Bruker AV2 400 MHz or AVNEO 400 MHz spectrometer. The data was processed using ACD Labs, MestReNova or Topspin software. NMR Chemical shift values are reported in parts per million (ppm) and calibrated to the centre of the residual solvent peak set (s = singlet, br = broad, d = doublet, t = triplet, q = quartet, m = multiplet). Tensiometry measurements were undertaken using the Biolin Scientific Theta Attension optical tensiometer. The data was processed using Biolin OneAttension software. A Hamilton (309) syringe was used for the measurements. The melting point for each compound was measured using Stuart SMP10 melting point apparatus. High resolution mass spectrometry was performed using a Bruker microTOF-Q mass spectrometer and spectra recorded and processed using Bruker's Compass Data Analysis software. Infrared spectra were obtained using a Shimadzu IR-Affinity-1 model Infrared spectrometer. The data are analysed in wavenumbers (cm^{-1}) using IRsolution software. Dynamic Light Scattering (DLS) and Zeta Potential studies were obtained using an Anton Paar LitesizerTM 500 and processed using KalliopeTM Professional or using a Malvern Zetasizer Nano ZS. Cellular growth curve measurements obtained using Thermo Scientific Multiscan Go 1510-0318C plate reader and recorded using the SkanIt Software 4.0 and a Clariostar plater reader using MARS data analysis software.

Tensiometry studies

All the samples were prepared in a EtOH:H₂O (1:19) solution. All samples underwent an annealing process in which the various solutions were heated to approximately 40 °C before being allowed to cool to room temperature, allowing each sample to reach a thermodynamic minimum. All samples were prepared through serial dilution of the most concentrated sample. Three surface tension

measurements were obtained for each sample at a given concentration, using the pendant drop method. These average values were then used to calculate the Critical Micelle Concentration (CMC).

DLS studies

Studies conducted with compounds were prepared in series with an aliquot of the most concentrated solution undergoing serial dilution. Sample sizes were kept to 1 mL. All solvents used for DLS studies were filtered to remove particulates from the solvents. Samples were heated to approximately 40 °C before being allowed to equilibrate for 1 hour at room temperature. A series of 10 'runs' were performed with each sample at 25 °C to give enough data to derive an appropriate average. In some instances, the raw correlation data indicated that a greater amount of time may be needed for the samples to reach a stable state. For this reason, only the last 9 'runs' were included in the average size distribution calculations.

Zeta potential studies

All solvents used for Zeta potential studies were filtered to remove particulates from the solvents. Samples were heated to approximately 40 °C, before being allowed to equilibrate at room temperature for 1 hour. A series of 10 'runs' were performed with each sample at 25 °C to give enough data to derive an appropriate average. In some instances, the raw correlation data indicated that a greater amount of time may be needed for the samples to reach a stable state. For this reason, only the last 9 'runs' were included in the average size distribution calculations.

High-resolution mass spectrometry studies

Chemical samples were dissolved in HPLC-grade methanol at a concentration of 1 mg/mL before being further diluted 1 in 100 in methanol. 10 µL of the sample was injected into a flowing stream of 10 mM ammonium acetate in 95% methanol in water (flow rate: 0.02 mL/min) and the flow directed into the electrospray source of the mass spectrometer. Mass spectra were acquired in the negative ion mode and data processed in Bruker's Compass Data Analysis software.

Self-association and association constant calculation

All association and self-association constants were calculated using the freely available bindfit programme (<http://app.supramolecular.org/bindfit/>). All the data relating to the calculation of the association constants can be accessed online, through the links given for each complexation event.¹

Single-crystal X-ray studies

A suitable crystal of each amphiphile was selected and mounted on a Rigaku Oxford Diffraction Supernova diffractometer. The suitable crystal was kept at 100(1) K during data collection, using an Oxford Cryosystems 800-series Cryostream. Data were collected using Cu K α radiation at 293 K. Structures were solved with the ShelXT² or ShelXS structure solution programs via Direct Methods and refined with ShelXL³ by Least Squares minimisation. Olex2⁴ was used as an interface to all ShelX programs (CCDC 1964617-1964619). All non-hydrogen atoms were refined using anisotropic displacement parameters, and hydrogen atoms were placed at calculated positions.

Low level computational modelling

Computational calculations to identify primary hydrogen bond donating and accepting sites were conducted in line with studies reported by Hunter using Spartan 16''.⁵ Calculations were performed using semi-empirical PM6 methods, after energy minimisation calculations, to identify E_{max} , E_{min} and LogP values. PM6 was used over AM1 in line with research conducted by Stewart.⁶

Biological experiments ⁷

Preparation of Luria Broth media (LB): Yeast extract (5 g), tryptone (10 g) and sodium chloride (10 g) were dissolved in dH₂O (1 L) then divided into bottles and autoclaved.

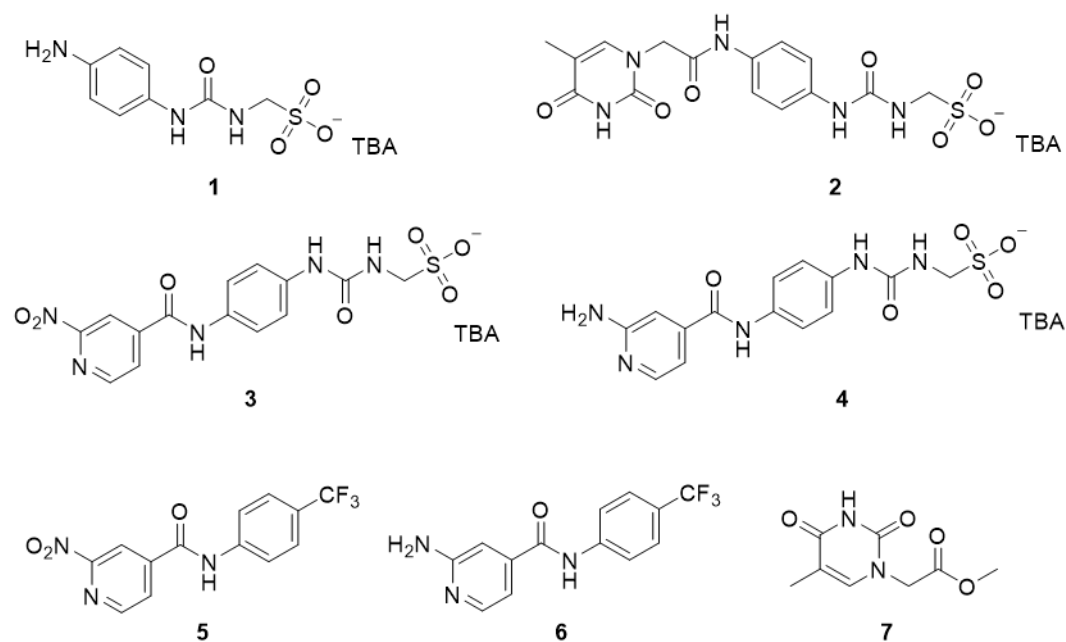
Preparation of McFarland standard: Barium chloride (1%, 50 μ L) was added to sulfuric acid (1 %, 9.95 mL) and mixed together. The optical density was recorded at 600 nm.

Preparation of antimicrobial compounds for screening: Compounds were dissolved in 5 % ethanol to make up 20 mM solutions on the day of experiment.

Preparation of Inoculum: An initial culture was made up by inoculating LB media (5 mL) with at least four single colonies of the desired bacteria under sterile conditions and incubating at 37 °C overnight. The following day, a subculture was made up using LB (5 mL) and the initial culture (50 µL), then incubated at 37°C until the culture had reached an optical density of 0.4 at 600 nm. Density was adjusted using sterile H₂O to equal 0.5 McFarland standard ($10^7 - 10^8$ cfu/mL), then a 1:10 dilution was carried out using sterile dH₂O (900 µL) and the McFarland adjusted suspension (100 µL). A final dilution (1:100) was carried using the 1:10 suspension (150 µL) and LB (14.85 mL) before use to achieve a final cell concentration of 10^5 cfu/mL.

Preparation of 96 well microplate for screening: 20 mM solutions of each compound to be tested were made up using 5 % ethanol. The 1:100 cell suspension (150 µL) was pipetted into the wells. Compound solutions (30 µL) were added into 6 wells on the plate so that 14 compounds could be screened on each plate. The final screening concentration for each compound was 3.3 mM in the well. These were incubated for 20 hours in a plate reader, with absorbance readings being taken at 600 nm every 15 minutes. Absorbance readings were plotted against time to produce growth curves.

Chemical structures



Chemical synthesis

Compound 2:⁸ *N*-Hydroxysuccinimide (NHS) (0.12 g, 1.03 mM) was added to a stirring solution of thymine-1-acetic acid (0.19 g, 1.03 mM) and compound **1**⁹ (0.50 g, 1.03 mM) in DMF (2 mL) at 0 °C and stirred for 30 mins. *N,N'*-Dicyclohexylcarbodiimide (DCC) (0.25 g, 1.23 mM) in DMF (2 mL) was added to the reaction mixture and the solution was then allowed to warm to room temperature overnight. Water (10 mL) was added and a precipitate was removed by filtration. The filtrate was then taken to dryness and DCM (20 mL) was added. The resultant precipitate was filtered, and dissolved in ethanol (20 mL) this process was repeated. The pure product was obtained by precipitation with acetone yielding a white solid. Yield 54 % (0.36 g, 0.55 mM); ¹H NMR (400 MHz, DMSO-*d*₆): δ (ppm): 0.93 (t, *J* = 14.60 Hz, 12H), 1.30 (m, 8H), 1.54 (m, 8H), 1.76 (s, 3H), 3.16 (m, 8H), 3.84 (d, *J* = 5.88 Hz, 2H), 4.46 (s, 2H), 6.40 (br s, NH), 7.30 (d, *J* = 8.88 Hz, 2H), 7.41 (d, *J* = 9.08 Hz, 2H), 7.51 (s, 1H), 8.70 (s, NH), 10.12 (s, NH), 11.34 (s, NH).

Compound 3: Compound **1**⁹ (0.20 g, 0.41 mM) was added to a stirring solution of 1-ethyl-3-(3-dimethylaminopropyl)carbodiimide (EDC) (0.09 g, 0.45 mM) and 2-nitroisonicotinic acid (0.07 g, 0.41

mM) in DMF (2 mL) in an ice-bath, and the mixture allowed to acclimatise to room temperature overnight. Water (10 mL) was added and separated with ethyl acetate (2 x 20 mL). The organic layer was dried, and the pure product obtained by precipitation with water as a bright yellow solid. Yield: 51 % (0.13 g, 0.21 mM); Melting point: > 200 °C; ^1H NMR (400 MHz, DMSO- d_6): δ (ppm): 0.93 (t, J = 14.68 Hz, 12H), 1.30 (m, 8H), 1.56 (m, 8H), 3.16 (m, 8H), 3.87 (d, J = 5.76 Hz, 2H), 6.47 (m, NH), 7.40 (d, J = 8.80 Hz, 2H), 7.63 (d, J = 8.92 Hz, 2H), 8.36 (d, J = 4.88 Hz, 1H), 8.78 (s, 1H), 8.81 (br s, NH), 8.87 (d, J = 4.96 Hz, 1H), 10.67 (br s, NH); $^{13}\text{C}\{^1\text{H}\}$ NMR (100 MHz, DMSO- d_6): δ (ppm): 13.5 (CH₃), 19.2 (CH₂), 23.1 (CH₂), 56.1 (CH₂), 57.5 (CH₃), 116.2 (ArCH), 117.6 (ArCH), 121.2 (ArCH), 127.8 (ArCH), 131.6 (ArC), 137.4 (ArC), 146.4 (ArC), 149.7 (ArCH), 154.6 (ArC), 157.0 (CO), 161.2 (CO); IR (film): ν (cm⁻¹) = 3333 (NH stretch), 1693 (C=O stretch), 1520 & 1312 (NO₂ stretch); HRMS for the sulfonate-urea ion (C₁₄H₁₂N₅O₇S⁻) (ESI⁻): m/z : act: 394.0440 [M]⁻ cal: 394.3385 [M]⁻.

Compound 4: Compound 3 (3.50 g, 0.55 mM), hydrazine hydrate (1.00 mL, 28.75 mM) and Pd/C 10 % (0.10 g) were heated at reflux overnight in ethanol (20 mL). The Pd/C 10 % was removed by filtration and the remaining solution taken to dryness. Pure product was obtained by precipitation with acetone as a white solid. Yield: 84 % (2.80 g, 0.46 mM); Melting point: > 200 °C; ^1H NMR (400 MHz, DMSO- d_6): δ (ppm): 0.93 (t, J = 7.24 Hz, 12H), 1.30 (m, 8H), 1.56 (m, 8H), 3.16 (m, 8H), 3.85 (d, J = 5.60 Hz, 2H), 6.20 (s, NH₂), 6.42 (m, NH), 6.85 (s, 1H), 6.91 (d, J = 4.96 Hz, 1H), 7.33 (d, J = 8.68 Hz, 2H), 7.58 (d, J = 8.64 Hz, 2H), 8.02 (d, J = 5.16 Hz, 1H), 8.74 (br s, NH), 10.15 (s, NH); $^{13}\text{C}\{^1\text{H}\}$ NMR (100 MHz, DMSO- d_6): δ (ppm): 13.6 (CH₃), 19.2 (CH₂), 23.1 (CH₂), 56.1 (CH₂), 57.5 (CH₃), 106.2 (CH), 109.4 (ArCH), 117.6 (ArCH), 121.0 (ArCH), 132.3 (ArC), 136.8 (ArC), 143.5 (ArC), 148.4 (ArCH), 154.6 (ArC), 160.3 (CO), 164.4 (CO); IR (film): ν (cm⁻¹) = 3329 (NH stretch), 1676 (C=O stretch); HRMS for the sulfonate-urea ion (C₁₄H₁₄N₅O₅S⁻) (ESI⁻): m/z : act: 364.0702 [M]⁻ cal: 364.3565 [M]⁻.

Compound 5: 1,1'-Carbonyldiimidazole (CDI) (0.39 g, 2.38 mM) was added to a stirring solution of 2-nitroisonicotinic acid (0.37 g, 2.17 mM) in chloroform (15 mL) and heated at reflux. After four hours 4-(trifluoromethyl) aniline (0.45 mL, 2.17 mM) was added to the mixture, which was heated at reflux

overnight. Crude product was diluted in chloroform (20 mL) and water (3 x 20 mL). The organic layer was reduced in volume and pure product was obtained by precipitation with hexane as a yellow solid. Yield: 54 % (0.37 g, 1.18 mM); Melting point: 195 °C; ^1H NMR (400 MHz, $\text{DMSO-}d_6$): δ (ppm): 7.77 (d, $J = 8.60$ Hz, 2H), 8.01 (d, $J = 8.52$ Hz, 2H), 8.37 (dd, $J = 1.36, 4.94$ Hz, 1H), 8.80 (s, 1H), 8.90 (d, $J = 4.88$ Hz, 1H), 11.09 (s, NH); $^{13}\text{C}\{^1\text{H}\}$ NMR (100 MHz, $\text{DMSO-}d_6$): δ (ppm): 116.3 (ArCH), 120.5 (ArCH), 124.5 (CF_3 , $J = 31.69$ Hz), 126.1 (ArCH, $J = 269.99$ Hz), 128.0 (ArCH, $J = 3.79$ Hz), 141.9 (ArC), 145.8 (ArC), 149.9 (ArCH), 156.9 (ArC), 162.4 (CO); IR (film): ν (cm^{-1}) = 3333 (NH stretch), 1662 (C=O stretch), 1535 & 1327 (N-O stretch); HRMS ($\text{C}_{13}\text{H}_8\text{F}_3\text{N}_3\text{O}_3$) (ESI $^-$): m/z : act: 310.0433 [M-H^+] $^-$ cal: 311.2202 [M-H^+] $^-$.

Compound 6: Hydrazine hydrate (0.50 mL, 10.00 mM) was added to a stirring solution of compound **5** (0.20 g, 0.64 mM) and Pd/C (0.05 g) in ethanol (20 mL) and was heated to 80 °C. The solution was filtered and taken to dryness and obtained as a white solid. Yield: 75 % (0.14 g, 0.48 mM); Melting point: > 200 °C; ^1H NMR (400 MHz, $\text{DMSO-}d_6$): δ (ppm): 6.27 (br s, NH_2), 6.88 (s, 1H), 6.93 (m, 1H), 7.72 (d, $J = 8.52$ Hz, 2H), 7.98 (d, $J = 8.60$ Hz, 2H), 8.07 (d, $J = 5.24$ Hz, 1H) 10.62 (br s, NH); $^{13}\text{C}\{^1\text{H}\}$ NMR (100 MHz, $\text{DMSO-}d_6$): δ (ppm): 106.3 (ArCH), 109.4 (ArCH), 120.2 (ArCH), 123.0 (q, $J = 31.87$ Hz, ArC), 123.9 (q, $J = 270.00$ Hz, CF_3), 126.0 (q, $J = 3.79$ Hz, ArCH), 142.5 (ArC), 143.0 (ArC), 148.4 (ArCH), 160.2 (CO), 165.5 (ArC); IR (film): ν (cm^{-1}) = 3304 (NH stretch), 1676 (C=O stretch); HRMS ($\text{C}_{13}\text{H}_{10}\text{F}_3\text{N}_3\text{O}$) (ESI $^-$): m/z : act: 280.0820 [M-H^+] $^-$ cal: 281.2382 [M-H^+] $^-$.

Compound 7: This compound was synthesised in line with previously published methods. Proton NMR were found to match previously published values.¹⁰ ^1H NMR (400 MHz, $\text{DMSO-}d_6$): δ (ppm): 1.75 (d, $J = 1.10$ Hz, 3H), 3.68 (s, 3H), 4.48 (s, 2H), 7.50 (d, $J = 1.2$ Hz, 1H), 11.43 (br s, NH).

Characterisation NMR

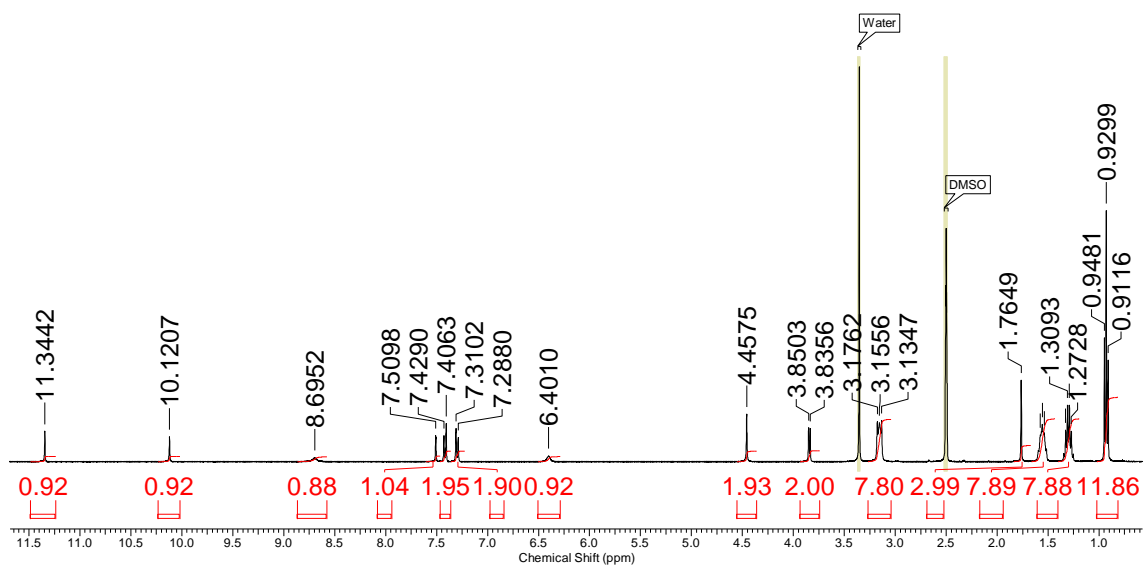


Figure S1 – ^1H NMR spectrum of **2** in $\text{DMSO}-d_6$ at 25 °C.

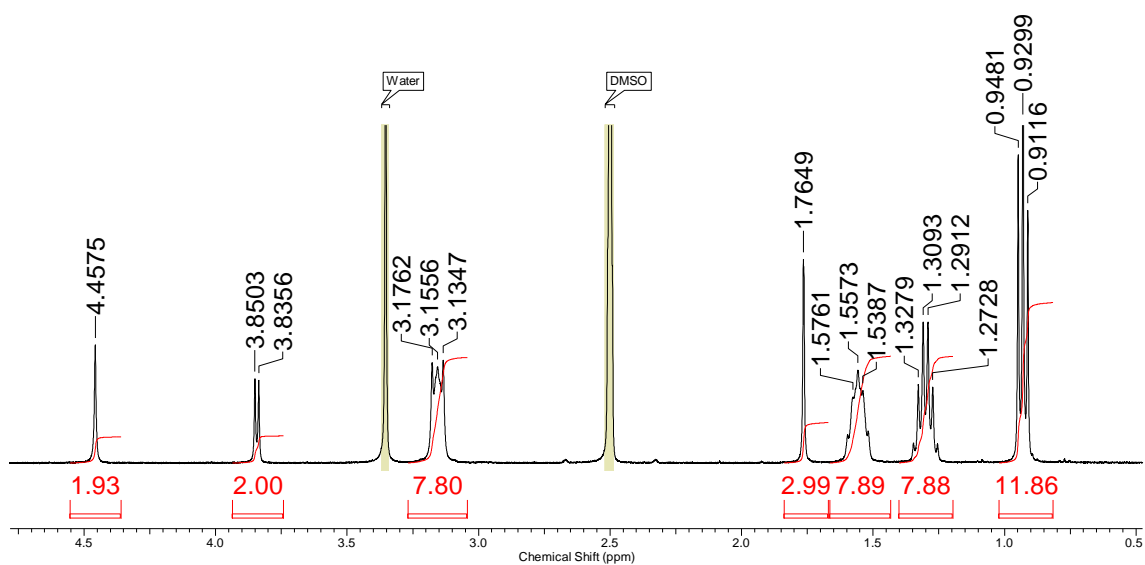


Figure S2 – Enlarged ^1H NMR spectrum of **2** in $\text{DMSO}-d_6$ at 25 °C.

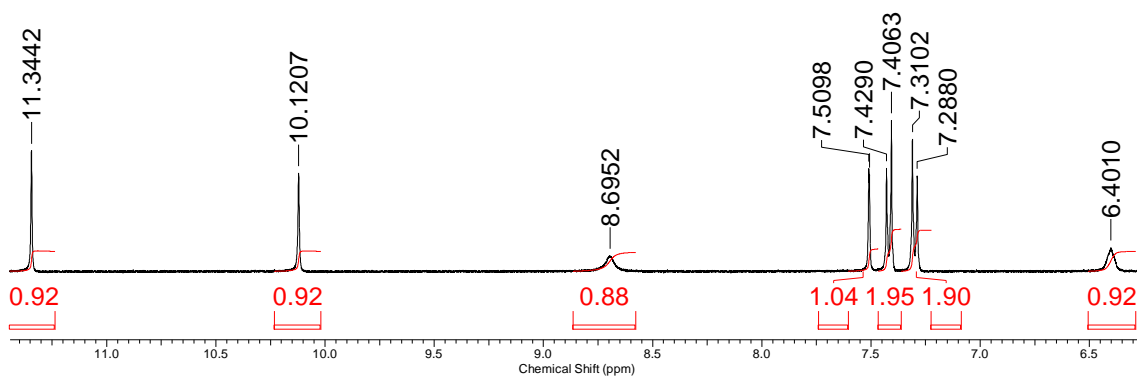


Figure S3 – Enlarged ^1H NMR spectrum of **2** in $\text{DMSO-}d_6$ at 25 °C.

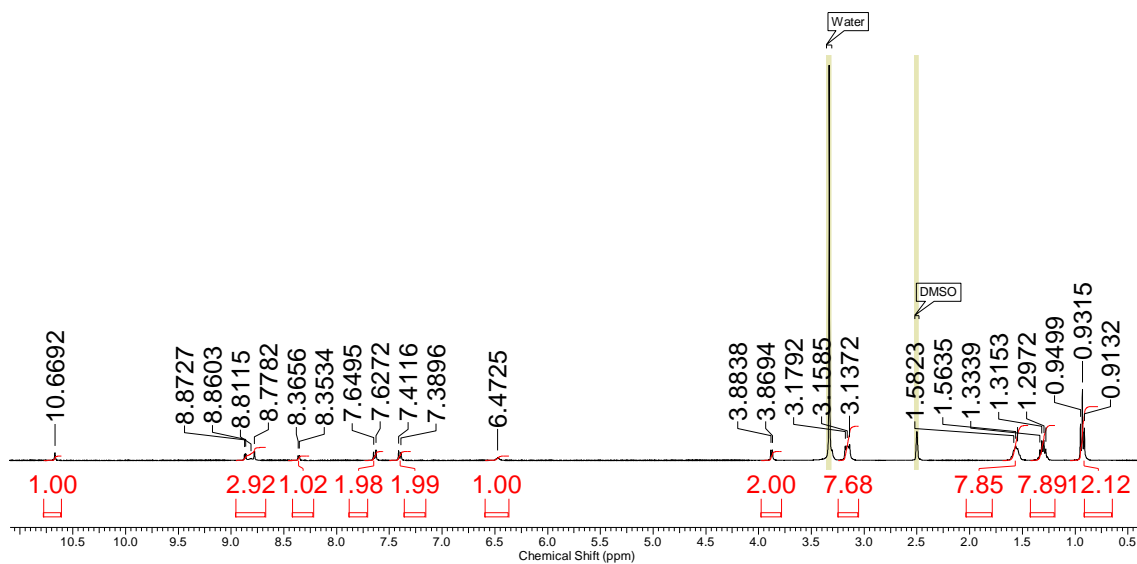


Figure S4 – ^1H NMR spectrum of **3** in $\text{DMSO-}d_6$ at 25 °C.

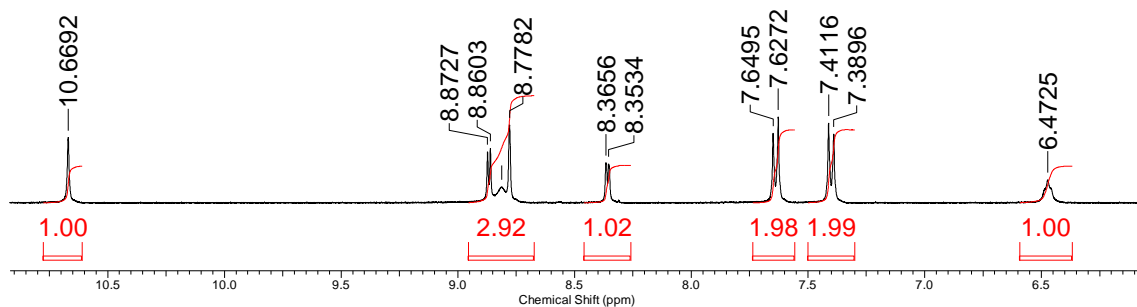


Figure S5 – Enlarged ^1H NMR spectrum of **3** in $\text{DMSO-}d_6$ at 25 $^\circ\text{C}$.

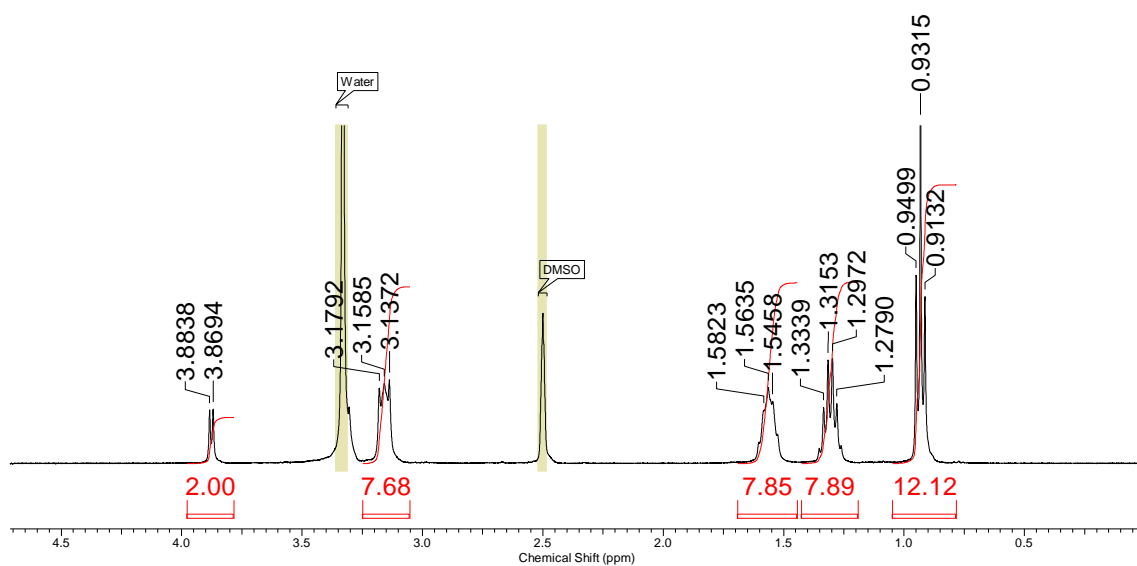


Figure S6 – Enlarged ^1H NMR spectrum of **3** in $\text{DMSO-}d_6$ at 25 $^\circ\text{C}$.

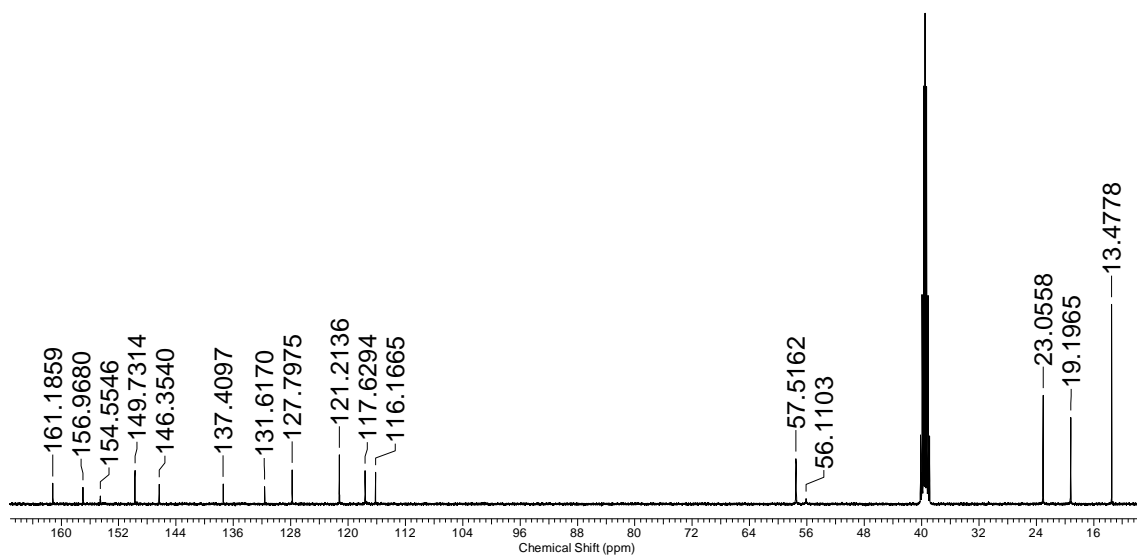


Figure S7 – $^{13}\text{C}\{^1\text{H}\}$ NMR spectrum of **3** in $\text{DMSO-}d_6$ at 25 °C.

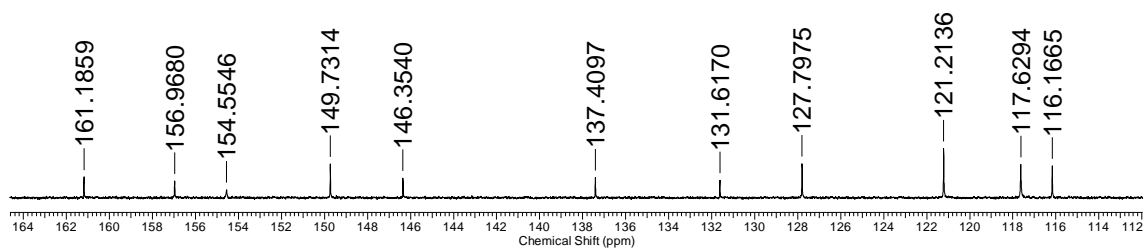


Figure S8 – Enlarged $^{13}\text{C}\{^1\text{H}\}$ NMR spectrum of **3** in $\text{DMSO-}d_6$ at 25 °C.

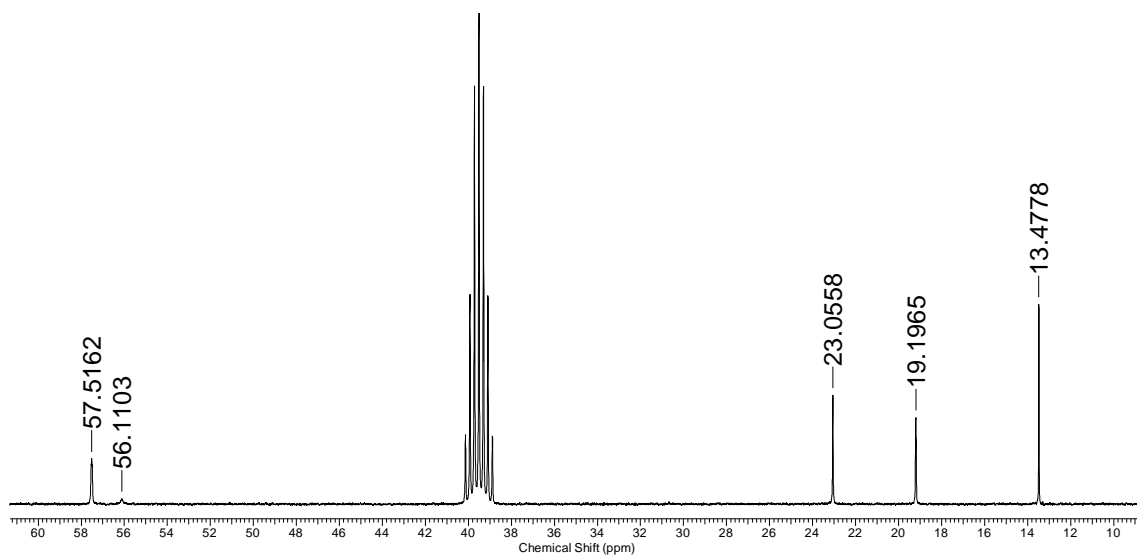


Figure S9 – Enlarged $^{13}\text{C}\{^1\text{H}\}$ NMR spectrum of **3** in $\text{DMSO-}d_6$ at 25 °C.

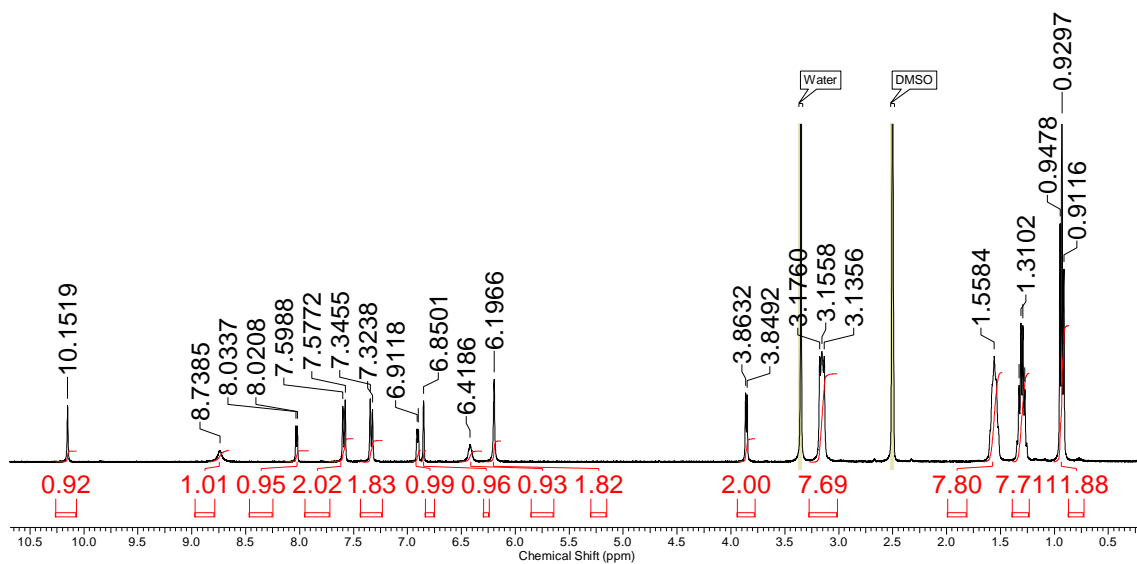


Figure S10 – ^1H NMR spectrum of **4** in $\text{DMSO-}d_6$ at 25 °C.

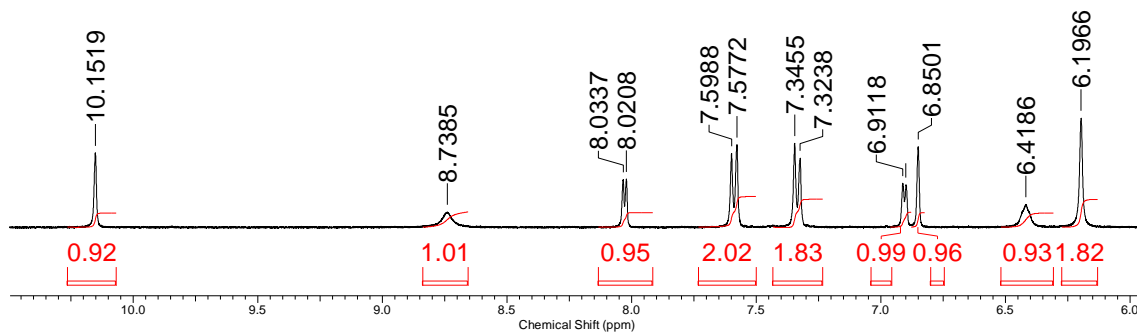


Figure S11 – Enlarged ^1H NMR spectrum of **4** in $\text{DMSO-}d_6$ at 25 °C.

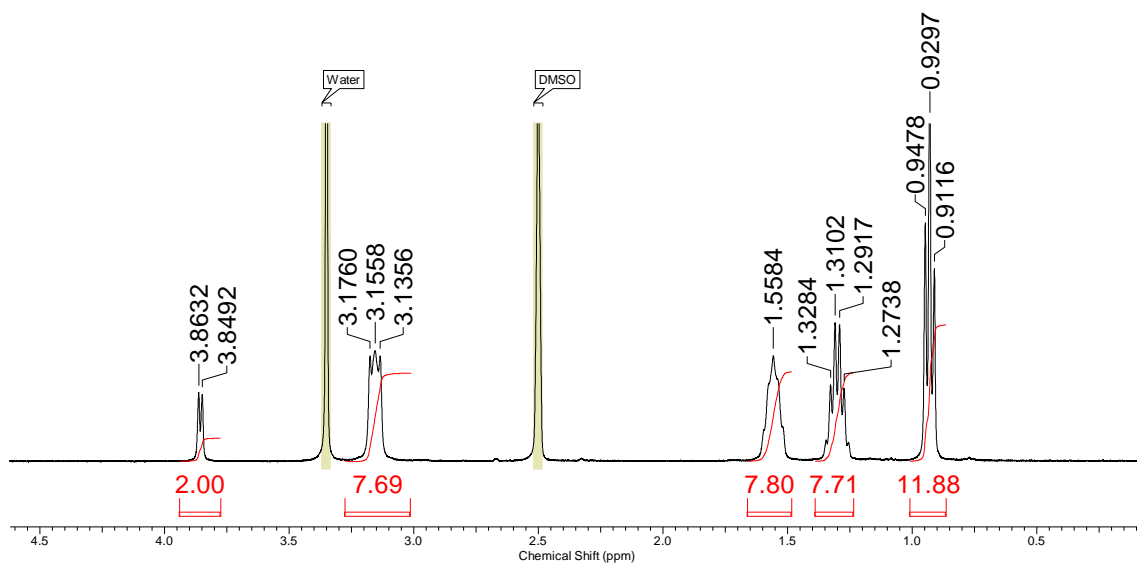


Figure S12 – Enlarged ^1H NMR spectrum of **4** in $\text{DMSO-}d_6$ at 25 °C.

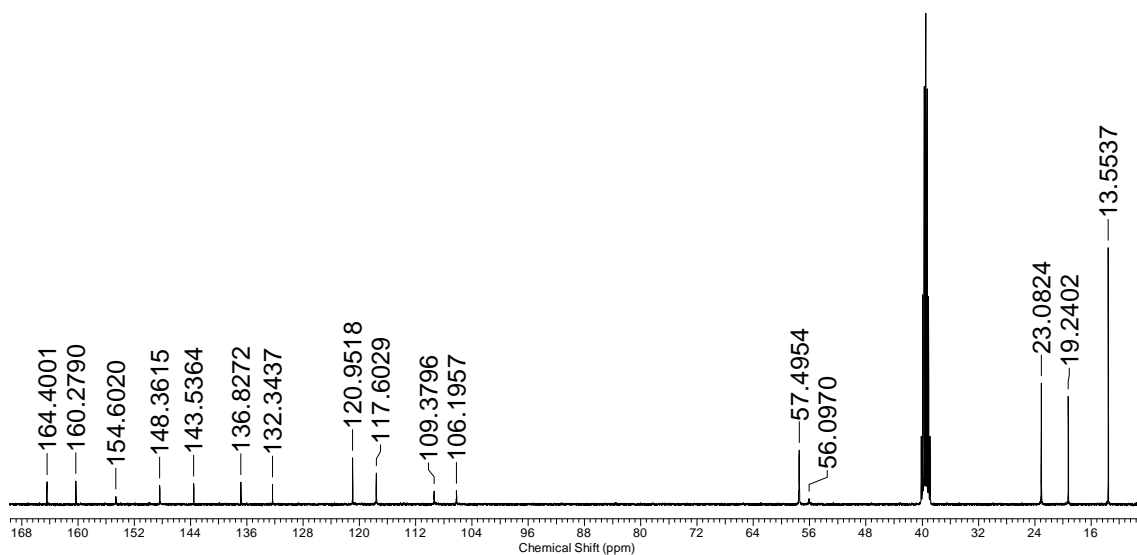


Figure S13 – $^{13}\text{C}\{^1\text{H}\}$ NMR spectrum of **4** in $\text{DMSO}-d_6$ at $25\text{ }^\circ\text{C}$.

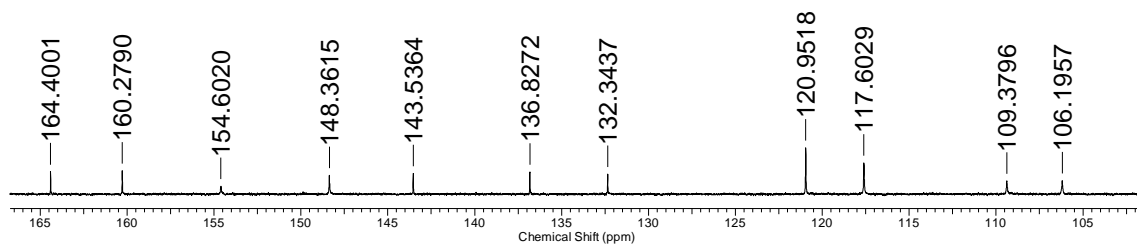


Figure S14 – Enlarged $^{13}\text{C}\{^1\text{H}\}$ NMR spectrum of **4** in $\text{DMSO}-d_6$ at $25\text{ }^\circ\text{C}$.

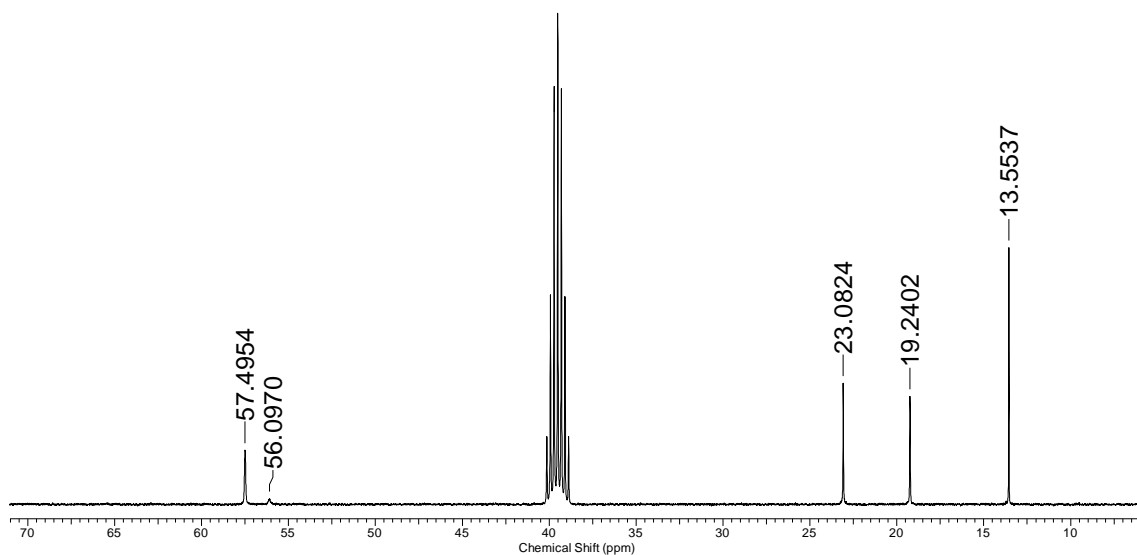


Figure S15 – Enlarged $^{13}\text{C}\{^1\text{H}\}$ NMR spectrum of **4** in $\text{DMSO}-d_6$ at $25\text{ }^\circ\text{C}$.

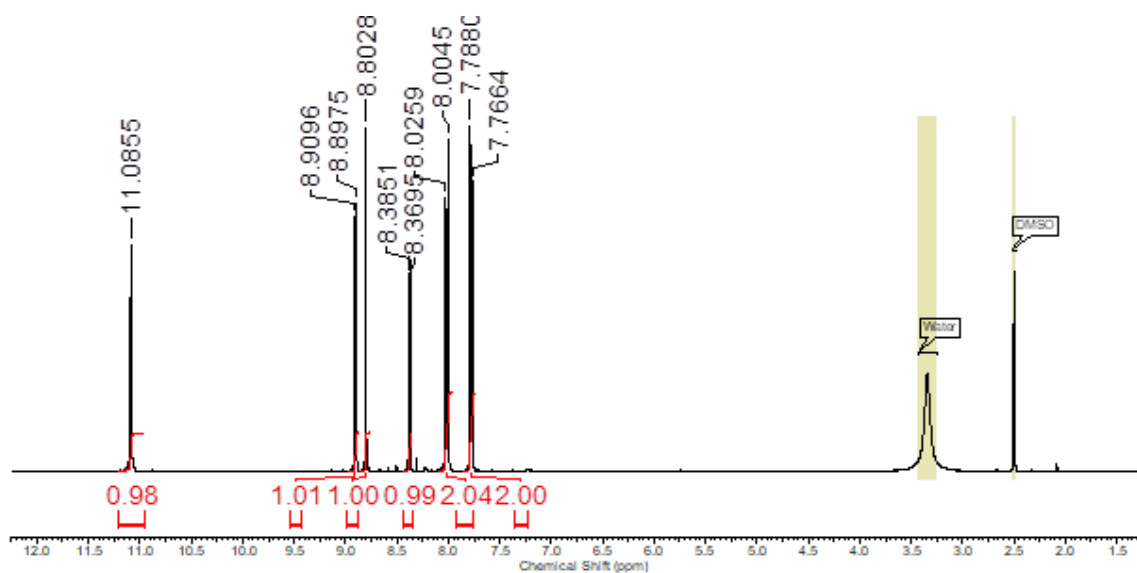


Figure S16 – ^1H NMR spectrum of **5** in $\text{DMSO}-d_6$ at $25\text{ }^\circ\text{C}$.

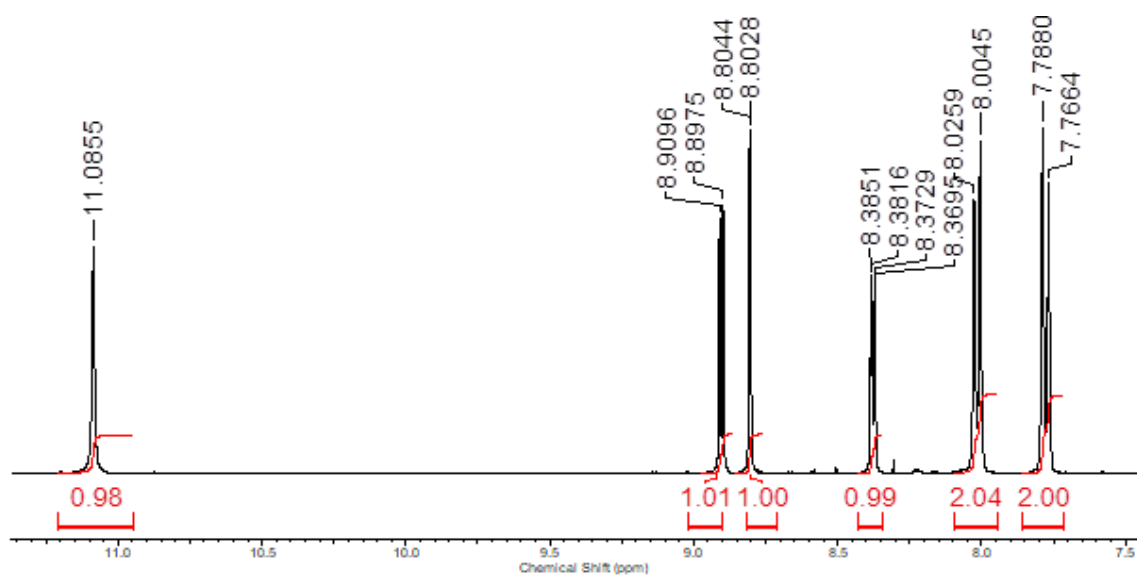


Figure S17 – Enlarged ^1H NMR spectrum of **5** in $\text{DMSO-}d_6$ at 25 °C.

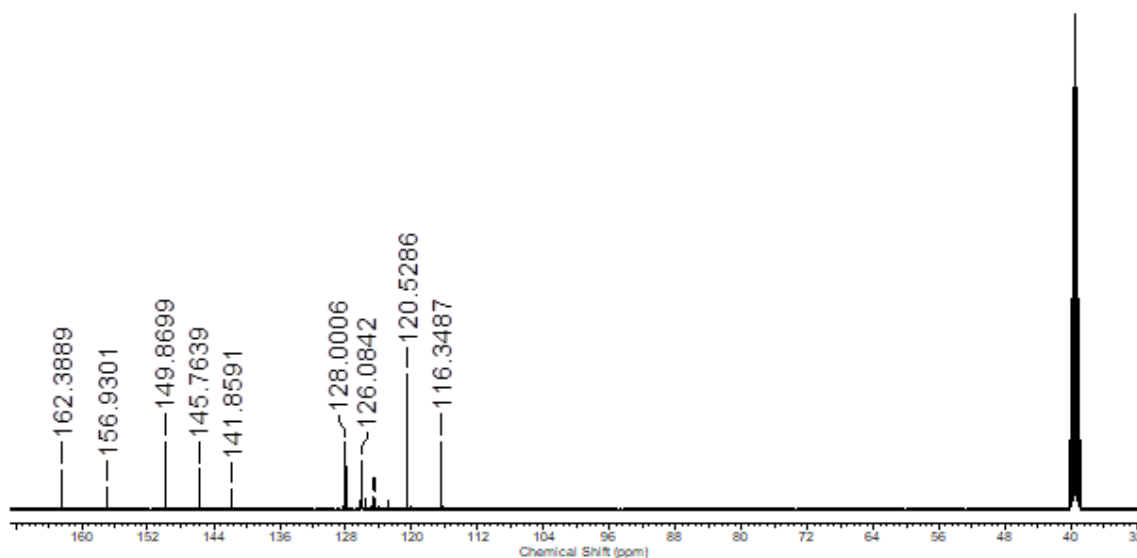


Figure S18 – $^{13}\text{C}\{^1\text{H}\}$ NMR spectrum of **5** in $\text{DMSO-}d_6$ at 25 °C.

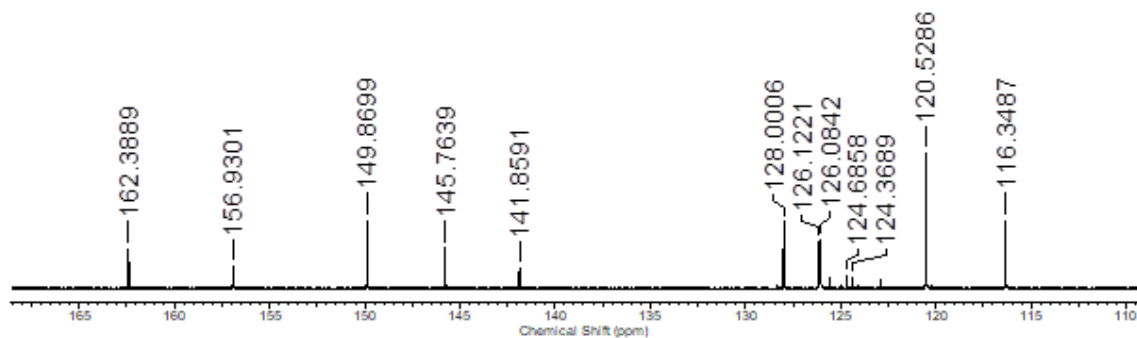


Figure S19 – Enlarged $^{13}\text{C}\{^1\text{H}\}$ NMR spectrum of **5** in $\text{DMSO-}d_6$ at 25 °C.

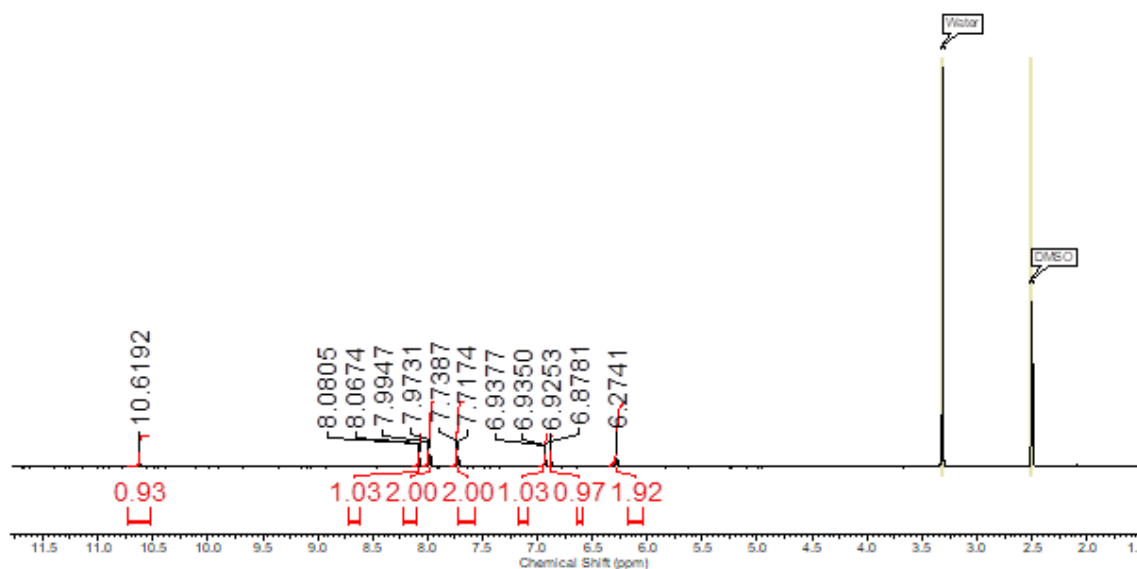


Figure S20 – ^1H NMR spectrum of **6** in $\text{DMSO-}d_6$ at 25 °C.

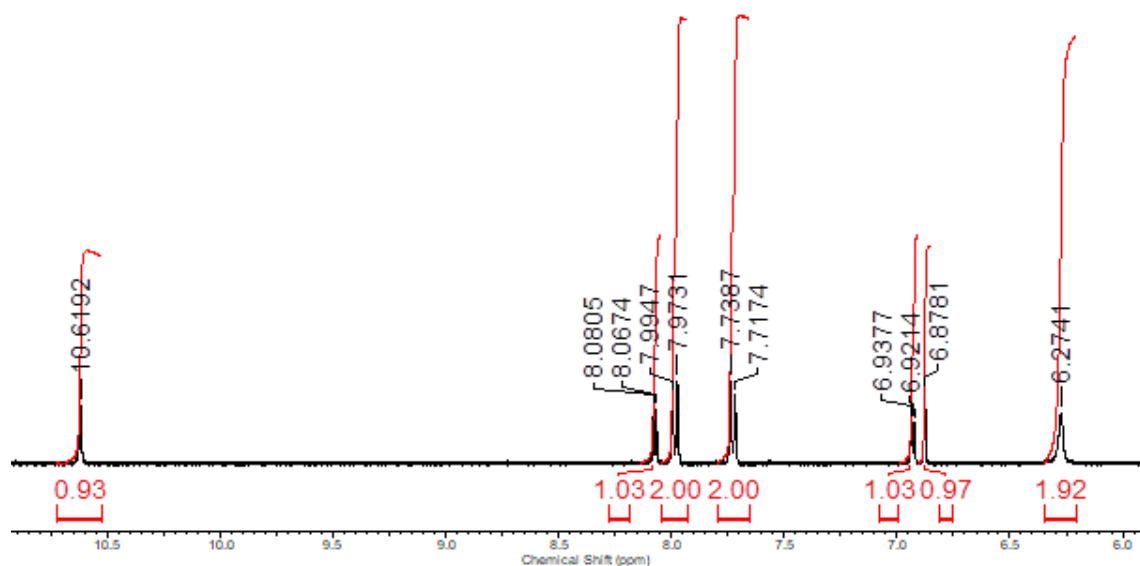


Figure S21 – Enlarged ^1H NMR spectrum of 6 in $\text{DMSO-}d_6$ at $25\text{ }^\circ\text{C}$.

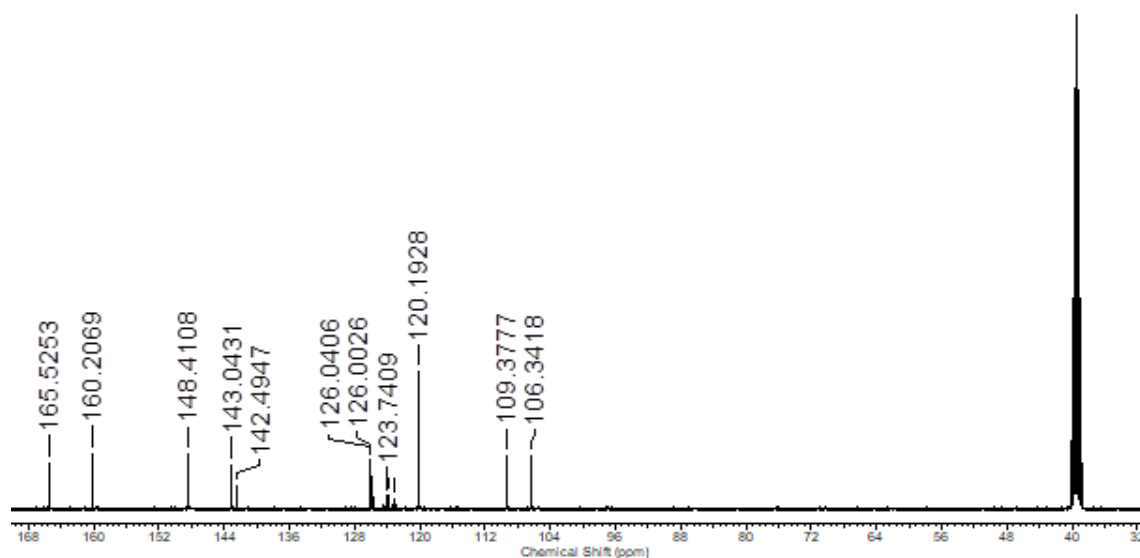


Figure S22 – $^{13}\text{C}\{^1\text{H}\}$ NMR spectrum of 6 in $\text{DMSO-}d_6$ at $25\text{ }^\circ\text{C}$.

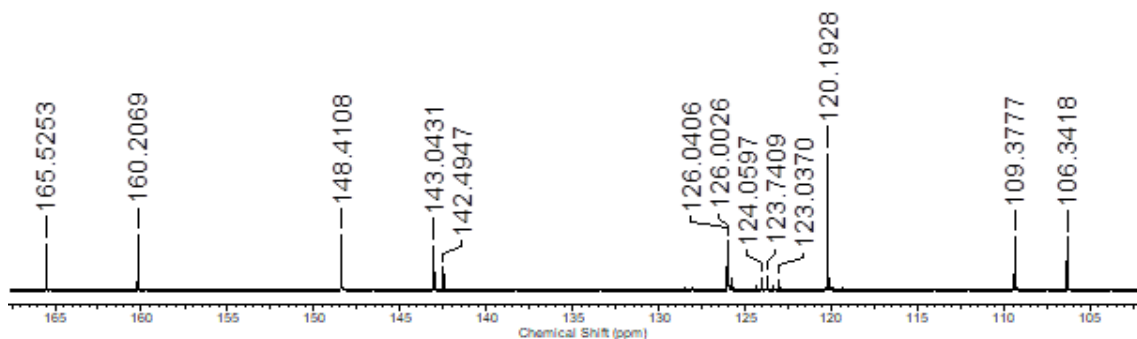


Figure S23 – Enlarged $^{13}\text{C}\{^1\text{H}\}$ NMR spectrum of **6** in $\text{DMSO}-d_6$ at 25 °C.

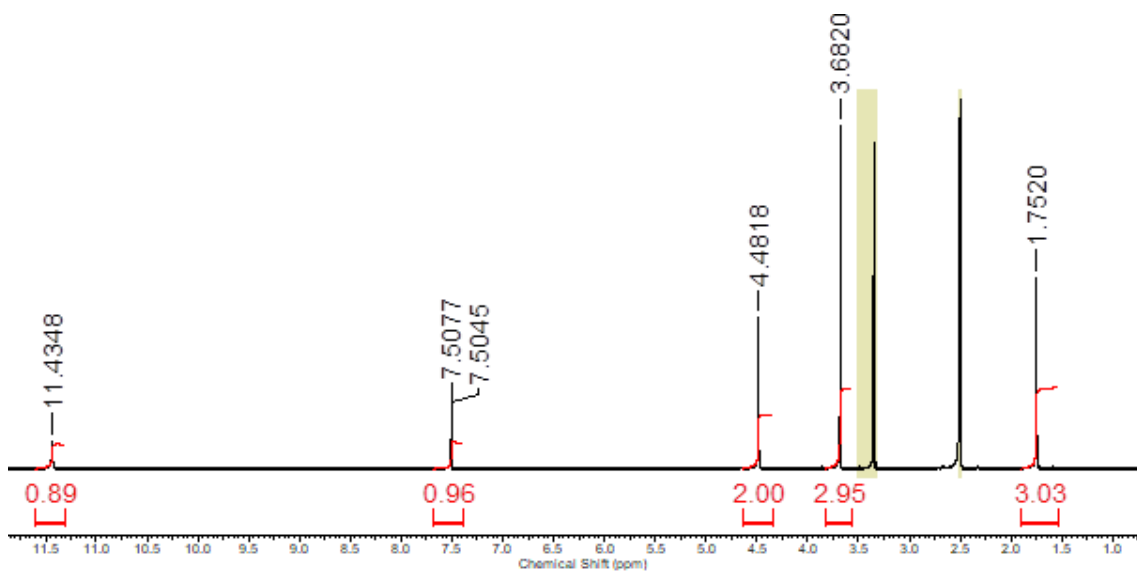


Figure S24 – ^1H NMR spectrum of **7** in $\text{DMSO}-d_6$ at 25 °C.

Single crystal X-ray structures

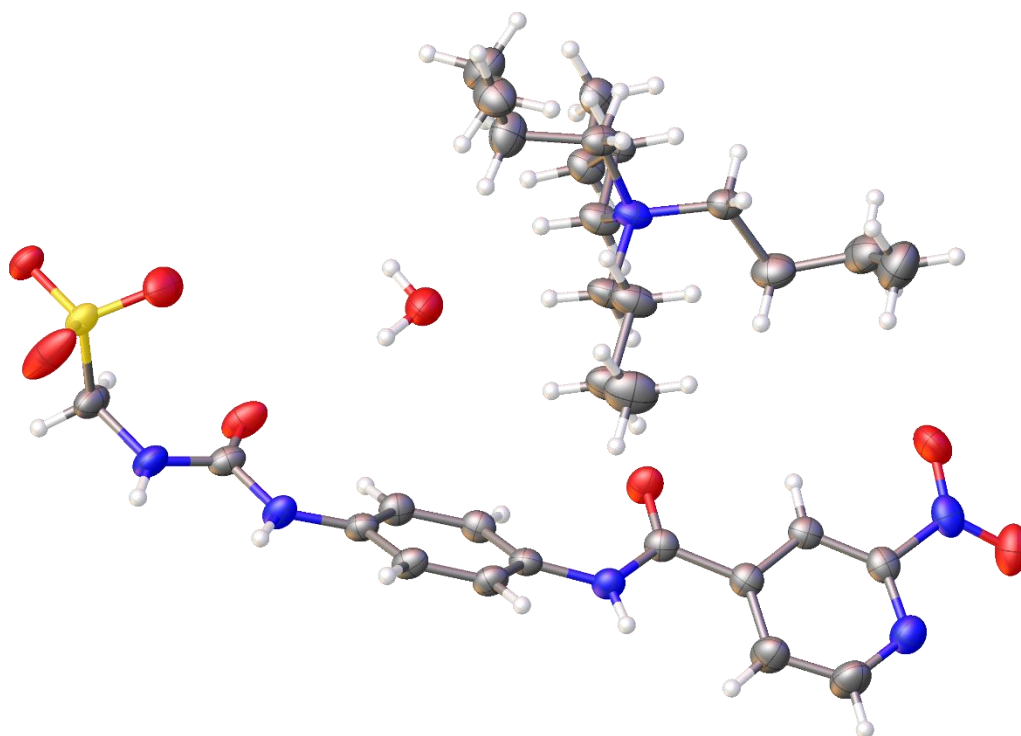


Figure S25 – Single crystal X-ray structure of **3**: red = oxygen; yellow = sulfur; blue = nitrogen; white = hydrogen; grey = carbon. CCDC 1964617, $C_{30}H_{48.67}N_6O_{7.34}S$ ($M = 642.83$): triclinic, space group $P\bar{1}$, $a = 12.3652(5) \text{ \AA}$, $b = 12.4302(5) \text{ \AA}$, $c = 13.2110(4) \text{ \AA}$, $\alpha = 74.723(3)^\circ$, $\beta = 68.913(3)^\circ$, $\gamma = 64.151(4)^\circ$, $V = 1691.23(12) \text{ \AA}^3$, $Z = 2$, $T = 150(1) \text{ K}$, $CuK\alpha = 1.5418 \text{ \AA}$, $D_{\text{calc}} = 1.262 \text{ g/cm}^3$, 11325 reflections measured ($7.230 \leq 2\theta \leq 133.200$), 5979 unique ($R_{\text{int}} = 0.0236$, $R_{\text{sigma}} = 0.0309$) which were used in all calculations. The final R_1 was 0.0411 ($I > 2\sigma(I)$) and wR_2 was 0.1062 (all data).

Table S1 – Hydrogen bond distances and angles observed for **3**, calculated from the single crystal X-ray structure shown in Figure S25.

Hydrogen bond donor	Hydrogen atom	Hydrogen bond acceptor	Hydrogen bond length (D•••A) (Å)	Hydrogen bond angle (D-H•••A) (°)
N1	H1	O2	2.823 (3)	140.34 (11)
N2	H2	O2	2.8291 (19)	152.52 (10)
N3	H3	O2	2.8897(18)	159.07 (9)
O8	H8B	O4	3.618(5)	153.1 (3)
O8	H8A	N4	2.872(4)	170.3 (3)

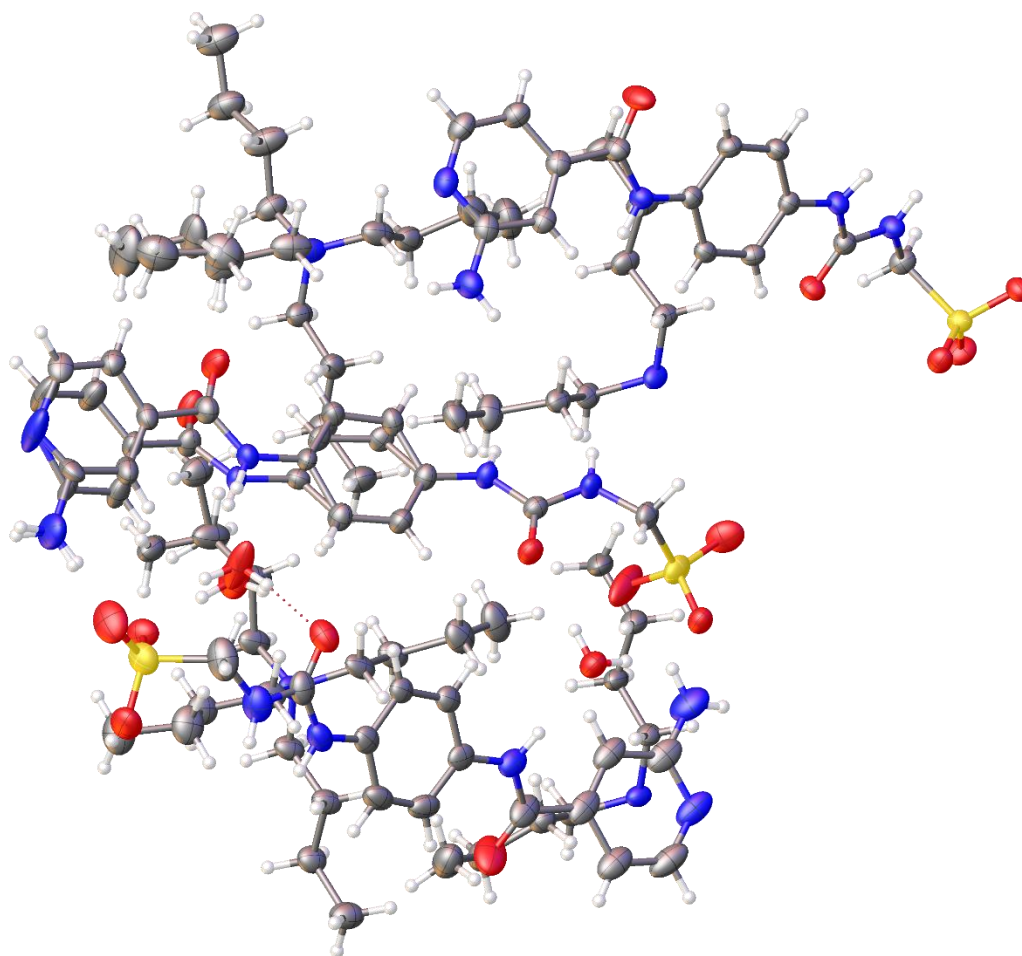


Figure S26 – Single crystal X-ray structure of **4**: red = oxygen; yellow = sulfur; blue = nitrogen; white = hydrogen; grey = carbon. CCDC 1964619, C₉₀H₁₅₄N₁₈O₁₇S₃ (M = 1856.48): monoclinic, space group P 2₁/n, a = 18.9400(6) Å, b = 8.6626(2) Å, c = 60.1390(20) Å, $\alpha = 90^\circ$, $\beta = 95.558(3)^\circ$, $\gamma = 90^\circ$, V = 9820.6(5) Å³, Z = 4, T = 100(1) K, CuK α = 1.5418 Å, D_{calc} = 1.256 g/cm³, 65730 reflections measured (6.756 ≤ 2 θ ≤ 142.048), 18811 unique (R_{int} = 0.0544, R_{sigma} = 0.0527) which were used in all calculations. The final R₁ was 0.0631 (I > 2 σ (I)) and wR₂ was 0.1507 (all data).

Table S2 – Hydrogen bond distances and angles observed for **4**, calculated from the single crystal X-ray structure shown in Figure S26.

Hydrogen bond donor	Hydrogen atom	Hydrogen bond acceptor	Hydrogen bond length (D•••A) (Å)	Hydrogen bond angle (D-H•••A) (°)
N1	H1	O12	3.24083 (7)	144.2563 (14)
N1	H1	O13	3.31040 (11)	143.0169 (11)
N2	H2	O12	2.88367 (9)	167.3009 (2)
N3	H3	O3	2.92408 (9)	164.6884 (6)
N5	H5A	N14	3.20783 (11)	148.1951 (13)
N5	H5B	O2	3.08961 (11)	151.6867 (12)
N6	H6	O8	2.87580 (8)	144.8249 (12)
N7	H7A	O8	2.77260 (10)	161.7169 (9)
N8	H8A	O16	2.88984 (6)	156.2226 (5)
N10	H10A	N9	3.07164 (11)	171.6333 (4)
N10	H10B	O13	3.13207 (11)	162.9753 (8)
N11	H11	O2	2.85340 (8)	152.8255 (10)
N12	H12	O2	2.86090 (11)	146.9218 (14)
N13A	H13A	O17A	2.73388 (9)	157.7786 (10)
N13B	H13B	O17B	2.98338 (10)	162.2477 (7)
N15	H15A	O6	3.45158 (8)	121.2813 (14)
N15	H15B	N14	3.00295 (11)	161.6067 (8)
N15	H15C	N4	3.00295 (11)	145.2453 (15)
N15	H15D	O7	2.96426 (10)	170.5745 (4)
O16	H16A	O11	2.88665 (11)	159.3766 (11)
O16	H16B	O14	2.81433 (10)	174.5841 (3)
O17A	H17A	O9	2.86566 (6)	165.9885 (3)
O17A	H17B	O7	2.77279 (11)	162.8523 (8)
O17B	H17C	O9	2.64585 (6)	169.59267 (9)
O17B	H17D	O7	2.73774 (10)	161.9488 (10)

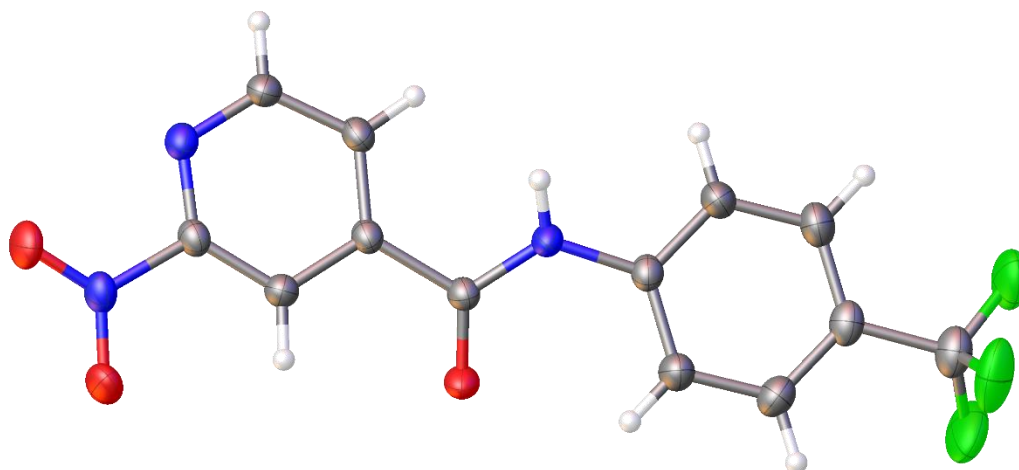


Figure S27 – Single crystal X-ray structure of compound **5**: red = oxygen; blue = nitrogen; white = hydrogen; grey = carbon; green = fluorine. CCDC 1964618, $C_{13}H_8F_3N_3O_3$ ($M = 311.22$): triclinic, space group $P-1$, $a = 4.9833(3) \text{ \AA}$, $b = 6.9376(3) \text{ \AA}$, $c = 18.1030(10) \text{ \AA}$, $\alpha = 90.645(4)^\circ$, $\beta = 94.990(5)^\circ$, $\gamma = 93.826(4)^\circ$, $V = 622.01(5) \text{ \AA}^3$, $Z = 2$, $T = 150(1) \text{ K}$, $CuK\alpha = 1.5418 \text{ \AA}$, $D_{\text{calc}} = 1.662 \text{ g/cm}^3$, 3628 reflections measured ($9.810 \leq 2\theta \leq 133.166$), 2182 unique ($R_{\text{int}} = 0.0321$, $R_{\text{sigma}} = 0.0448$) which were used in all calculations. The final R_1 was 0.0399 ($I > 2\sigma(I)$) and wR_2 was 0.1073 (all data).

Table S3 – Hydrogen bond distances and angles observed for **5**, calculated from the single crystal X-ray structure shown in Figure S27.

Hydrogen bond donor	Hydrogen atom	Hydrogen bond acceptor	Hydrogen bond length (D...A) (\AA)	Hydrogen bond angle (D-H...A) ($^\circ$)
O1	H1	N1	3.059 (2)	152.61 (13)

Mass spectrum data

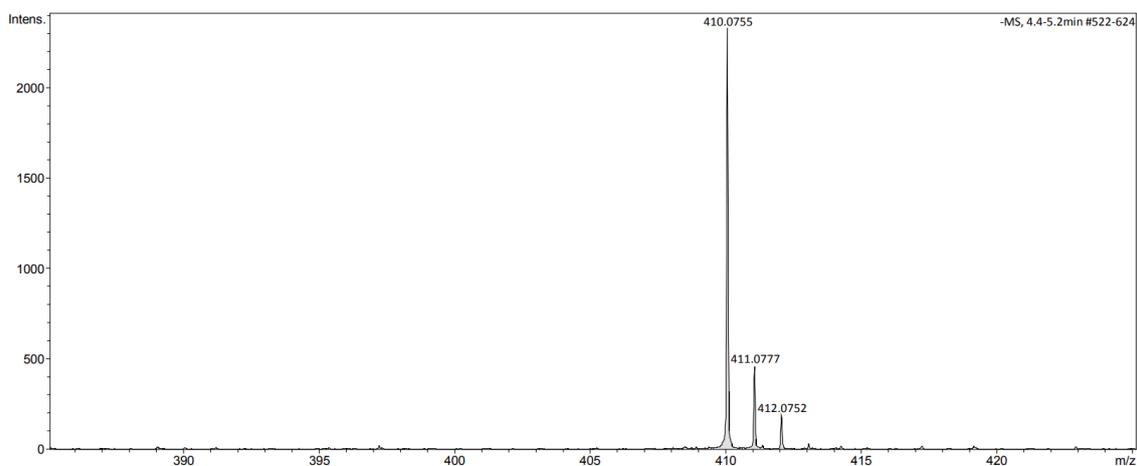


Figure S28 – High-resolution ESI⁻ mass spectrum collected for **2**.

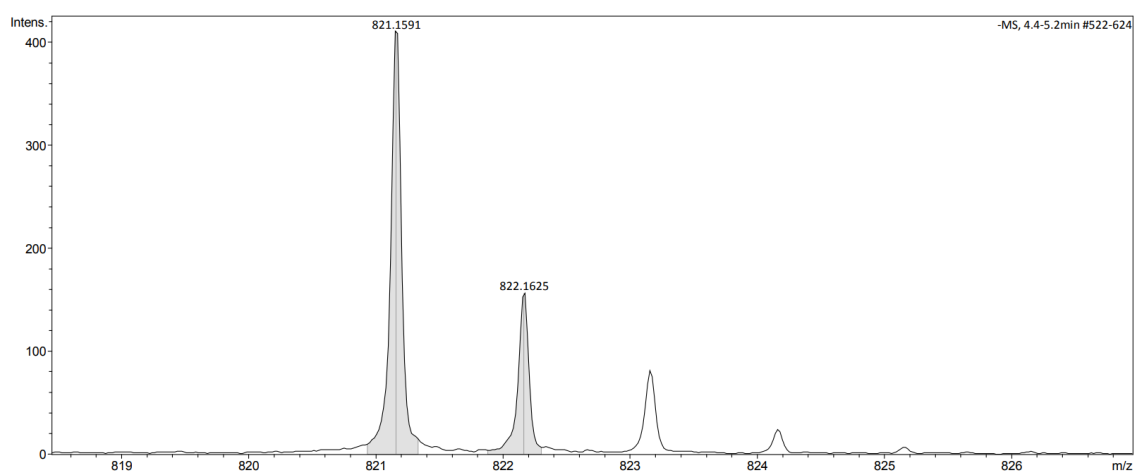


Figure S29 – High-resolution ESI⁻ mass spectrum collected for **2**.

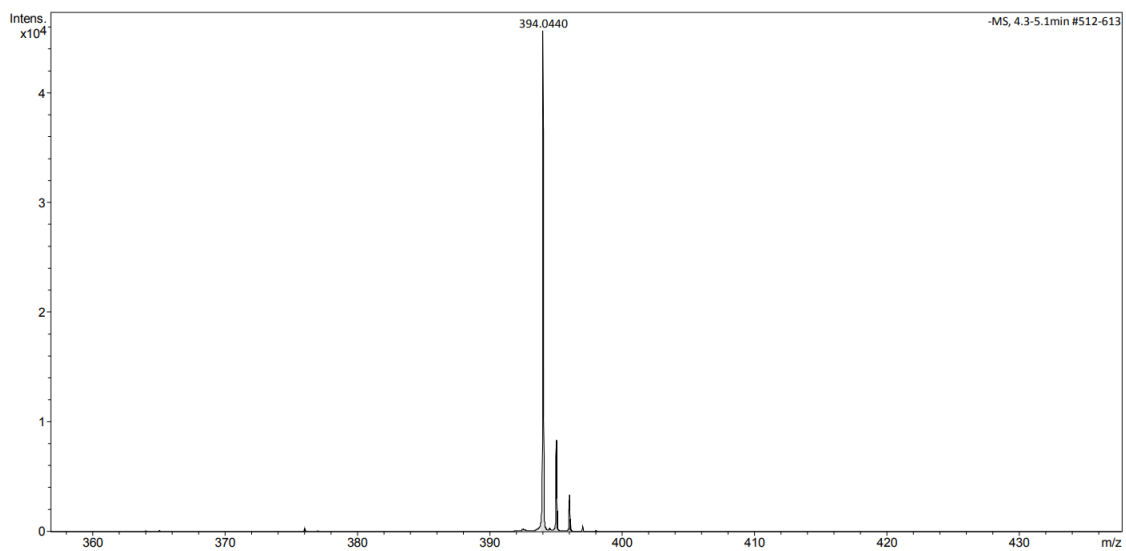


Figure S30 – High-resolution ESI^{-ve} mass spectrum collected for **3**.

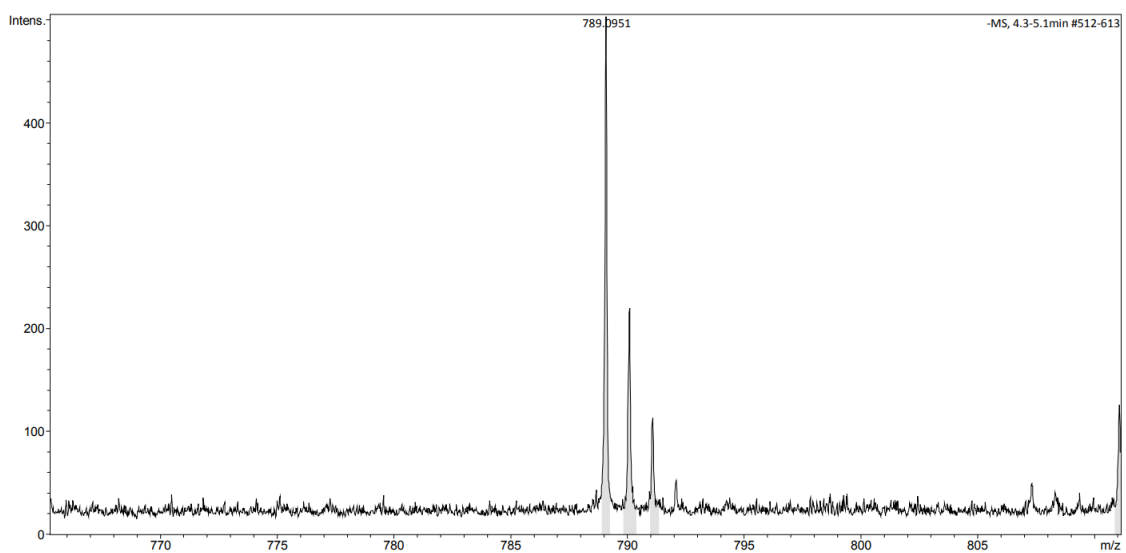


Figure S31 – High-resolution ESI^{-ve} mass spectrum collected for **3**.

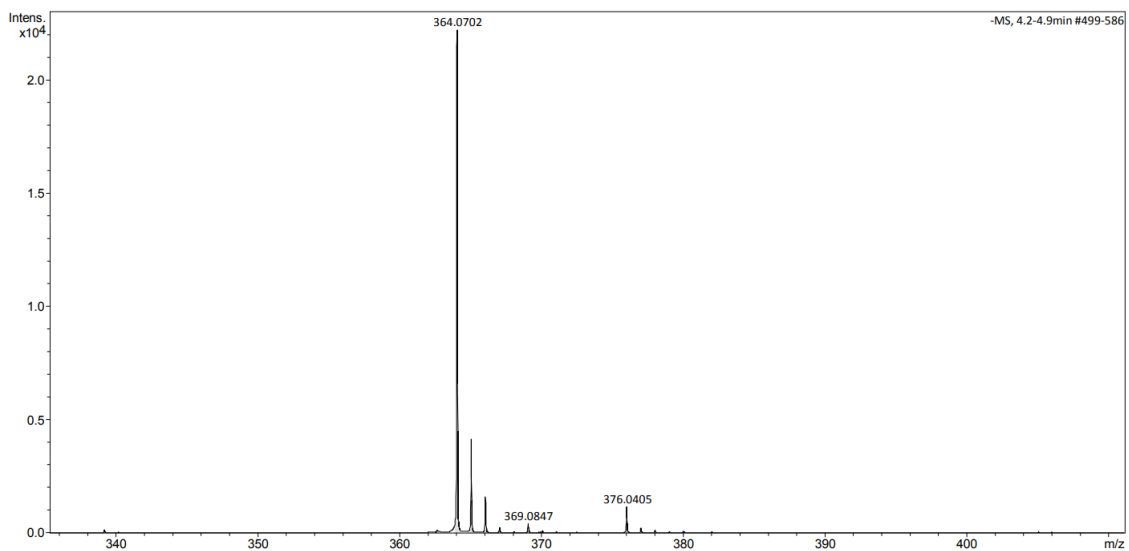


Figure S32 – High-resolution ESI⁻ mass spectrum collected for **4**.

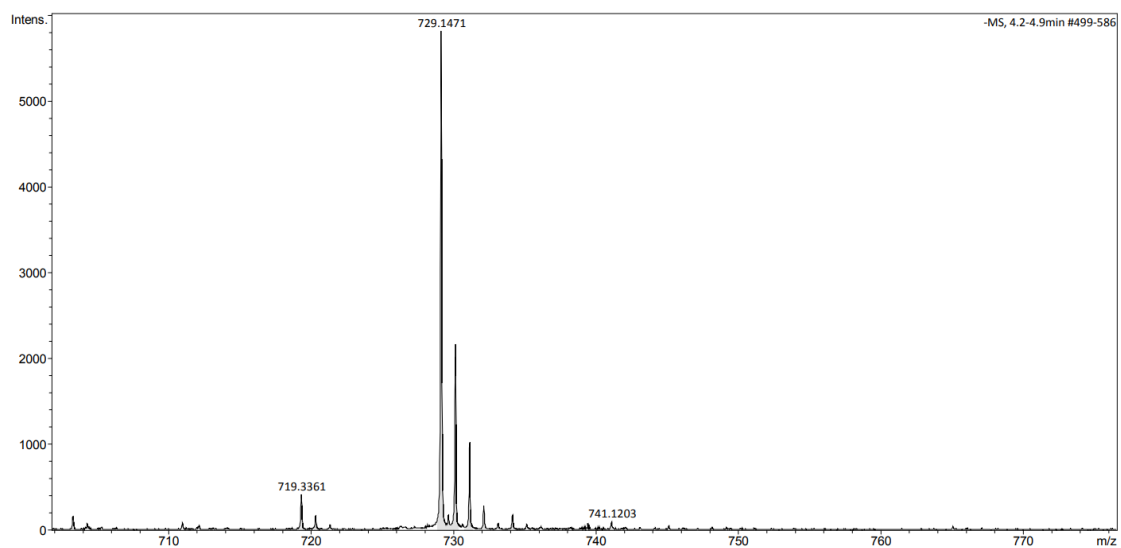


Figure S33 – High-resolution ESI⁻ mass spectrum collected for **4**.

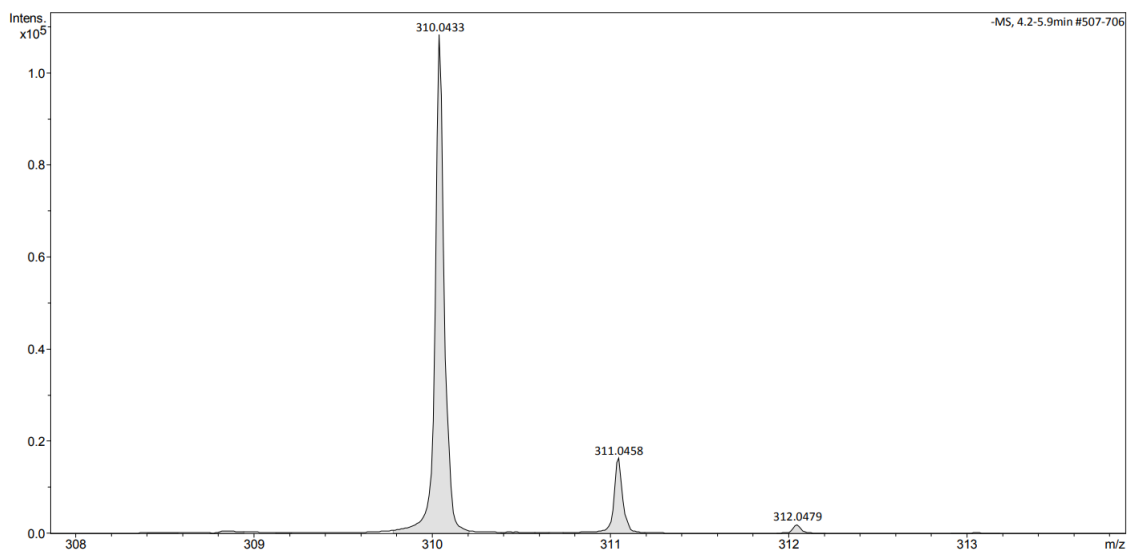


Figure S34 – High-resolution ESI^{-ve} mass spectrum collected for 5.

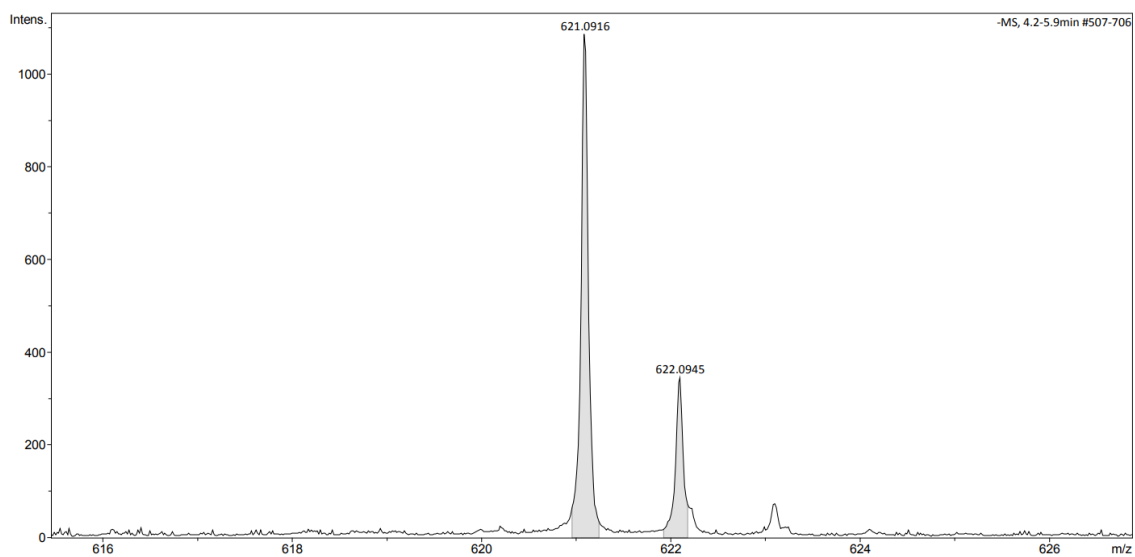


Figure S35 – High-resolution ESI^{-ve} mass spectrum collected for 5.

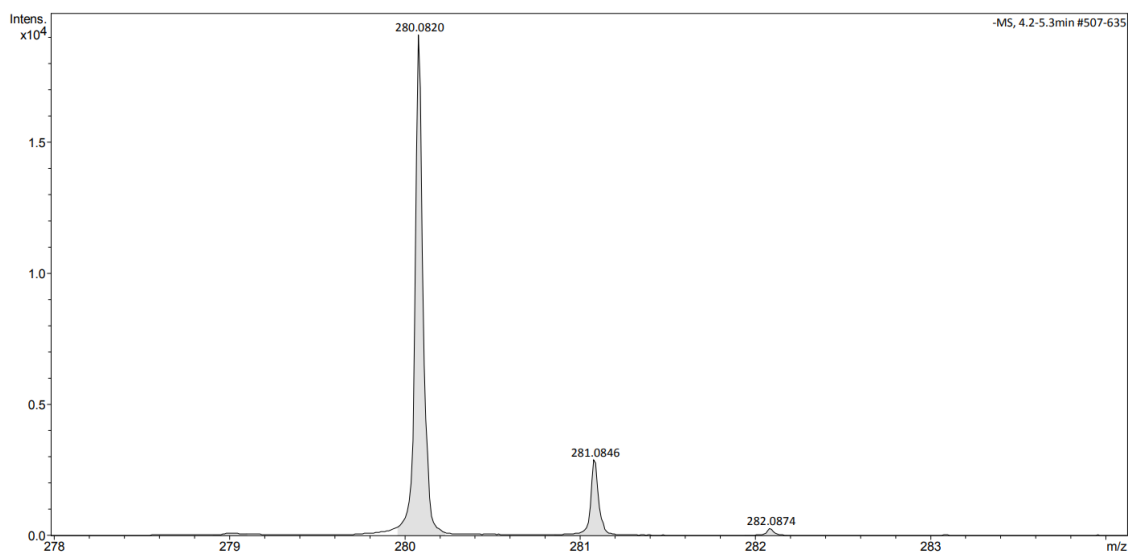


Figure S36 – High-resolution ESI⁻ mass spectrum collected for **6**.

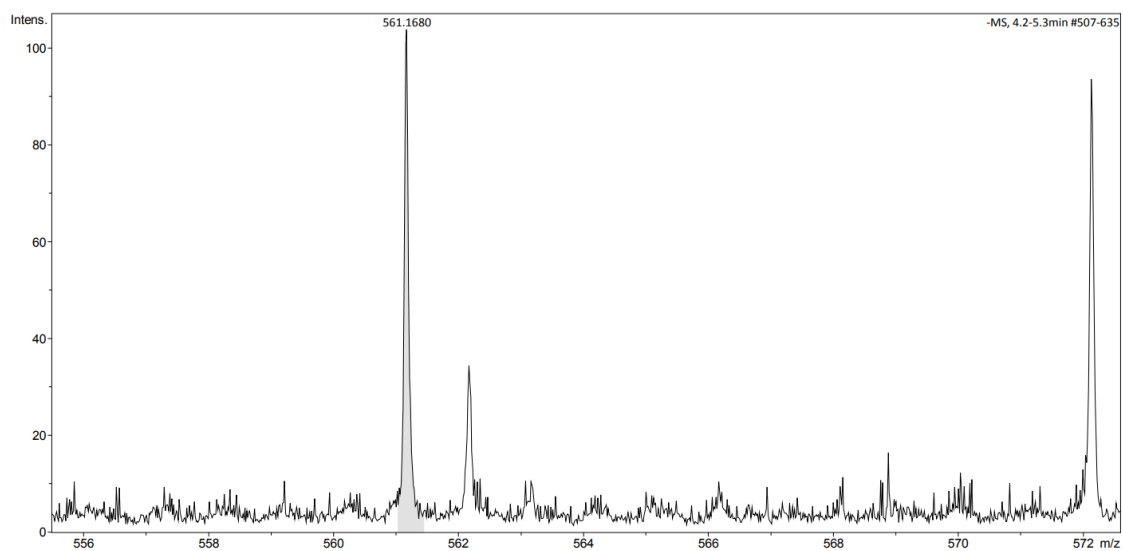


Figure S37 – High-resolution ESI⁻ mass spectrum collected for **6**.

Table S4 – High-resolution mass spectrometry theoretical and experimentally derived values for compounds **2-4**.

SSA	m/z [M] ⁻		m/z [M + M + H] ⁺	
	Theoretical	Actual	Theoretical	Actual
2	410.3815	410.0755	821.7700	821.1591
3	394.3385	394.0440	789.6840	789.0951
4	364.3565	364.0702	729.7200	729.1471

Table S5 – High-resolution mass spectrometry theoretical and experimentally derived values for compounds **5**, **6**.

Compound	m/z [M – H] ⁺		m/z [M + M] ⁻	
	Theoretical	Actual	Theoretical	Actual
5	310.2132	310.0433	621.4334	621.0916
6	280.2312	280.0820	561.4694	561.1680

¹H NMR quantitative studies

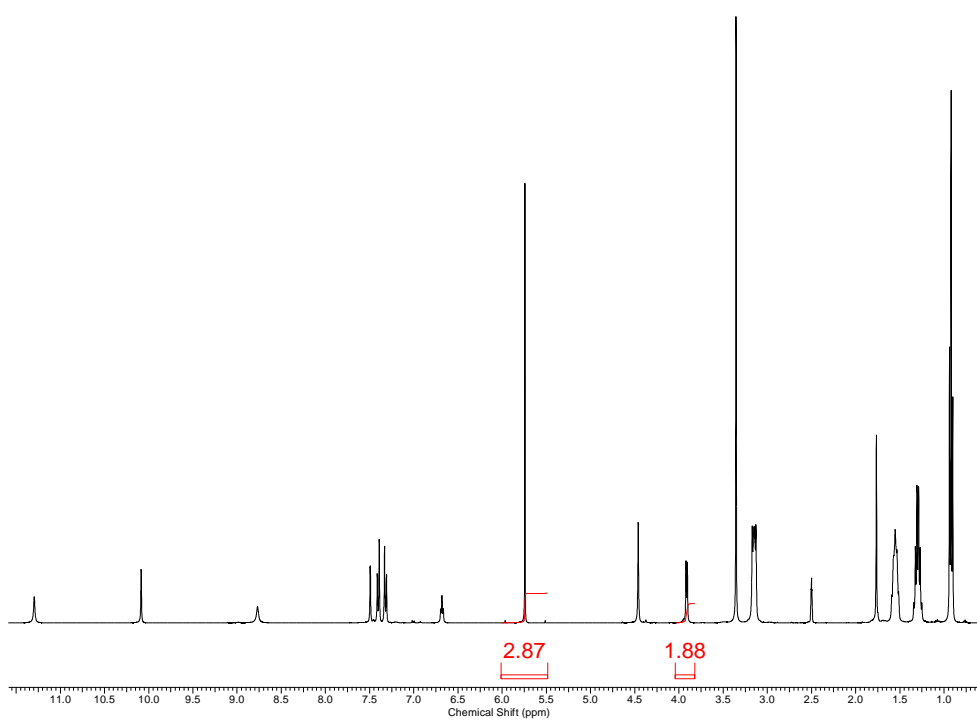


Figure S38 – ¹H NMR spectrum (*d*₁ = 60 s) of compound **2** (111.12 mM) in DMSO-*d*₆/1.0% DCM. Comparative integration indicates 6% of the anionic component of **2** has become NMR silent.

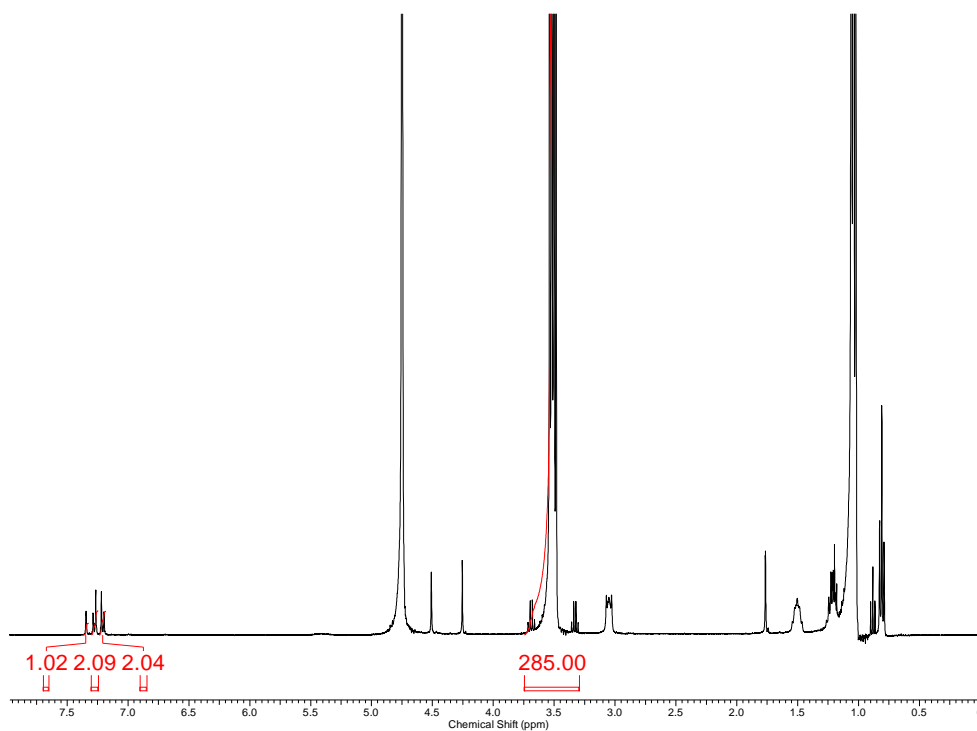


Figure S39 – ^1H NMR spectrum ($d_1 = 60$ s) of compound **2** (6.00 mM) in D_2O /5.0 % EtOH. Comparative integration indicates 0 % of the anionic component of **2** has become NMR silent.

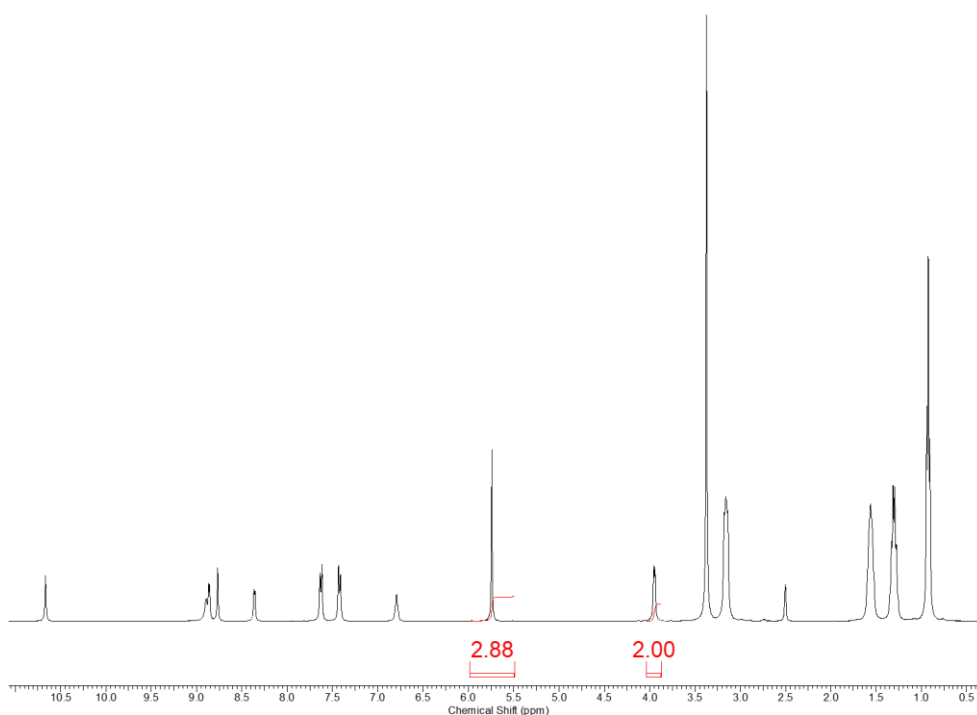


Figure S40 – ^1H NMR spectrum ($d_1 = 60$ s) of compound **3** (111.12 mM) in $\text{DMSO-}d_6$ /1.0 % DCM. Comparative integration indicates 0 % of the anionic component of **3** has become NMR silent.

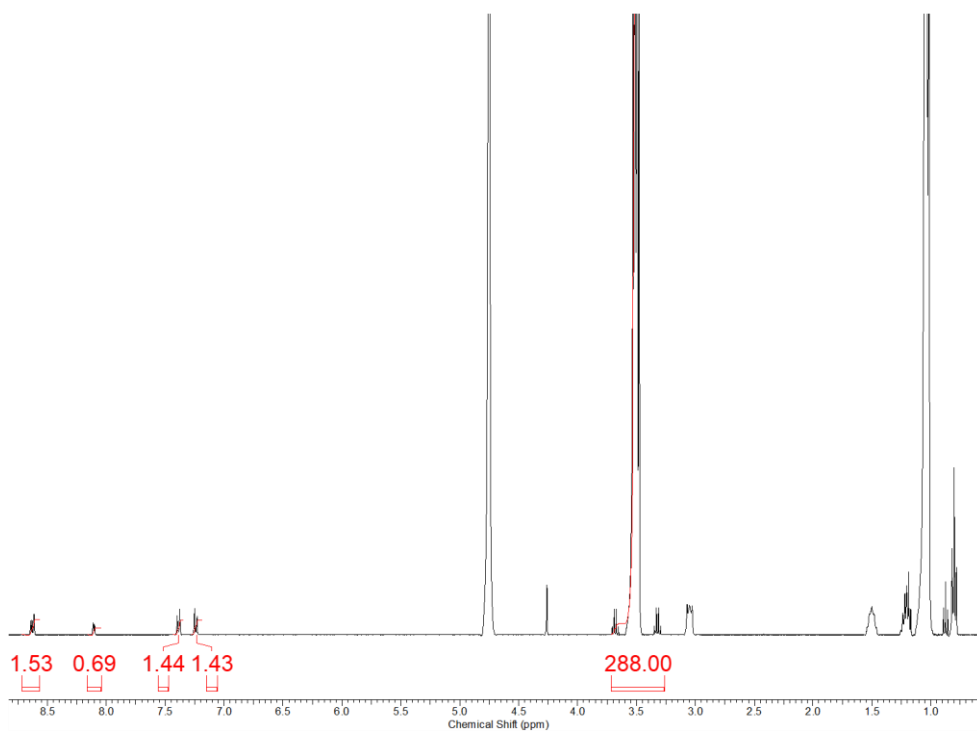


Figure S41 – ^1H NMR spectrum ($d_1 = 60$ s) of compound **3** (6.00 mM) in D_2O /5.0 % EtOH. Comparative integration indicates 29 % of the anionic component of **3** has become NMR silent.

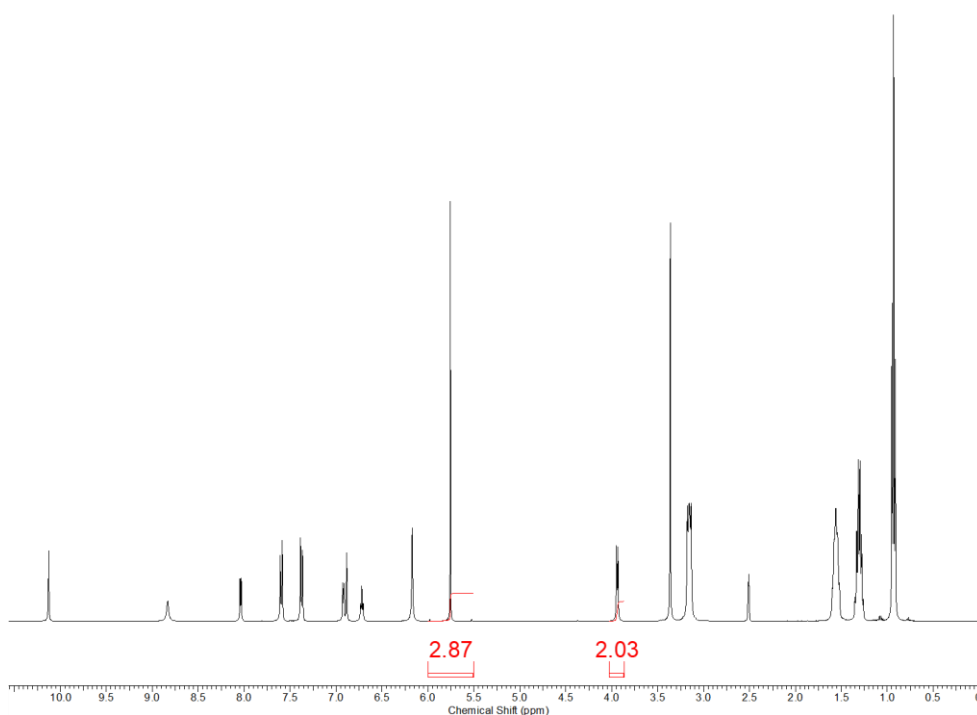


Figure S42 – ^1H NMR spectrum ($d_1 = 60$ s) of compound **4** (111.12 mM) in $\text{DMSO-}d_6$ /1.0 % DCM. Comparative integration indicates 0 % of the anionic component of **4** has become NMR silent.

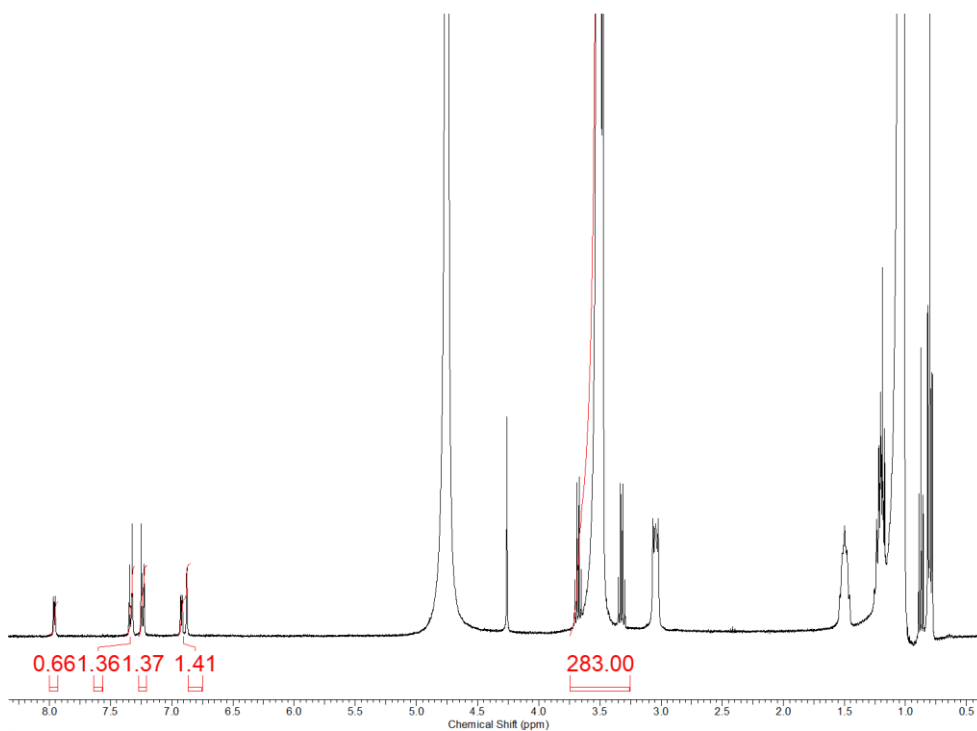


Figure S43 – ^1H NMR spectrum ($d_1 = 60$ s) of compound **4** (6.00 mM) in D_2O /5.0 % EtOH. Comparative integration indicates 32 % of the anionic component of **4** has become NMR silent.

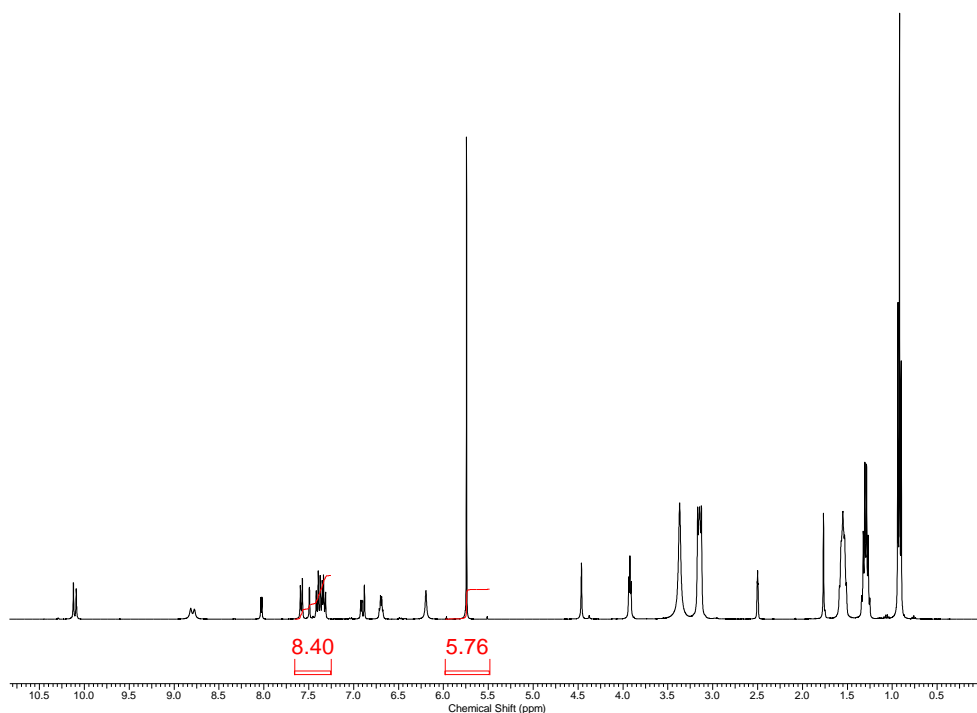


Figure S44 – ^1H NMR spectrum ($d_1 = 60$ s) of compound **2** (55.56 mM) and compound **4** (55.56 mM) in $\text{DMSO}-d_6$ /1.0 % DCM. Comparative integration indicates 7 % of the anionic component of **2** and **4** has become NMR silent.

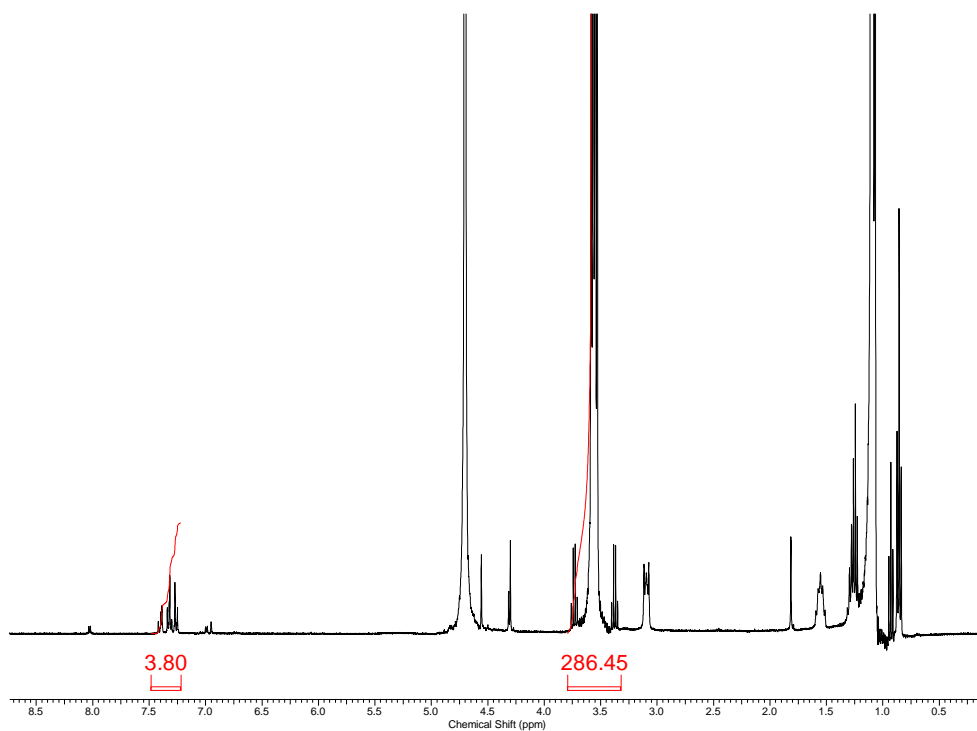


Figure S45 – ^1H NMR spectrum ($d_1 = 60$ s) of compound **2** (3.00 mM) and compound **4** (3.00 mM) in D_2O / 5.0 % EtOH.

Comparative integration indicates 58 % of the anionic component of **2** and **4** has become NMR silent.

^1H NMR DOSY studies

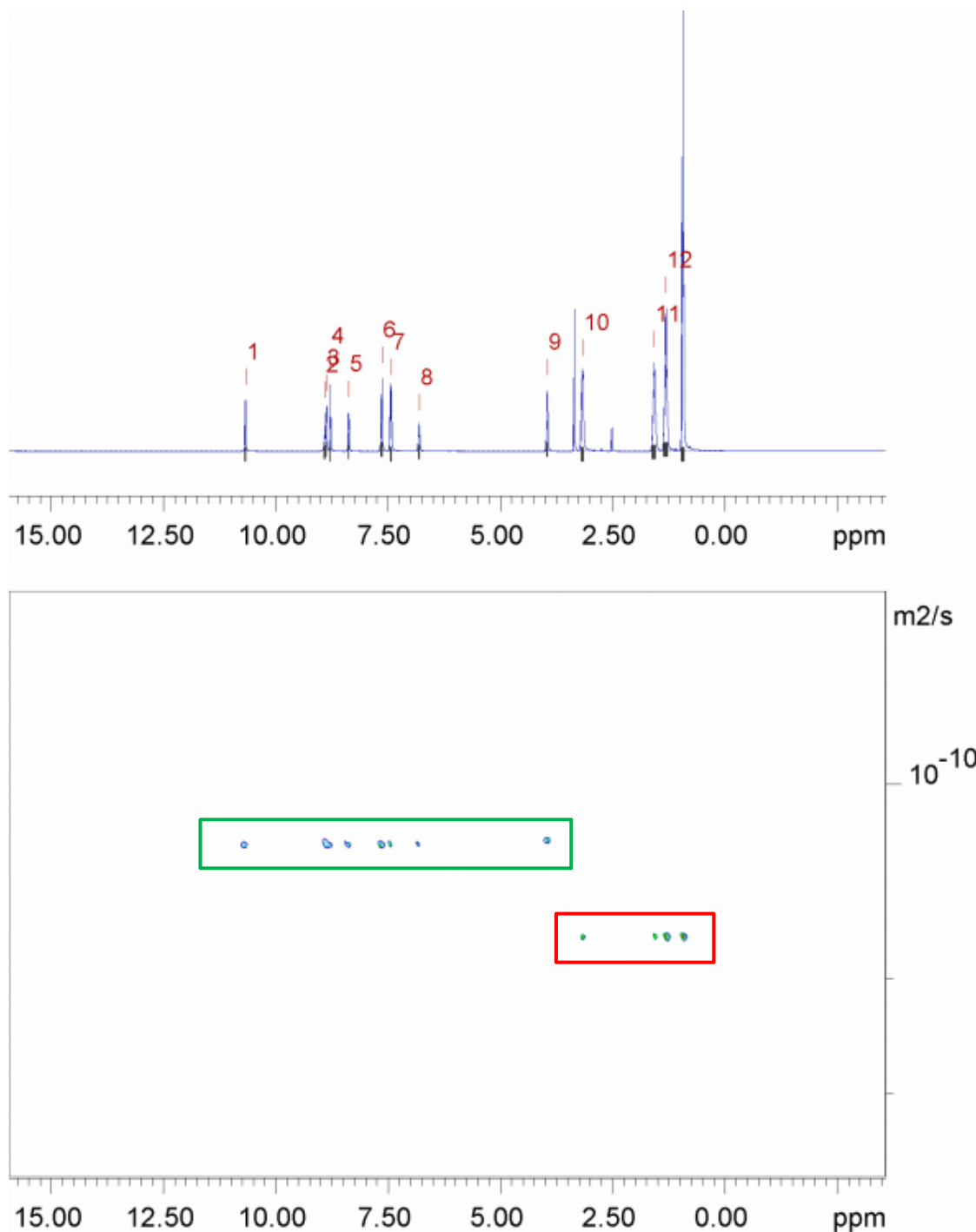


Figure S46 – ^1H DOSY NMR spectrum of compound **3** (111.12 mM) in $\text{DMSO}-d_6$ conducted at 25 $^\circ\text{C}$. Anionic component highlighted in green, TBA counter cation highlighted in red.

Table S6 – Diffusion data obtained from ^1H DOSY NMR spectrum of compound **3** (111.12 mM) in $\text{DMSO-}d_6$ conducted at 25 °C.

Peak name	F2 [ppm]	D [m ² /s]	error
1	10.670	1.23e-10	1.265e-14
2	8.906	1.23e-10	2.190e-14
3	8.871	1.23e-10	9.310e-15
4	8.777	1.23e-10	9.960e-15
5	8.371	1.23e-10	1.037e-14
6	7.634	1.23e-10	5.860e-15
7	7.429	1.24e-10	5.840e-15
8	6.804	1.23e-10	1.461e-14
9	3.948	1.23e-10	6.315e-15
10	3.166	1.71e-10	4.747e-15
11	1.569	1.71e-10	4.661e-15
12	1.309	1.71e-10	3.502e-15
13	0.931	1.71e-10	1.818e-15

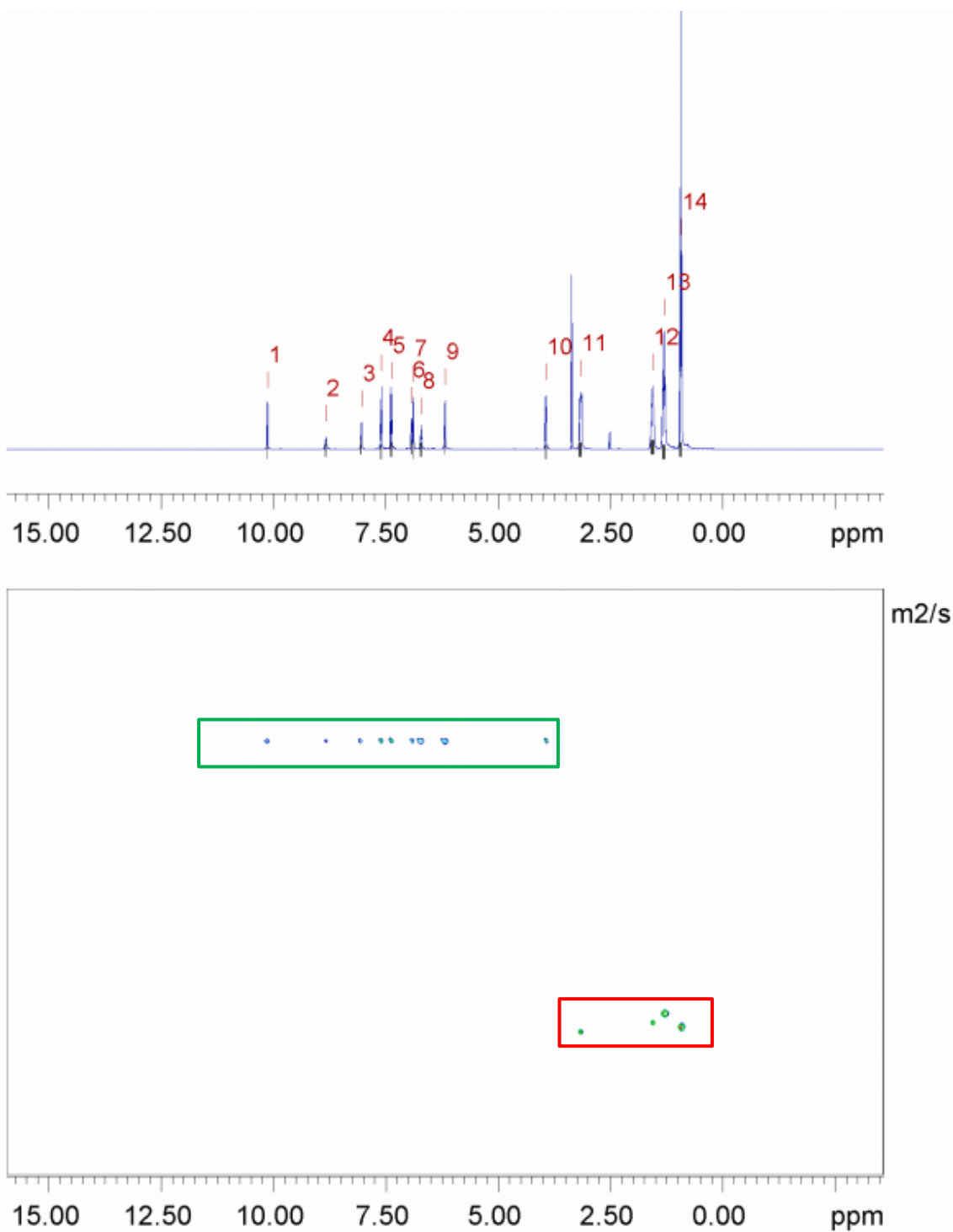


Figure S47 – ^1H DOSY NMR spectrum of compound **4** (111.12 mM) in $\text{DMSO-}d_6$ conducted at 25 °C. Anionic component highlighted in green, TBA counter cation highlighted in red.

Table S7 – Diffusion data obtained from ¹H DOSY NMR spectrum of compound **4** (111.12 mM) in DMSO-*d*₆ conducted at 25 °C.

Peak name	F2 [ppm]	D [m ² /s]	error
1	10.128	1.13e-10	9.945e-15
2	8.830	1.13e-10	2.220e-14
3	8.037	1.13e-10	1.083e-14
4	7.595	1.13e-10	5.575e-15
5	7.372	1.13e-10	5.491e-15
6	6.918	1.13e-10	9.468e-15
7	6.880	1.13e-10	8.380e-15
8	6.709	1.13e-10	1.383e-14
9	6.175	1.13e-10	7.963e-15
10	3.931	1.12e-10	5.805e-15
11	3.156	1.62e-10	5.040e-15
12	1.557	1.60e-10	4.653e-15
13	1.301	1.58e-10	3.186e-15
14	0.926	1.61e-10	1.630e-15

Table S8 – Hydrodynamic diameter, calculated from average diffusion constants for the anionic and cationic components of **3** and **4** in DMSO-*d*₆ at 25 °C.

Compound	Anion (nm)	Cation (nm)
3	1.78	1.28
4	1.94	1.37

^1H NMR self-association studies

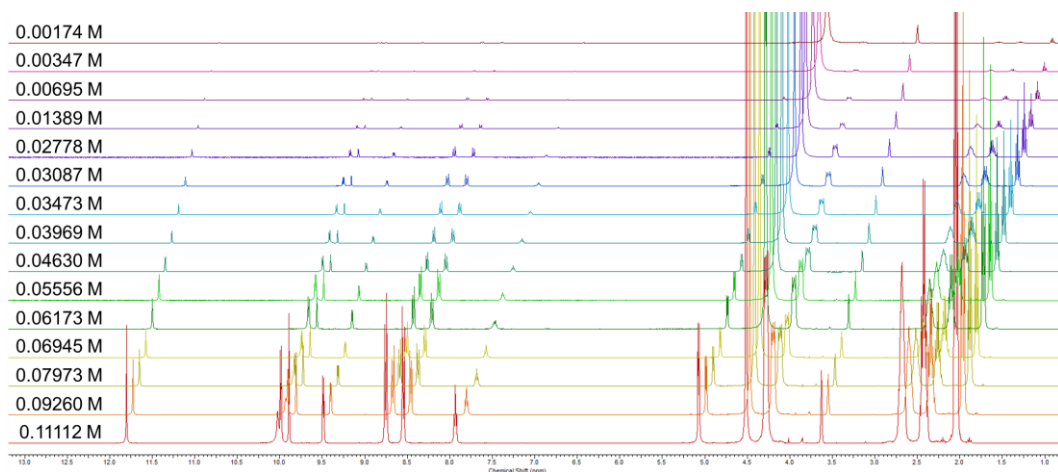


Figure S48 – ^1H NMR stack plot of compound **3** in a $\text{DMSO-}d_6$ 0.5% H_2O solution. Samples were prepared in series with an aliquot of the most concentrated solution undergoing serial dilution at 25 °C.

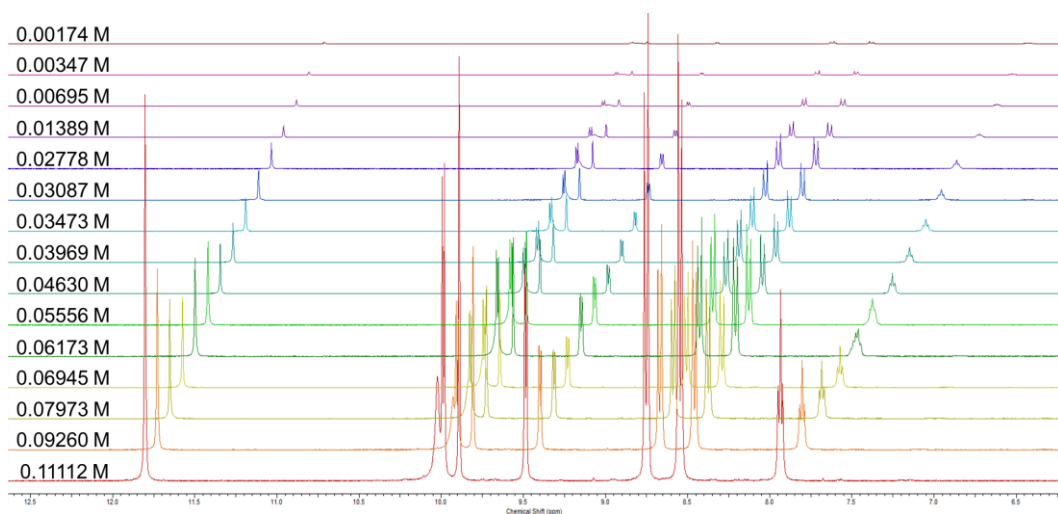


Figure S49 – Enlarged ^1H NMR stack plot of compound **3** in a $\text{DMSO-}d_6$ 0.5% H_2O solution. Samples were prepared in series with an aliquot of the most concentrated solution undergoing serial dilution at 25 °C.

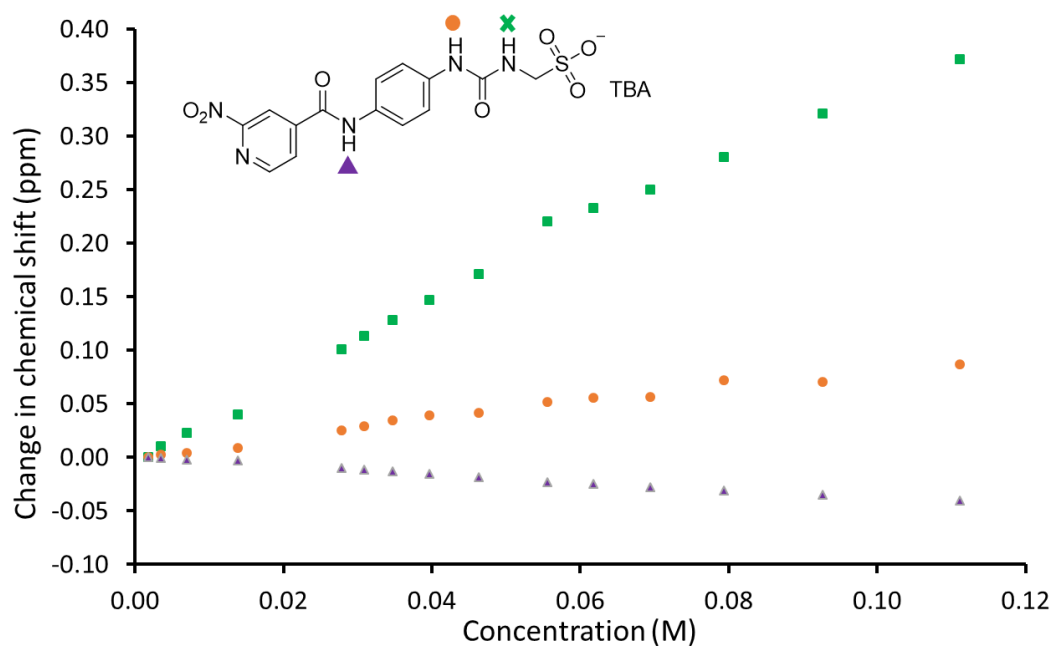


Figure S50 – Graph showing the ^1H NMR down-field change in chemical shift of NH resonances with increasing concentration of compound **3** in $\text{DMSO-}d_6$ 0.5 % H_2O (25 °C).

Self-association constant calculation

Table S9 – Self-association constants calculated from ^1H NMR dilution study data for compound **3** in $\text{DMSO-}d_6$ 0.5 % H_2O .

Values calculated from data gathered from the two urea NHs.

EK Model (M^{-1})		CoEK Model (M^{-1})		
K_e	K_{dim}	K_e	K_{dim}	ρ
1.41 ($\pm 1.5\%$)	0.71 ($\pm 0.7\%$)	10.91 ($\pm 3.4\%$)	5.45 ($\pm 1.7\%$)	0.30 ($\pm 10.0\%$)
Link for EK	http://app.supramolecular.org/bindfit/view/090bee18-4a16-4728-9d3a-565b04666500			
Link for CoEK	http://app.supramolecular.org/bindfit/view/573b0ca3-687a-437f-bff5-3ded4a748198			

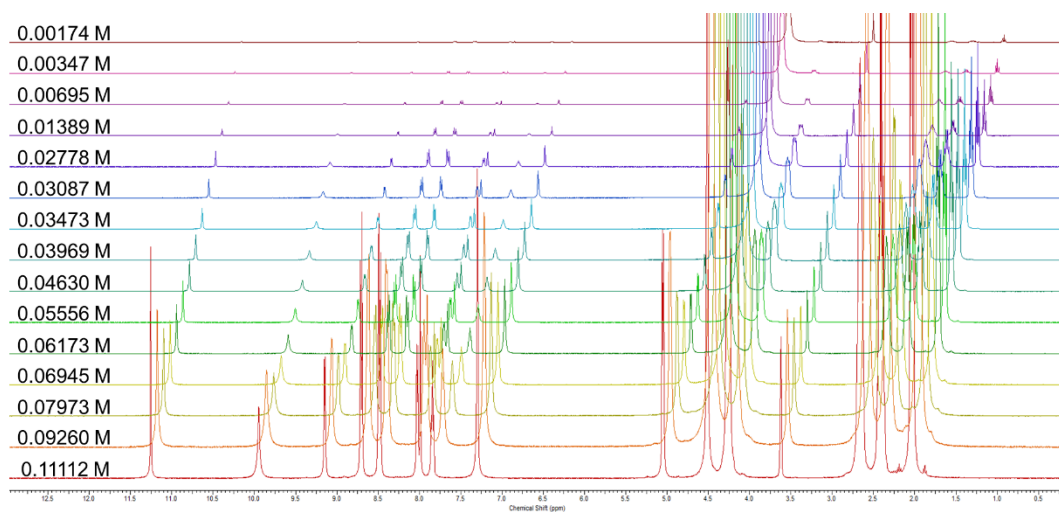


Figure S51 – ^1H NMR stack plot of compound **4** in a $\text{DMSO-}d_6$ 0.5 % H_2O solution. Samples were prepared in series with an aliquot of the most concentrated solution undergoing serial dilution.

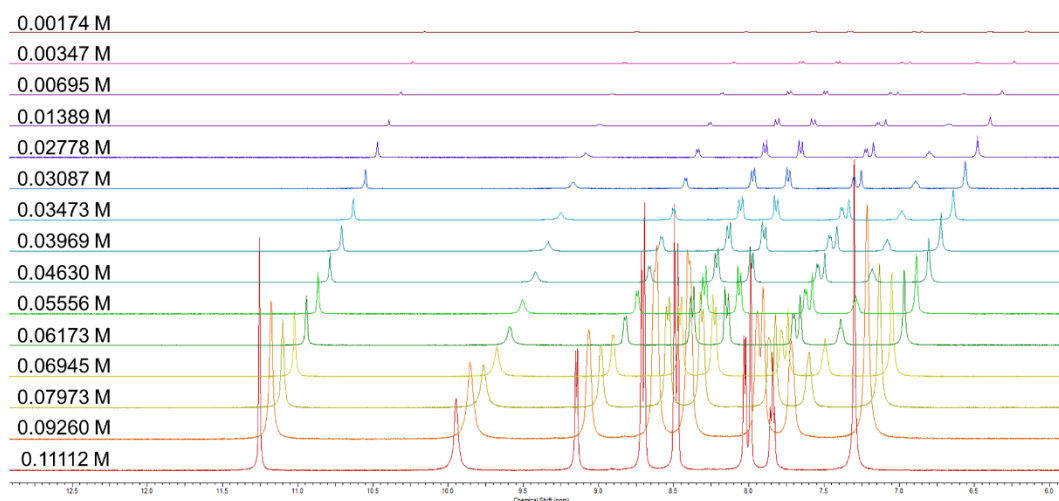


Figure S52 – Enlarged ^1H NMR stack plot of compound **4** in a $\text{DMSO-}d_6$ 0.5 % H_2O solution. Samples were prepared in series with an aliquot of the most concentrated solution undergoing serial dilution.

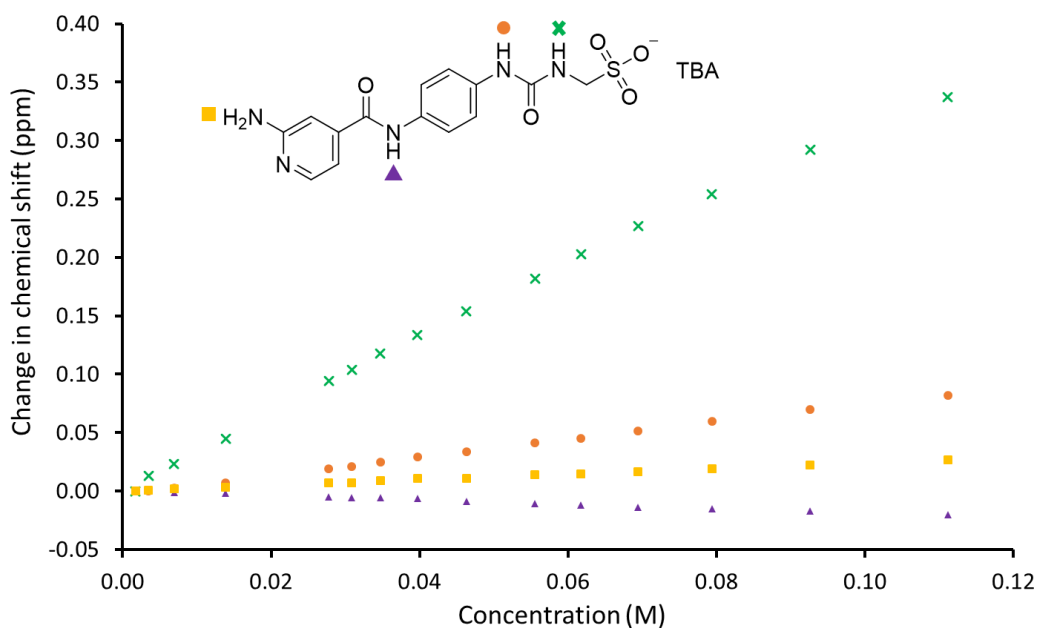


Figure S53 – Graph showing the ^1H NMR down-field change in chemical shift of NH resonances with increasing concentration of compound 4 in DMSO- d_6 0.5 % H_2O (25 °C).

Self-association constant calculation

Table S10 – Self-association constants calculated from ^1H NMR dilution study data for compound 4 in DMSO- d_6 0.5 % H_2O . Values calculated from data gathered from the two urea NHs.

EK Model (M^{-1})		CoEK Model (M^{-1})		
K_e	K_{dim}	K_e	K_{dim}	ρ
1.78 ($\pm 0.6\%$)	0.89 ($\pm 0.3\%$)	8.32 ($\pm 3.1\%$)	4.16 ($\pm 1.6\%$)	0.50 ($\pm 5.2\%$)
Link for EK	http://app.supramolecular.org/bindfit/view/005255d3-873e-49e1-b066-d6b551ddc6fd			
Link for CoEK	http://app.supramolecular.org/bindfit/view/96557a3e-c430-4e14-9bc4-11cc00d92277			

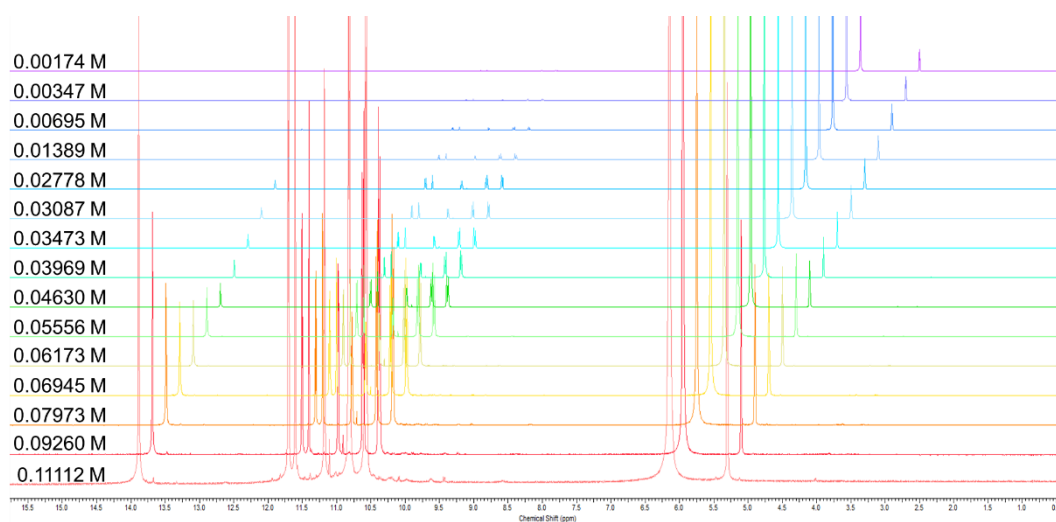


Figure S54 – ^1H NMR stack plot of compound **5** in a $\text{DMSO-}d_6$ 0.5 % H_2O solution. Samples were prepared in series with an aliquot of the most concentrated solution undergoing serial dilution.

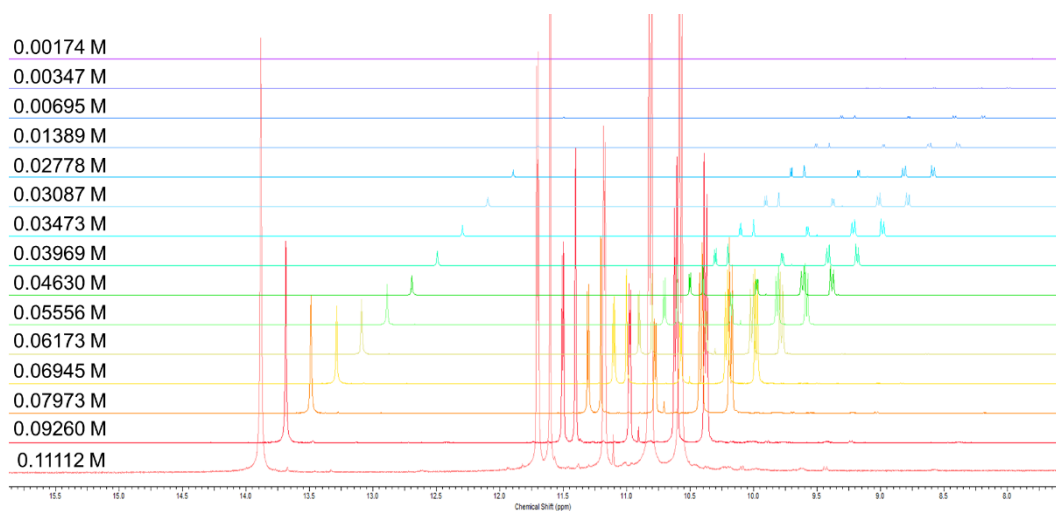


Figure S55 –Enlarged ^1H NMR stack plot of compound **5** in a $\text{DMSO-}d_6$ 0.5 % H_2O solution. Samples were prepared in series with an aliquot of the most concentrated solution undergoing serial dilution.

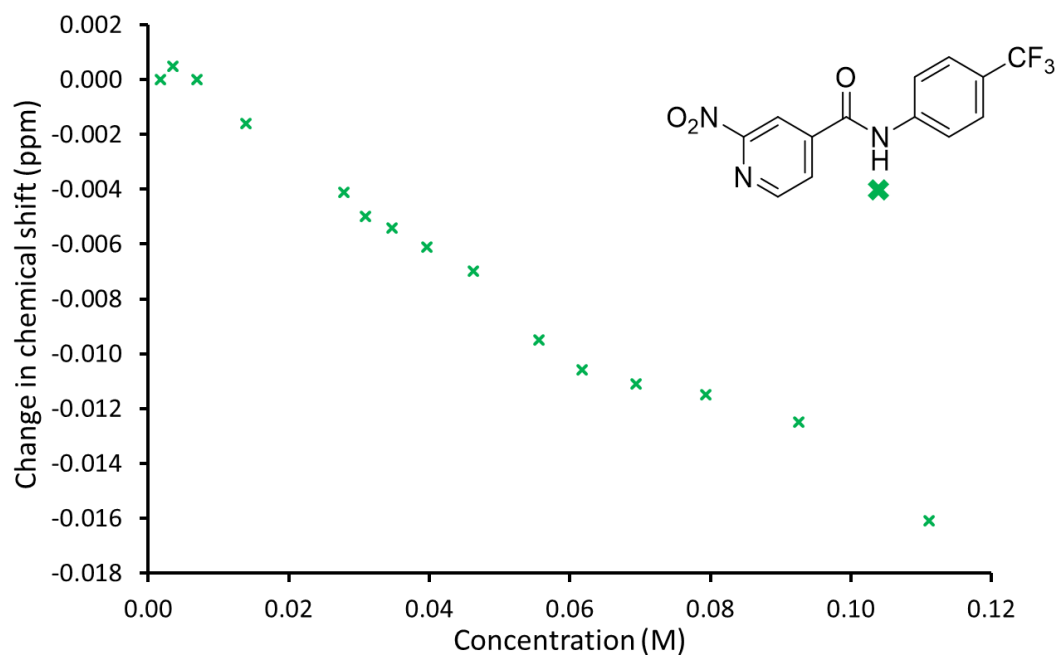


Figure S56 – Graph showing the ^1H NMR down-field change in chemical shift of NH resonances with increasing concentration of compound **5** in $\text{DMSO-}d_6$ 0.5 % H_2O (25 °C).

Self-association constant calculation

Table S11 – Self-association constants calculated from ^1H NMR dilution study data for compound **5** in $\text{DMSO-}d_6$ 0.5 % H_2O .

Values calculated from data gathered from the amide NH.

EK Model (M^{-1})		CoEK Model (M^{-1})		
K_e	K_{dim}	K_e	K_{dim}	ρ
2.27 (\pm 4.9 %)	1.13 (\pm 2.4 %)	13.68 (\pm 11.0 %)	6.84 (\pm 5.5 %)	0.29 (\pm 38.3 %)
Link for EK	http://app.supramolecular.org/bindfit/view/7867a53f-bd11-4638-9ee1-7c8e9cf91ea4			
Link for CoEK	http://app.supramolecular.org/bindfit/view/f9ad1bb2-9aa3-4018-a401-11bf1606ab34			

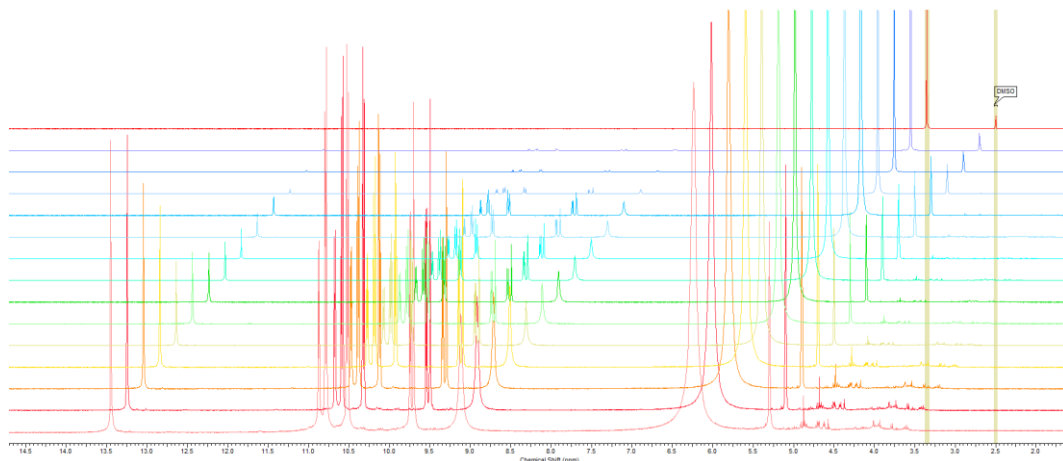


Figure S57 – ^1H NMR stack plot of compound **6** in a $\text{DMSO-}d_6$ 0.5 % H_2O solution. Samples were prepared in series with an aliquot of the most concentrated solution undergoing serial dilution from 0.1112 M to 0.00174 M.

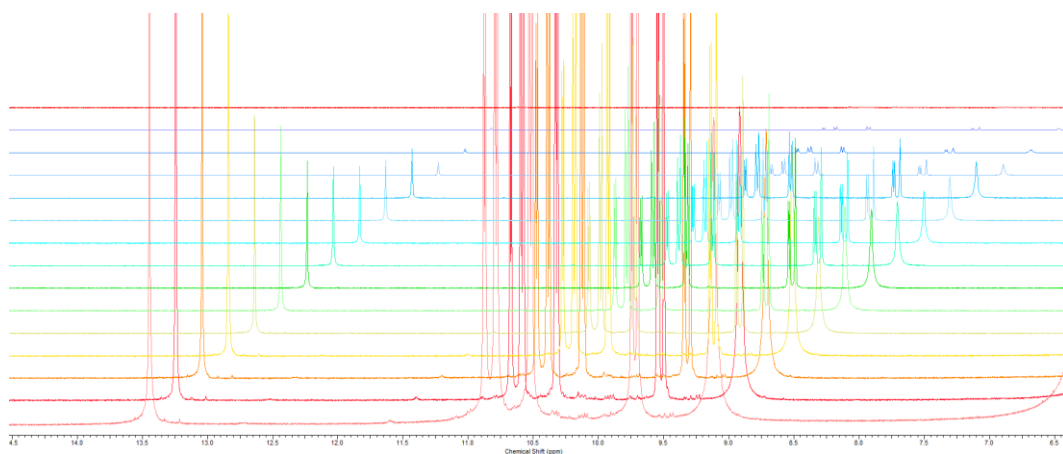


Figure S58 – Enlarged ^1H NMR stack plot of compound **6** in a $\text{DMSO-}d_6$ 0.5 % H_2O solution. Samples were prepared in series with an aliquot of the most concentrated solution undergoing serial dilution from 0.1112 M to 0.00174 M.

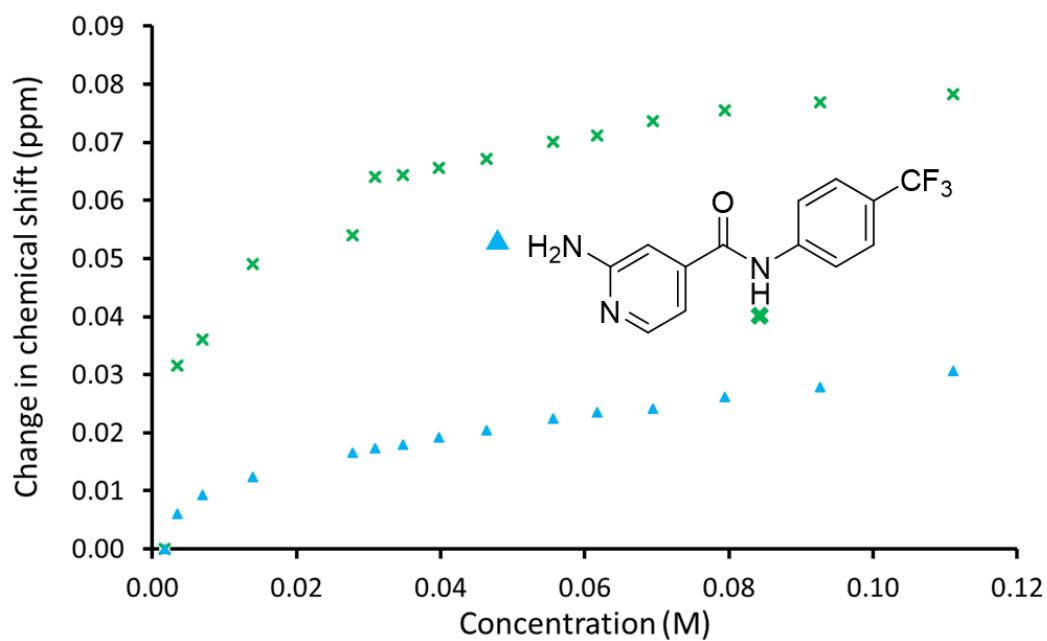


Figure S59 – Graph showing the ^1H NMR down-field change in chemical shift of NH resonances with increasing concentration of compound **6** in $\text{DMSO-}d_6$ 0.5 % H_2O (25 °C).

Table S12 – Self-association constants calculated from ¹H NMR dilution study data for compound 6 in DMSO-*d*₆ 0.5 % H₂O.

NH group	EK Model (M ⁻¹)		CoEK Model (M ⁻¹)		
	K _e	K _{dim}	K _e	K _{dim}	ρ
All NH's	356.59 (± 11.7 %)	178.30 (± 5.8 %)	675.15 (± 18.3 %)	337.58 (± 9.2 %)	2.69 (± 30.5 %)
Amine NH	515.43 (± 3.9 %)	257.72 (± 1.9 %)	1715.66 (± 8.9 %)	857.83 (± 4.4 %)	1.99 (± 13.4 %)
Amide NH	20.97 (± 9.8 %)	10.49 (± 4.9 %)	9.80 (± 30.2 %)	4.90 (± 15.1 %)	2.08 (± 57.6 %)
Link for EK	http://app.supramolecular.org/bindfit/view/7867a53f-bd11-4638-9ee1-7c8e9cf91ea4				
Link for CoEK	http://app.supramolecular.org/bindfit/view/f9ad1bb2-9aa3-4018-a401-11bf1606ab34				

^1H NMR titration study data

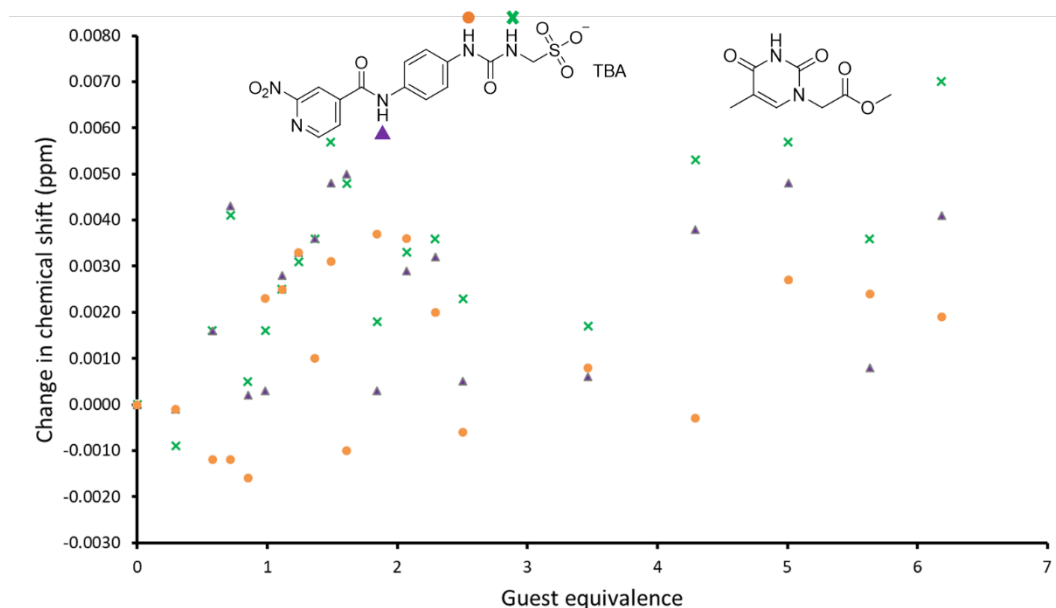


Figure S60 – A graph showing the downfield ^1H NMR change in chemical shift for the NHs of compound 3 (host) with increasing the concentration of compound 7 (guest) in a $\text{DMSO}-d_6 - 0.5\% \text{H}_2\text{O}$ solution (25°C).

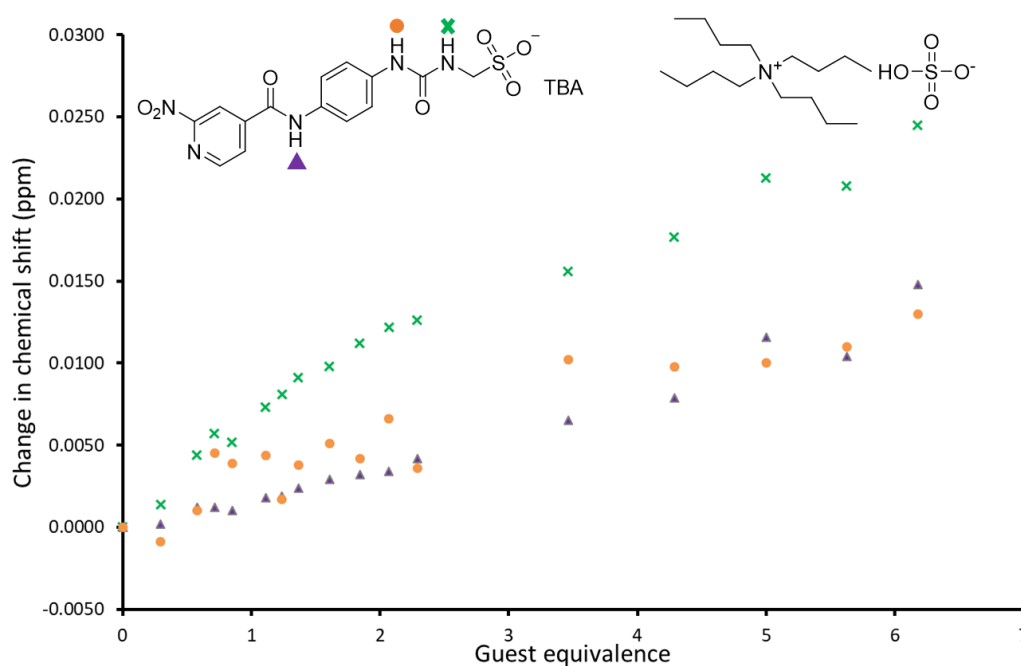


Figure S61 – A graph showing the downfield ^1H NMR change in chemical shift for the NHs of compound 3 (host) with increasing the concentration of $\text{TBA}\cdot\text{HSO}_4$ (guest) in a $\text{DMSO}-d_6 - 0.5\% \text{H}_2\text{O}$ solution (25°C).

Table S13 – Association constants (M^{-1}) calculated for compound **3** (host) titrated against TBA•HSO₄ (guest) in a DMSO-*d*₆ – 0.5% H₂O solution (25 °C) – Figure S61.

Host: Guest	1: 1		1: 2		2: 1	
NH	K	K ₁₁	K ₁₂	K ₁₁	K ₂₁	
Cross	23.16 (± 6.3 %)	28.33 (± 4.3 %)	<i>a</i>	<i>b</i>	<i>b</i>	
Link to 1:1	http://app.supramolecular.org/bindfit/view/37658304-d8b5-4cb6-9e10-31755a2ab682					
Link to 1:2	http://app.supramolecular.org/bindfit/view/43718c5b-d1f7-430a-b989-46e760f9ece6					
Link to 2:1	N/A					
Circle	15.52 (± 16.2 %)	7011.20 (± 1295 %)	4.30 (± 24.0 %)	<i>c</i>	<i>d</i>	
Link to 1:1	http://app.supramolecular.org/bindfit/view/983eb7f1-5228-4152-8d29-f9f713ce34e7					
Link to 1:2	http://app.supramolecular.org/bindfit/view/8aa46054-3bfb-4e2f-8e8f-bc37400edae1					
Link to 2:1	http://app.supramolecular.org/bindfit/view/0cc717bd-4dbc-477b-92c8-7bb36e5d893e					
Triangle	<i>b</i>	<i>c</i>	<i>d</i>	<i>a</i>	155.36 (± 4.6 %)	
Link to 1:1	N/A					
Link to 1:2	http://app.supramolecular.org/bindfit/view/9f73dc58-f2ca-4fc8-8687-26ad227197ab					
Link to 2:1	http://app.supramolecular.org/bindfit/view/15907068-693a-4b98-a7ed-a27e5f087c10					

a – negative association constant calculated. *b* – data could not be fitted. *c* – association constant < 0.1 M⁻¹. *d* – association constant > 1 x 10⁴ M⁻¹.

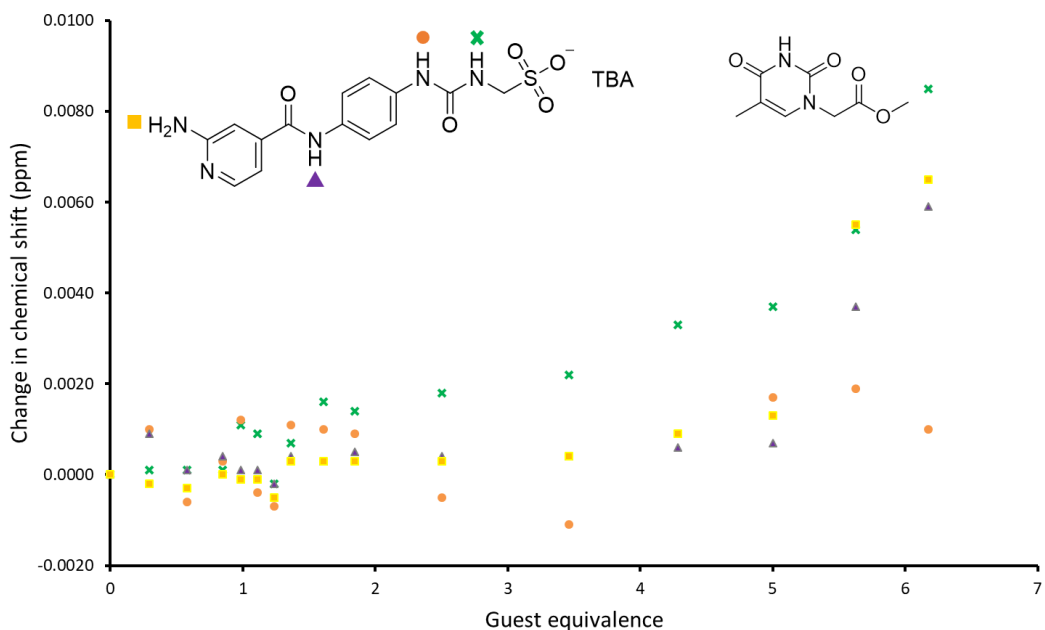


Figure S62 – A graph showing the downfield ¹H NMR change in chemical shift for the NHs of compound 4 (host) with increasing the concentration of compound 7 (guest) in a DMSO-*d*₆ – 0.5% H₂O solution (25 °C).

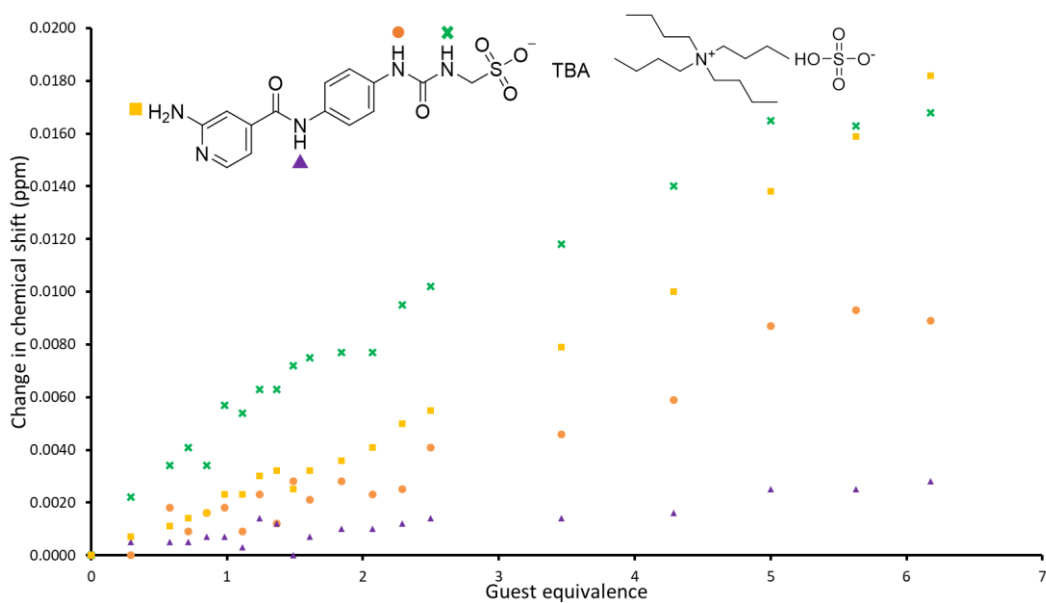


Figure S63 – A graph showing the downfield ¹H NMR change in chemical shift for the NHs of compound 5 (host) with increasing the concentration of TBA•HSO₄ (guest) in a DMSO-*d*₆ – 0.5% H₂O solution (25 °C).

Table S14 – Association constants (M^{-1}) calculated for the NH's in compound **4** (host) titrated against TBA•HSO₄ (guest) in a DMSO-*d*₆ – 0.5% H₂O solution (25 °C).

Host: Guest	1: 1	1: 2		2: 1	
NH	K	K ₁₁	K ₁₂	K ₁₁	K ₂₁
Cross	26.04 (± 4.9 %)	717.09 (± 52.7 %)	7.93 (± 8.3 %)	<i>a</i>	<i>b</i>
Link to 1:1	http://app.supramolecular.org/bindfit/view/ea74b735-8d07-406a-bdf1-d61778639ac7				
Link to 1:2	http://app.supramolecular.org/bindfit/view/bdc87a62-a031-4a3c-aa79-4356d41bb020				
Link to 2:1	http://app.supramolecular.org/bindfit/view/8ca06bd8-5fb3-408c-81ba-b06a4f64f2c5				
Square	<i>a</i>	<i>c</i>	<i>b</i>	<i>c</i>	<i>b</i>
Link to 1:1	http://app.supramolecular.org/bindfit/view/40307ed4-40cd-455d-a4ce-514d6a14cc6a				
Link to 1:2	http://app.supramolecular.org/bindfit/view/60a474da-34c2-4e89-91d5-a6b12757f215				
Link to 2:1	http://app.supramolecular.org/bindfit/view/9ec95d55-2903-4fc0-9806-1362bbb14d6				

a – association constant < 0.1 M⁻¹. *b* – association constant > 1 x 10⁴ M⁻¹. *c* – negative association constant calculated.

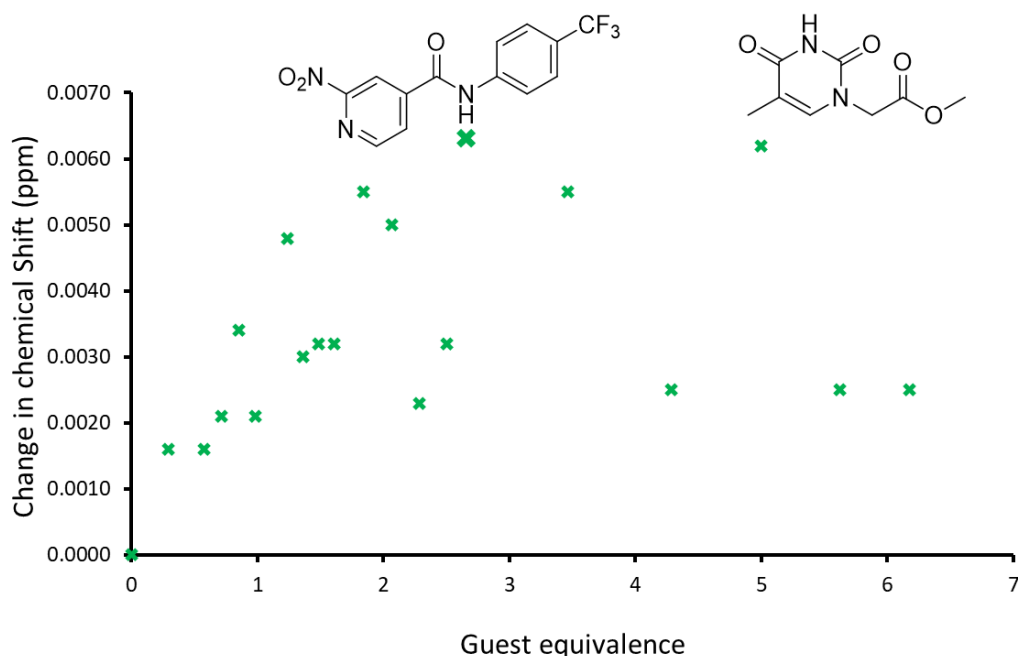


Figure S64 – A graph showing the downfield ¹H NMR change in chemical shift for the NHs of compound **5** (host) with increasing the concentration of compound **7** (guest) in a DMSO-*d*₆ – 0.5% H₂O solution (25 °C).

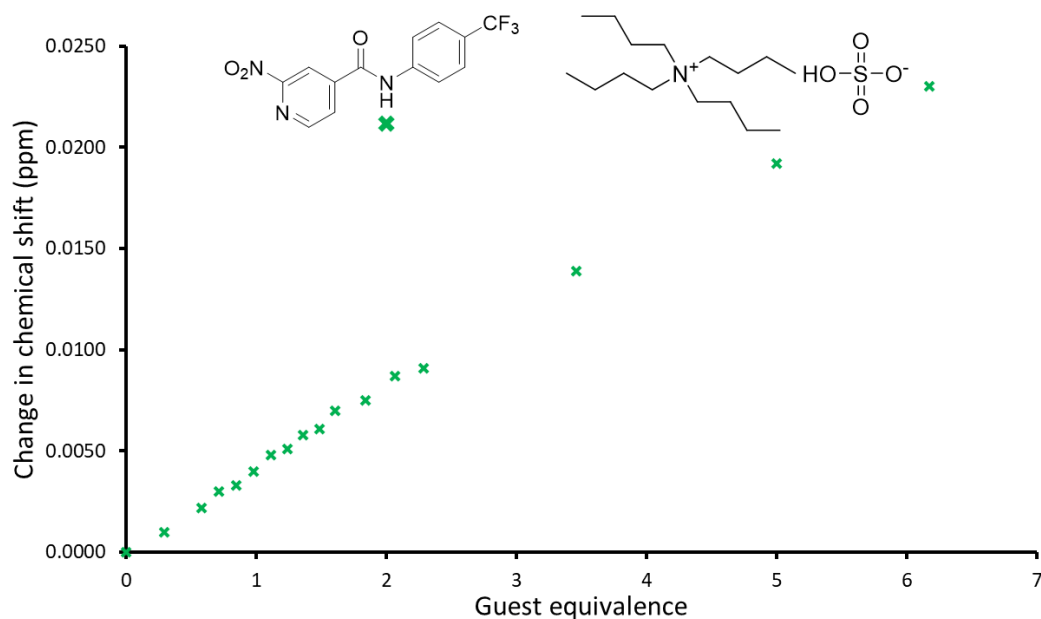


Figure S65 – A graph showing the downfield ^1H NMR change in chemical shift for the NHs of compound **5** (host) with increasing the concentration of TBA•HSO₄ (guest) in a DMSO-*d*₆ – 0.5% H₂O solution (25 °C).

Table S15 – Association constants (M^{-1}) calculated for the amide NH in compound **5** (host) titrated against TBA•HSO₄ (guest) in a DMSO-*d*₆ – 0.5% H₂O solution (25 °C).

Host: Guest	1: 1	1: 2		2: 1	
NH	K	K ₁₁	K ₁₂	K ₁₁	K ₂₁
Cross	3.35 (± 1.1 %)	<i>a</i>	3.49 (± 1.8 %)	<i>b</i>	<i>b</i>
Link to 1:1	http://app.supramolecular.org/bindfit/view/f66937c8-9eab-4632-a8ff-b4085f79f1fc				
Link to 1:2	http://app.supramolecular.org/bindfit/view/0c7d2b13-9028-4787-a84c-f145c7f474d3				
Link to 2:1	http://app.supramolecular.org/bindfit/view/06b6b7a0-a00e-417f-bcf3-c8dec846d20d				

a – association constant > $1 \times 10^4 \text{ M}^{-1}$ *b* – negative association constant calculated.

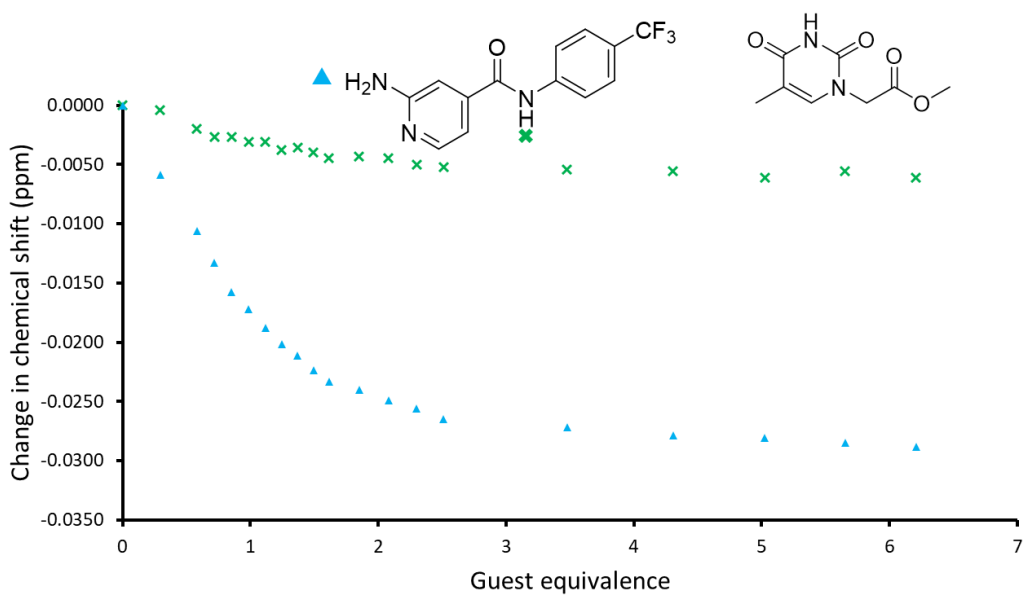


Figure S66 – A graph showing the downfield ^1H NMR change in chemical shift for the NHs of compound **6** (host) with increasing the concentration of compound **7** (guest) in a $\text{DMSO-}d_6$ – 0.5% H_2O solution (25 °C).

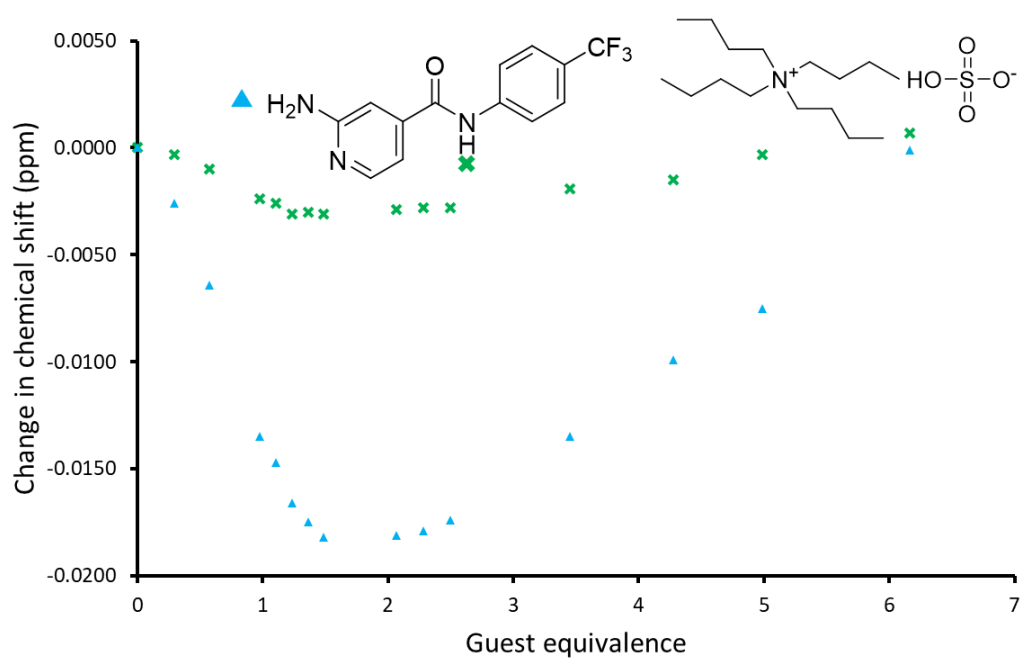


Figure S67 – A graph showing the downfield ^1H NMR change in chemical shift for the NHs of compound **6** (host) with increasing the concentration of $\text{TBA}\cdot\text{HSO}_4$ (guest) in a $\text{DMSO-}d_6$ – 0.5% H_2O solution (25 °C).

DLS data

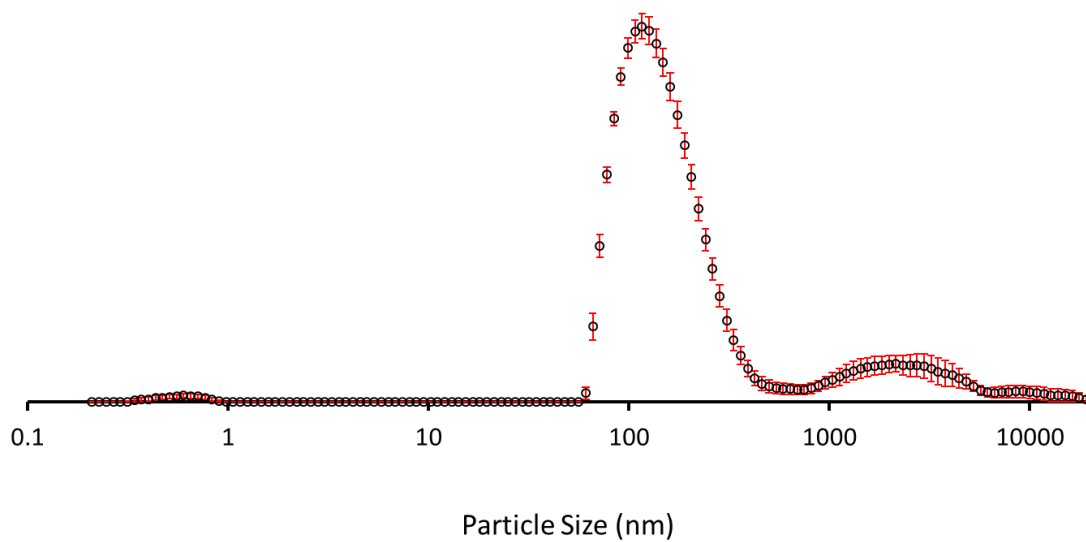


Figure S68 – Average intensity particle size distribution, calculated from 9 DLS runs, of aggregates formed by compound **2** at a concentration of 3.00 mM in a solution of EtOH: H₂O 1:19, after heating to 40 °C and cooling to 25 °C.

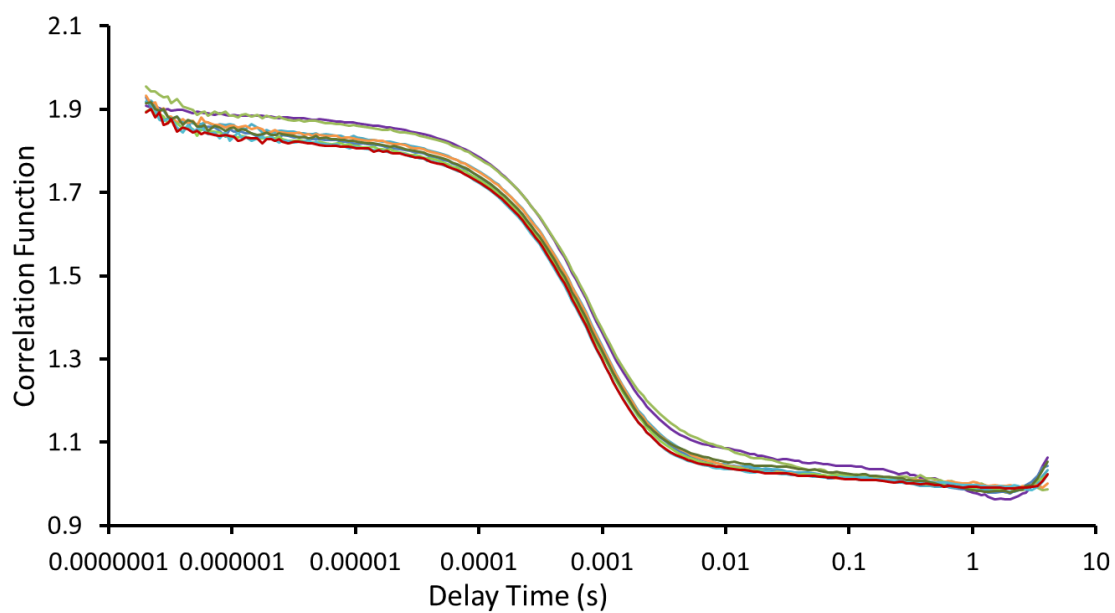


Figure S69 – Correlation function data for 9 DLS runs of compound **2** at a concentration of 3.00 mM in a solution of EtOH: H₂O 1:19, after heating to 40 °C and cooling to 25 °C.

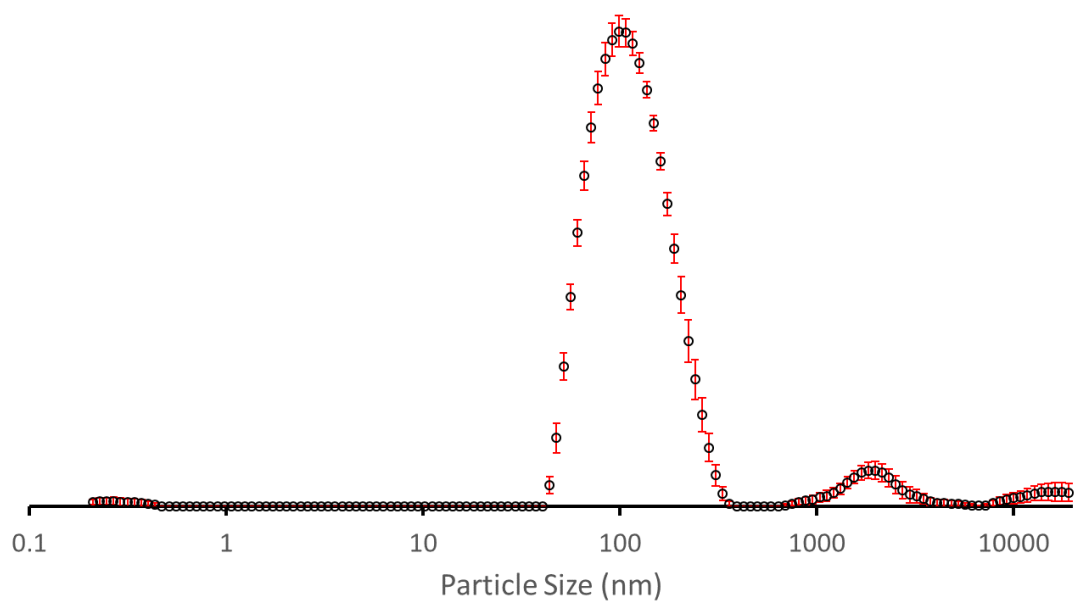


Figure S70 – Average intensity particle size distribution, calculated from 10 DLS runs, of aggregates formed by compound **2** at a concentration of 0.30 mM in a solution of EtOH: H₂O 1:19, after heating to 40 °C and cooling to 25 °C.

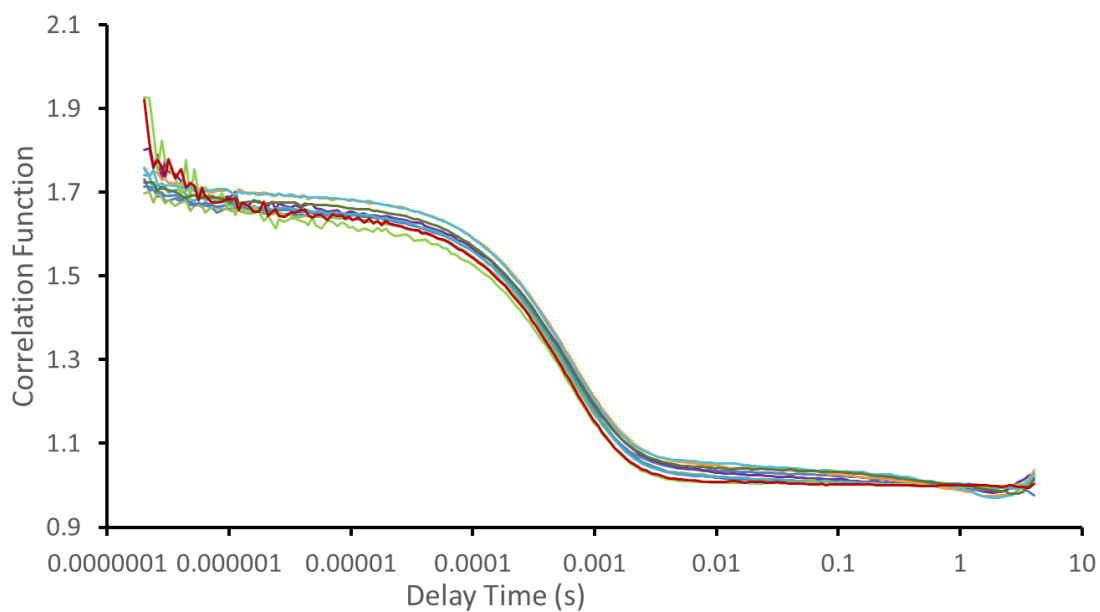


Figure S71 – Correlation function data for 10 DLS runs of compound **2** at a concentration of 0.30 mM in a solution of EtOH: H₂O 1:19, after heating to 40 °C and cooling to 25 °C.

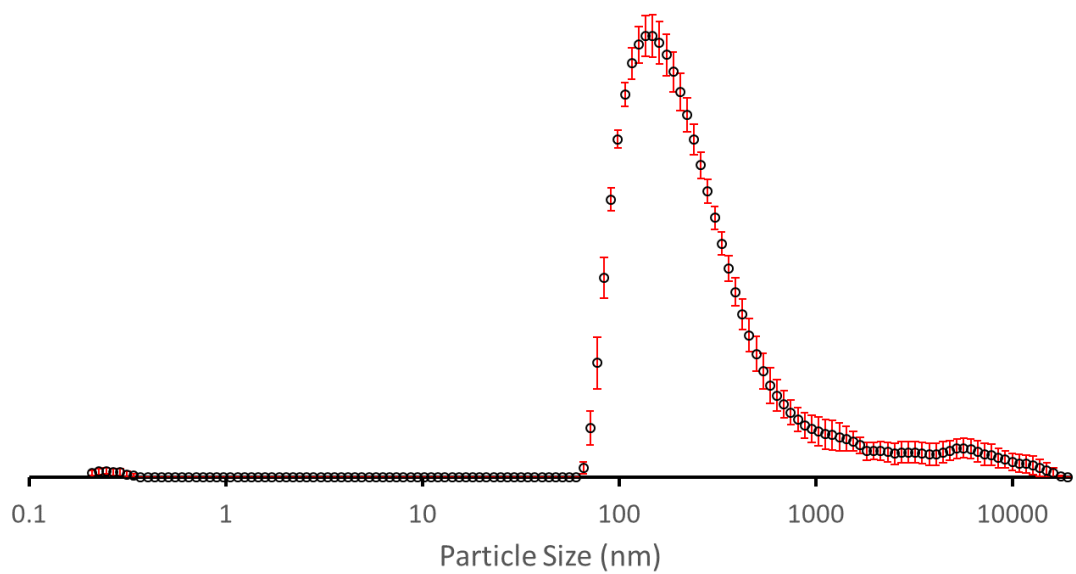


Figure 72 – Average intensity particle size distribution, calculated from 10 DLS runs, of aggregates formed by compound **3** at a concentration of 3.00 mM in a solution of EtOH: H₂O 1:19, after heating to 40 °C and cooling to 25 °C.

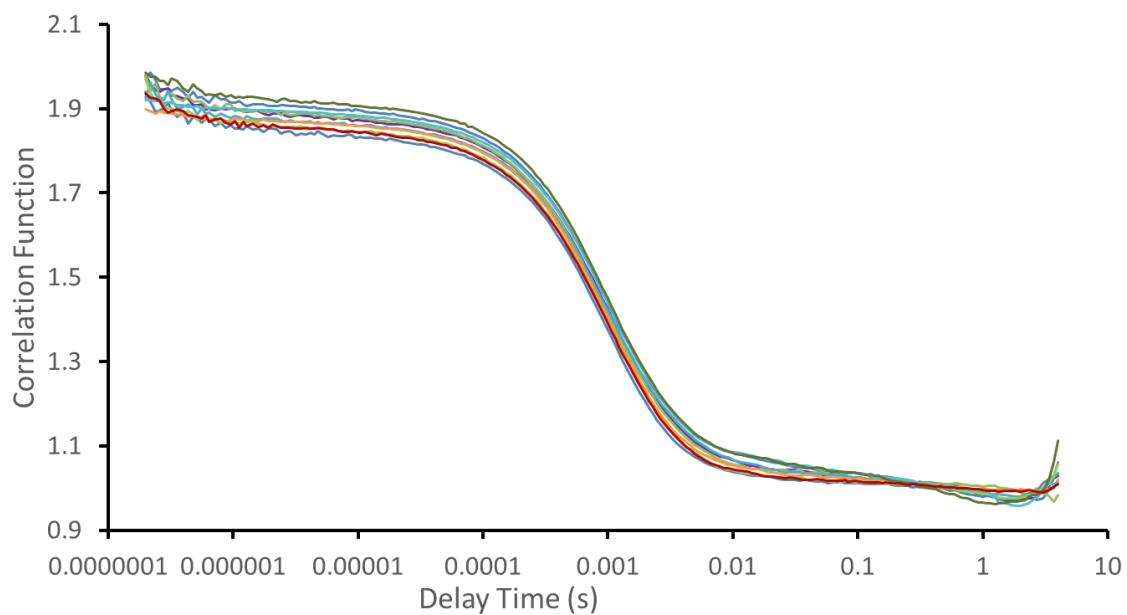


Figure S73 – Correlation function data for 10 DLS runs of compound **3** at a concentration of 3.00 mM in a solution of EtOH: H₂O 1:19, after heating to 40 °C and cooling to 25 °C.

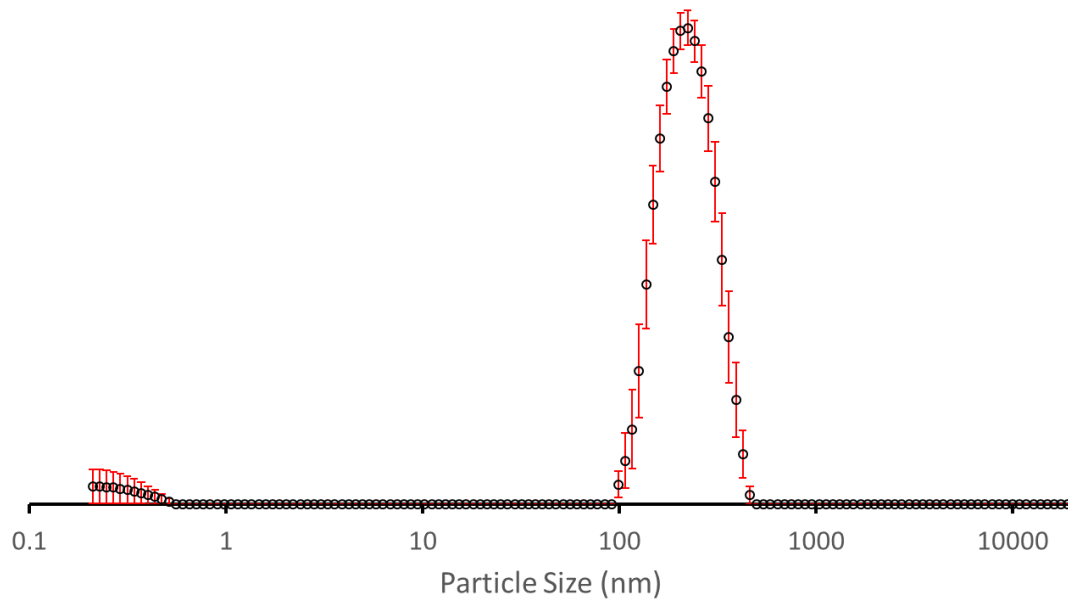


Figure S74 – Average intensity particle size distribution, calculated from 10 DLS runs, of aggregates formed by compound **3** at a concentration of 0.30 mM in a solution of EtOH: H₂O 1:19, after heating to 40 °C and cooling to 25 °C.

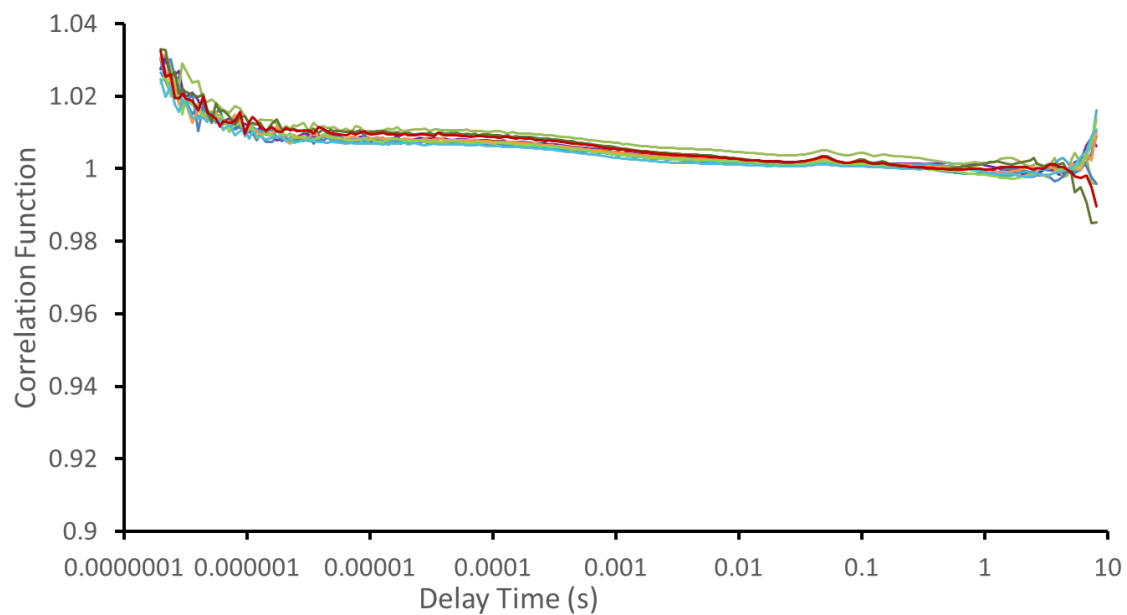


Figure S75 – Correlation function data for 10 DLS runs of compounds **3** at a concentration of 0.30 mM in a solution of EtOH: H₂O 1:19, after heating to 40 °C and cooling to 25 °C.

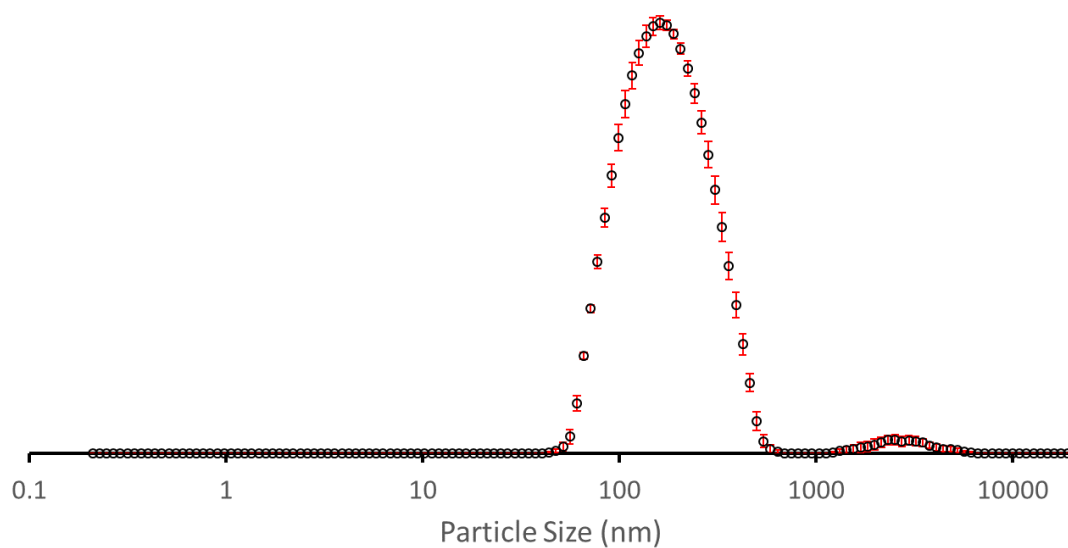


Figure S76 – Average intensity particle size distribution, calculated from 10 DLS runs, of aggregates formed by compound **4** at a concentration of 3.00 mM in a solution of EtOH: H₂O 1:19, after heating to 40 °C and cooling to 25 °C.

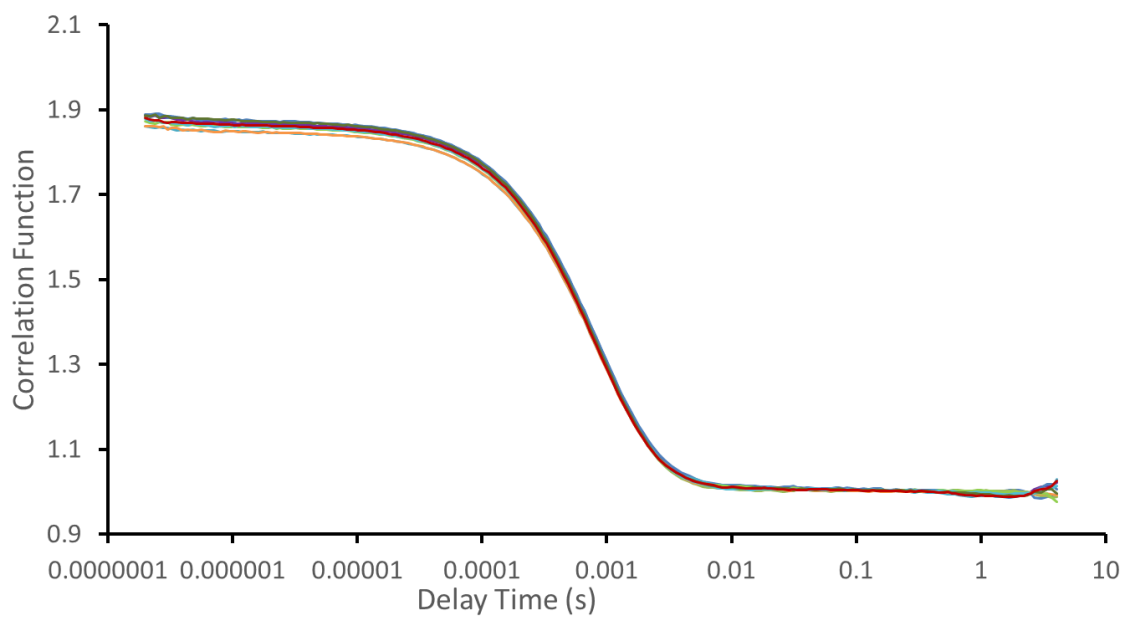


Figure S77 – Correlation function data for 10 DLS runs of compounds **4** at a concentration of 3.00 mM in a solution of EtOH: H₂O 1:19, after heating to 40 °C and cooling to 25 °C.

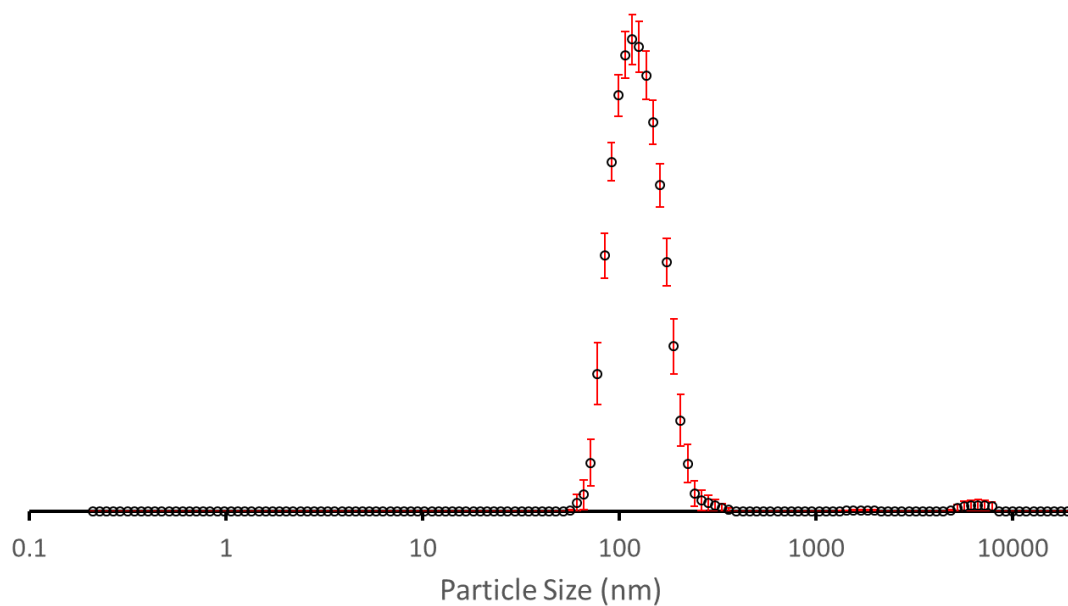


Figure S78 – Average intensity particle size distribution, calculated from 10 DLS runs, of aggregates formed by compound **4** at a concentration of 0.30 mM in a solution of EtOH: H₂O 1:19, after heating to 40 °C and cooling to 25 °C.

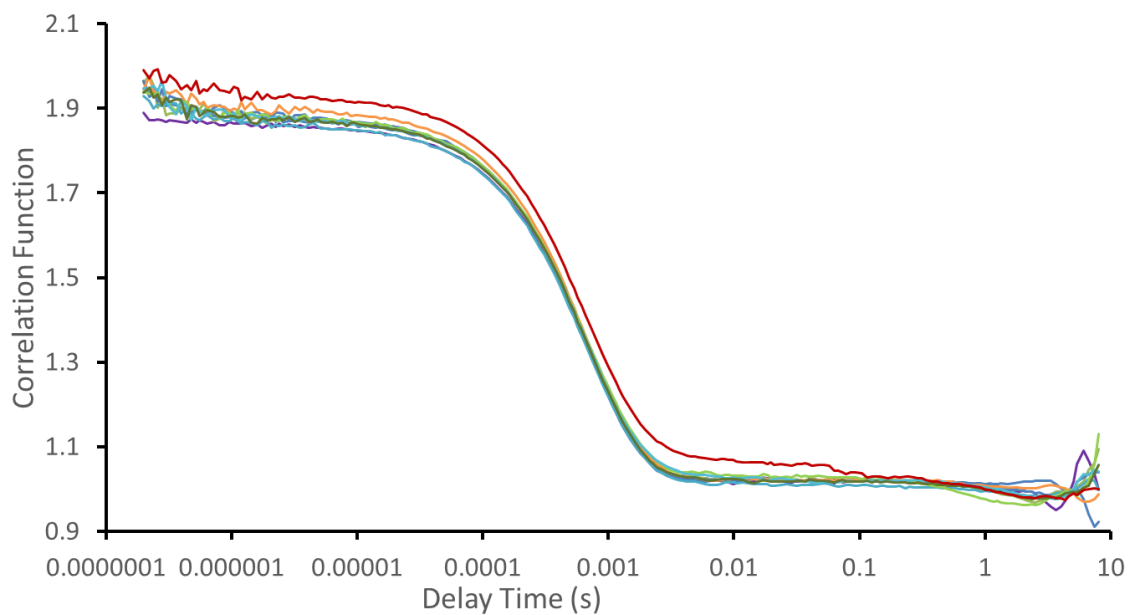


Figure S79 – Correlation function data for 10 DLS runs of compound **4** at a concentration of 0.30 mM in a solution of EtOH: H₂O 1:19, after heating to 40 °C and cooling to 25 °C.

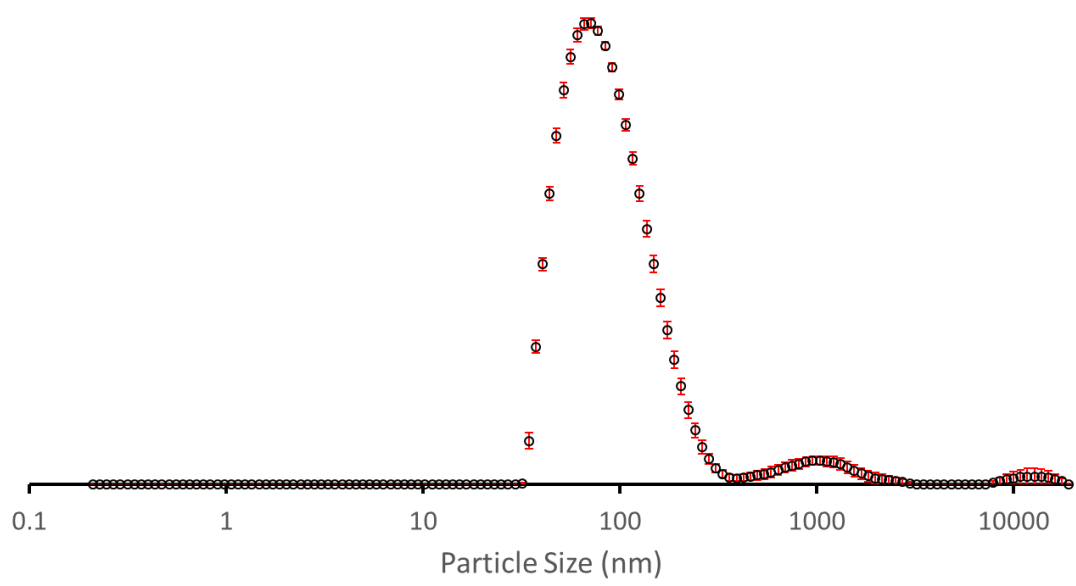


Figure S80 – Average intensity particle size distribution, calculated from 8 DLS runs, of aggregates formed by compounds **2** (1.50 mM) and **4** (1.50 mM) in a solution of EtOH: H₂O 1:19, after heating to 40 °C and cooling to 25 °C.

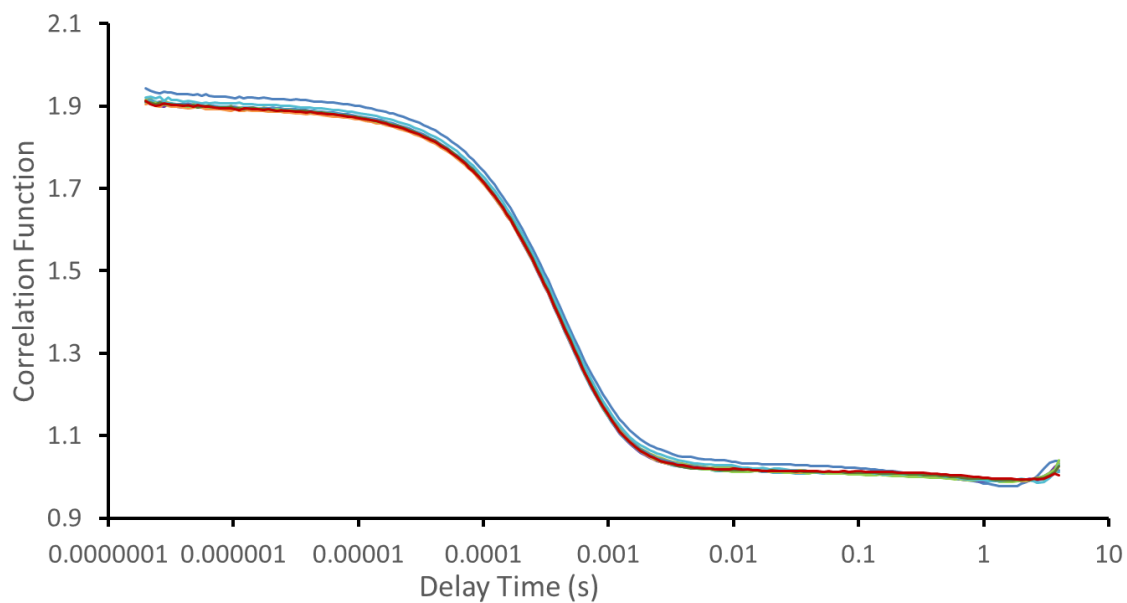


Figure S81 – Correlation function data for 10 DLS runs of a mixture of c compounds **2** (1.50 mM) and **4** (1.50 mM) in a solution of EtOH: H₂O 1:19, after heating to 40 °C and cooling to 25 °C

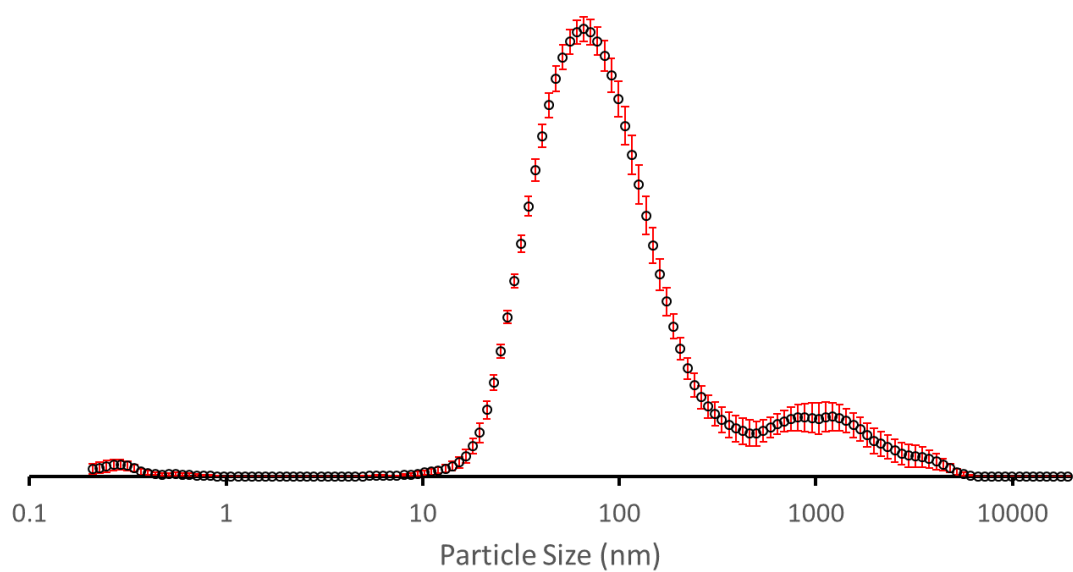


Figure S82 – Average intensity particle size distribution, calculated from 10 DLS runs, of aggregates formed by compounds **2** (0.15 mM) and **4** (0.15 mM) in a solution of EtOH: H₂O 1:19, after heating to 40 °C and cooling to 25 °C.

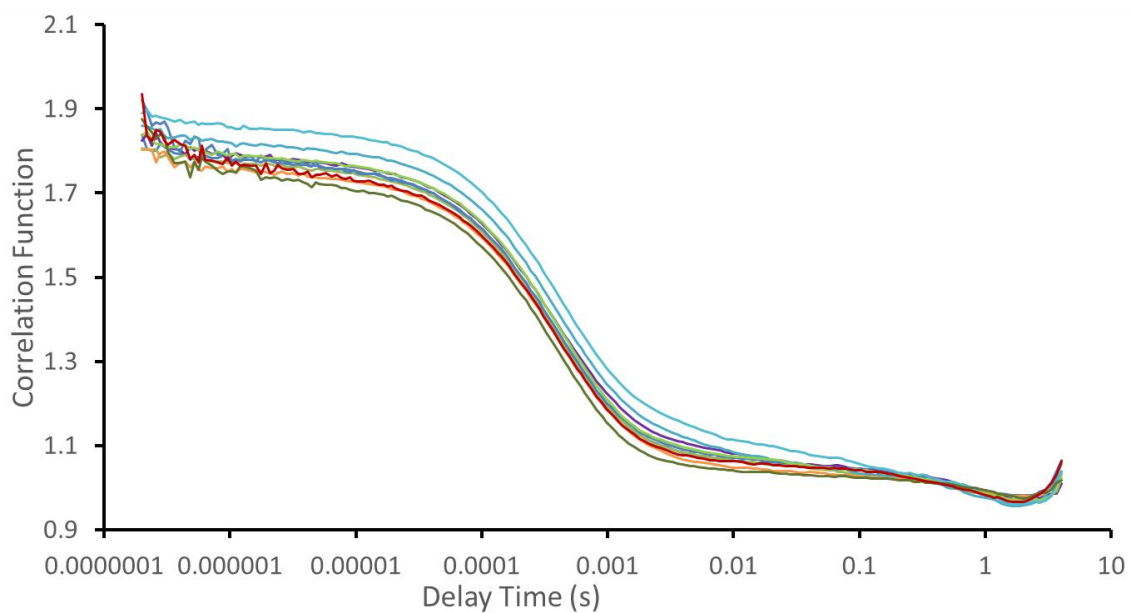


Figure S83 – Correlation function data for 10 DLS runs of a mixture of compounds **2** (1.50 mM) and **4** (1.50 mM) in a solution of EtOH: H₂O 1:19, after heating to 40 °C and cooling to 25 °C

Table S16 – Average intensity particle size distribution for compounds **2** - **4** and a mixture of compounds **2** and **4** in a 1:1 molar equivalence, calculated from 10 DLS runs at 3.00 mM and 0.30 mM. Samples were prepared in series, with an aliquot of the most concentrated solution undergoing serial dilution and measured after heating to 40 °C and cooling to 25 °C.

Compound	Peak maxima (nm)		PDI (%)	
	3 mM	0.3 mM	3 mM	0.3 mM
2	147.23 (\pm 7.4)	126.23 (\pm 2.85)	25.02 (\pm 0.7)	21.79 (\pm 0.3)
3	230.97 (\pm 12.81)	222.45 (\pm 9.70)	26.13 (\pm 0.78)	96.25 (\pm 3.23)
4	189.30 (\pm 2.96)	128.41 (\pm 2.66)	23.56 (\pm 0.41)	14.20 (\pm 2.52)
2 and 4	94.47 (\pm 2.0)	88.61 (\pm 3.9)	24.69 (\pm 0.4)	25.68 (\pm 0.8)

Zeta potential data

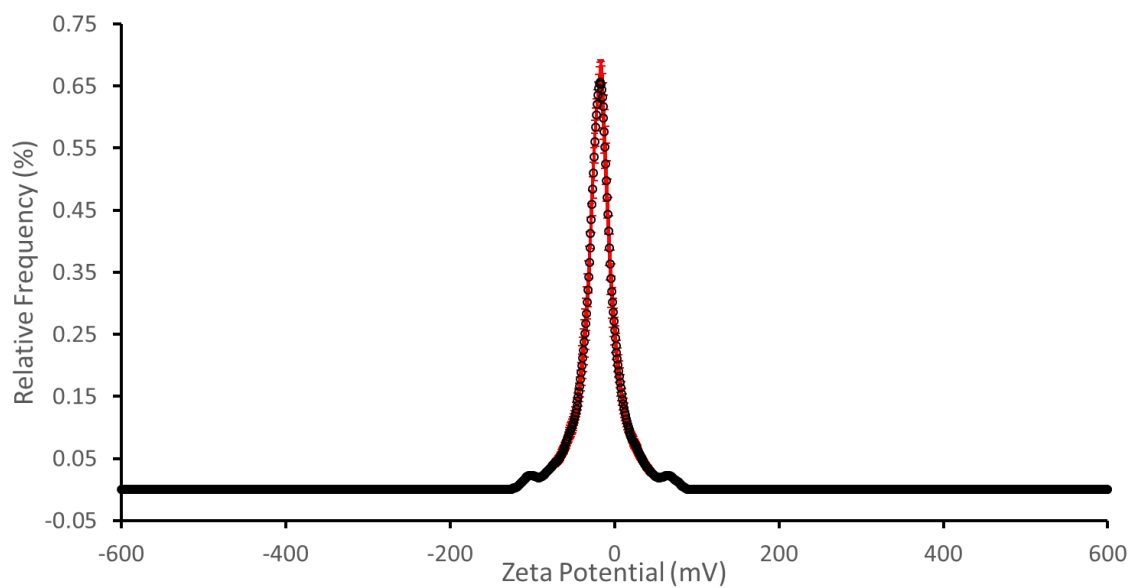


Figure S84 – The average zeta potential distribution calculated using 10 runs of compound **2** (3.00 mM) in an EtOH: H₂O (1:19) solution at 25 °C.

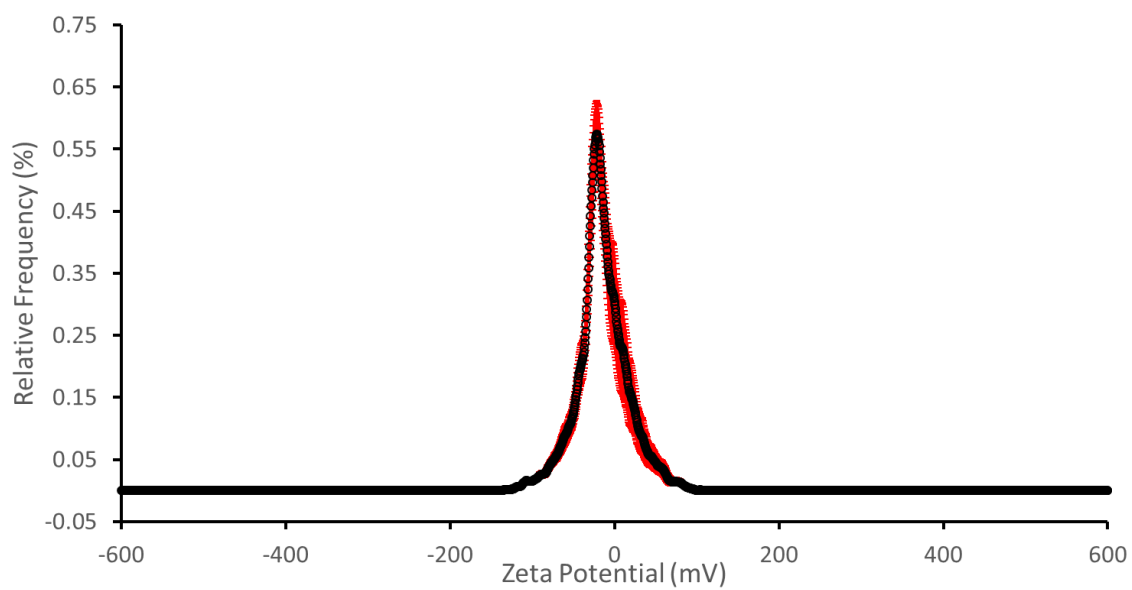


Figure S85 – The average zeta potential distribution calculated using 10 runs of compound **3** (3.00 mM) in an EtOH: H₂O (1:19) solution at 25 °C.

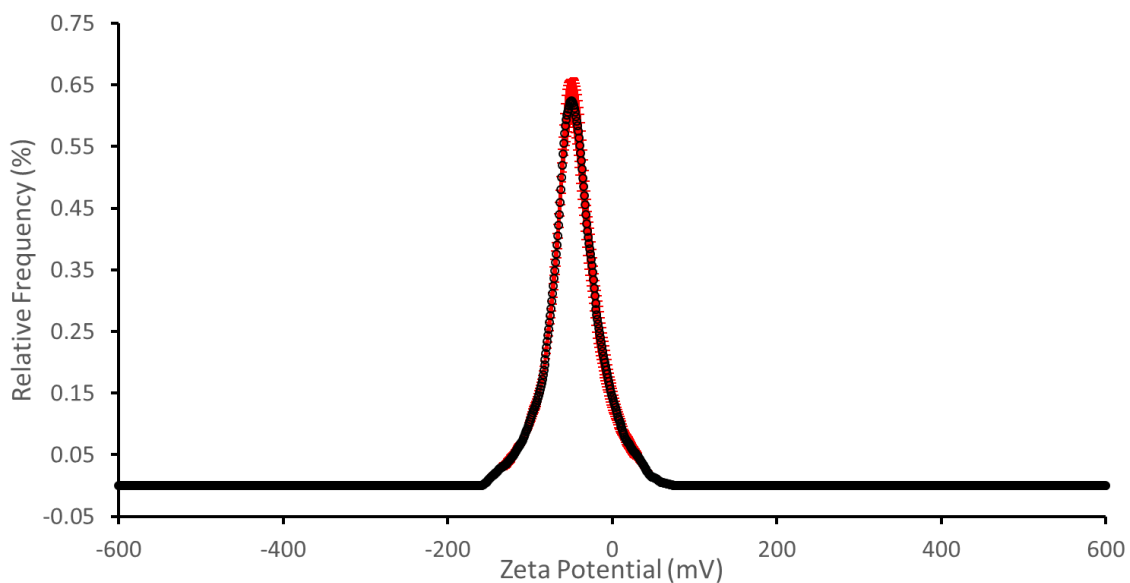


Figure 1 – The average zeta potential distribution calculated using 10 runs of compound **4** (3.00 mM) in an EtOH: H₂O (1:19) solution at 25 °C.

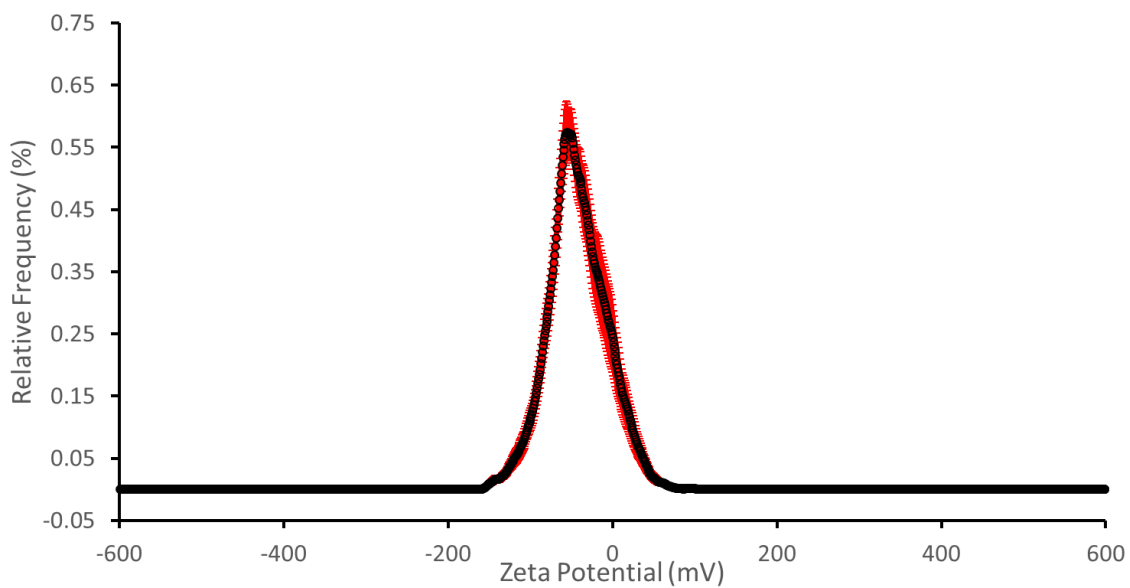


Figure S87 – The average zeta potential distribution calculated using 10 runs for a 1:1 mixture of compound **2** and **4** (total concentration = 3 mM) in an EtOH: H₂O (1:19) solution at 25 °C.

Table S17 – The average zeta potential distribution calculated using 10 runs for compounds **2-4** and a mixture of **2** and **4**, supplied as a 1:1 mixture at 3.00 mM, in an EtOH: H₂O (1:19) solution at 25 °C.

Compound	Mean Zeta Potential (mV)
2	-14.40
3	- 32.05
4	- 53.75
2 and 4	- 43.00

Critical micelle concentration

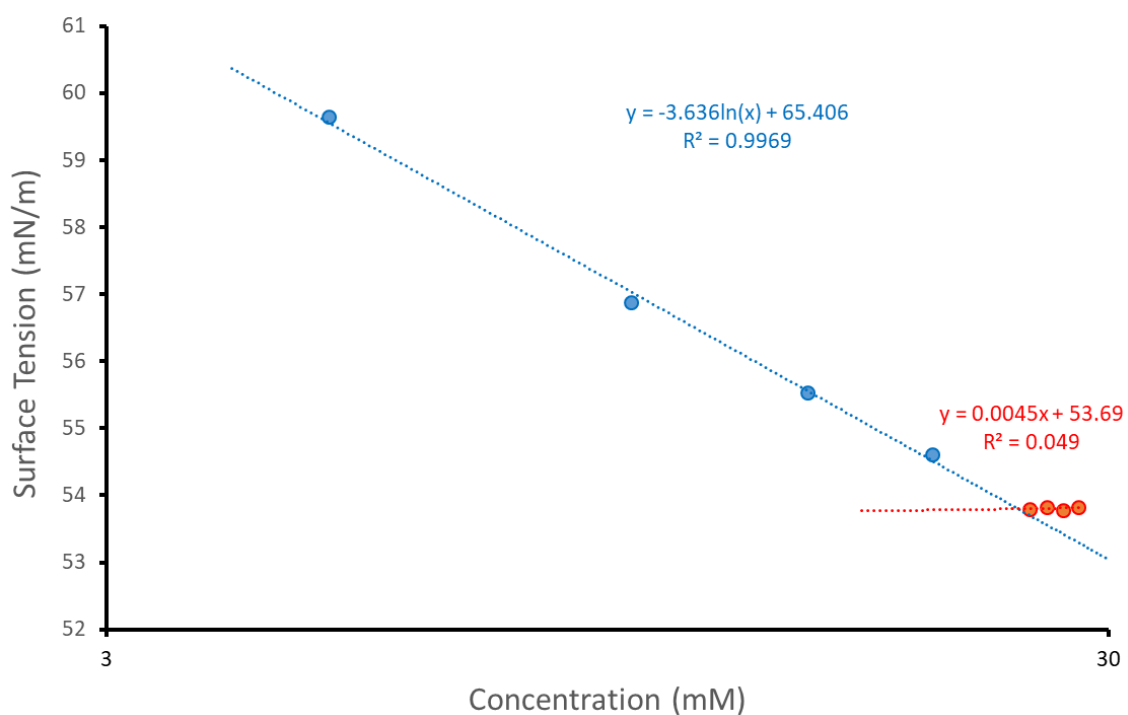


Figure S88 – Calculation of CMC for compound **2** in an EtOH: H₂O 1:19 mixture using surface tension measurements.

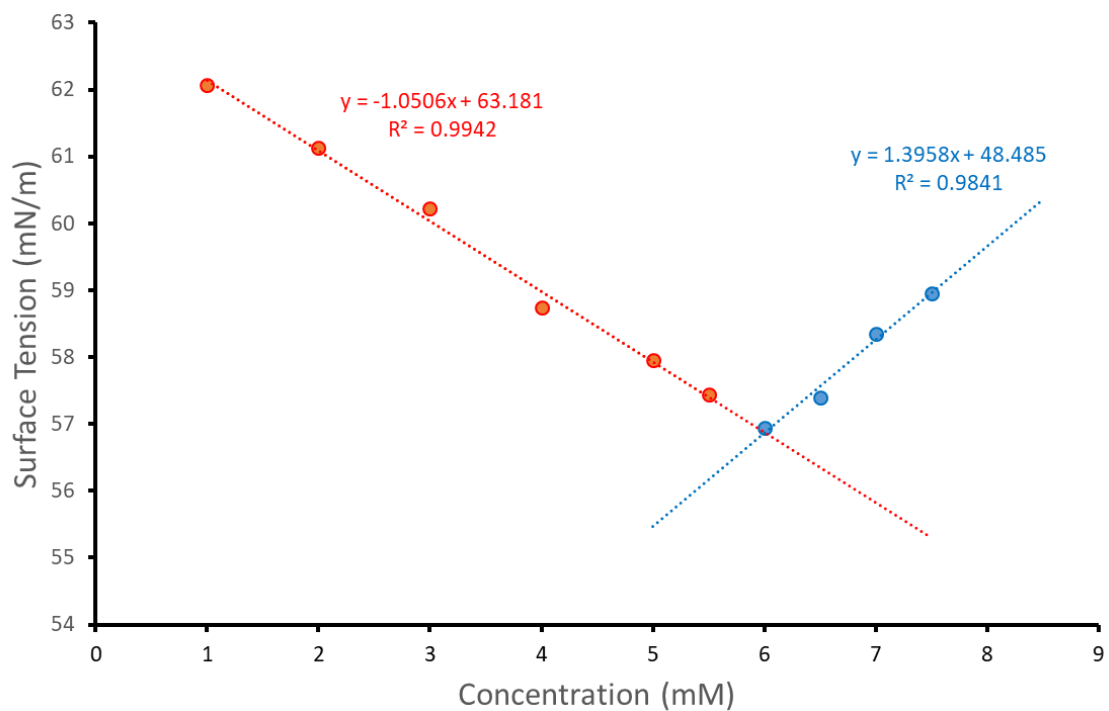


Figure S89 – Calculation of CMC for compound 3 in an EtOH: H₂O 1:19 mixture using surface tension measurements.

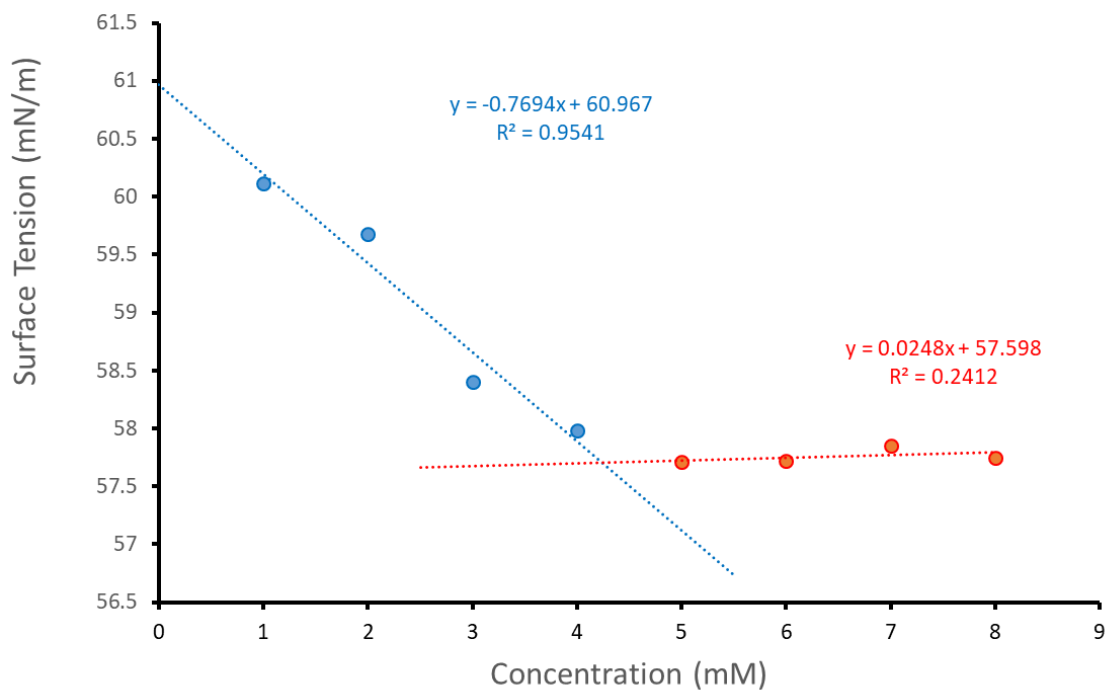


Figure S90 – Calculation of CMC for compound 4 in an EtOH: H₂O 1:19 mixture using surface tension measurements.

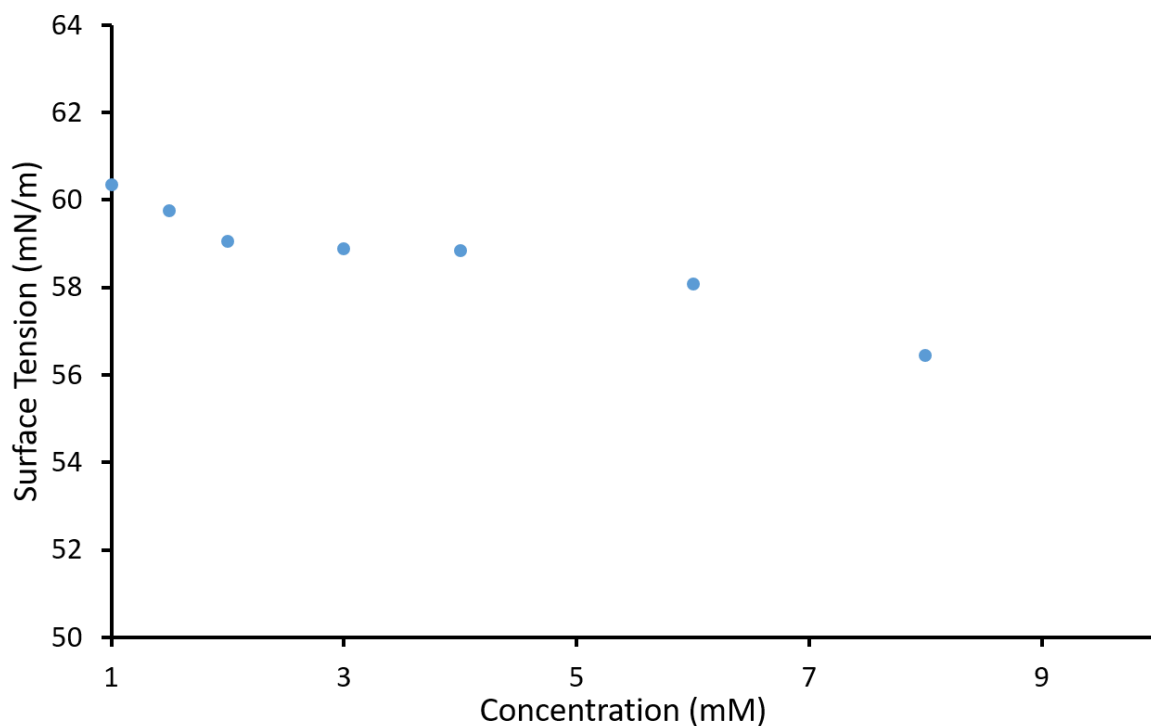


Figure S91 – Calculation of CMC for compounds **2** and **4** supplied in a 1:1 molar ratio in an EtOH: H₂O 1:19 mixture using surface tension measurements. Concentration given represents the total number of moles of both **2** and **4**.

Table S18 – Overview of CMC and surface tension (obtained at CMC) measurements for compounds **2-4** at 25°C

Compound	CMC (mM)	Surface tension at CMC (mN/m)
2	24.98	53.70
3	6.00	56.87
4	4.24	57.70
2 and 4	>10.00	Could not be determined

Low level in-silico modelling

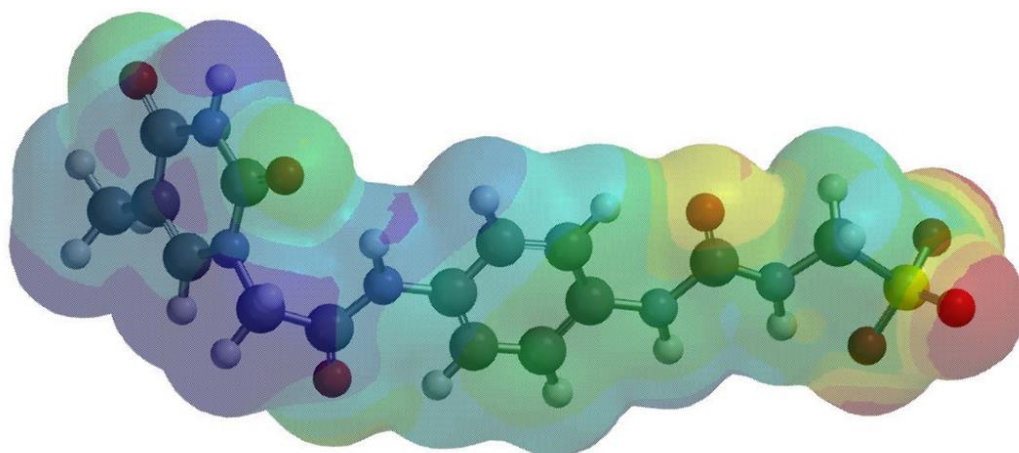


Figure S92 – Electrostatic potential map calculated for the anionic component of **2**.

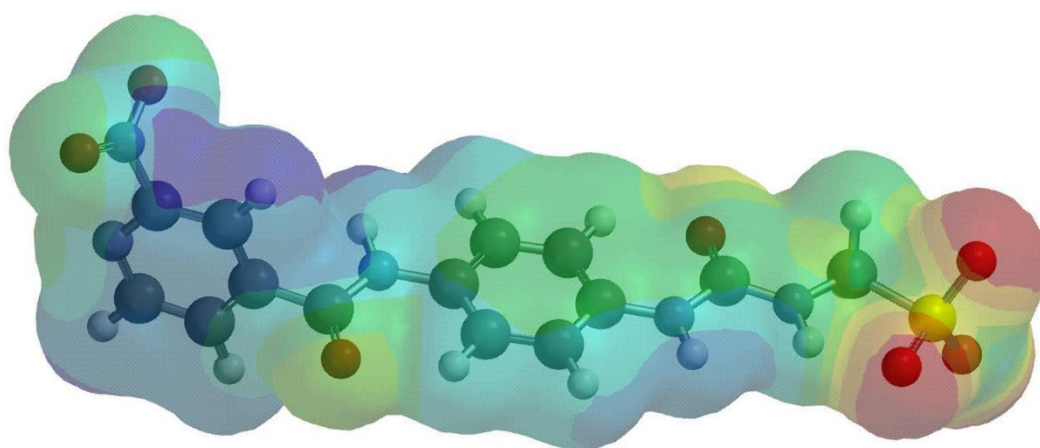


Figure S93 – Electrostatic potential map calculated for the anionic component of **3**.

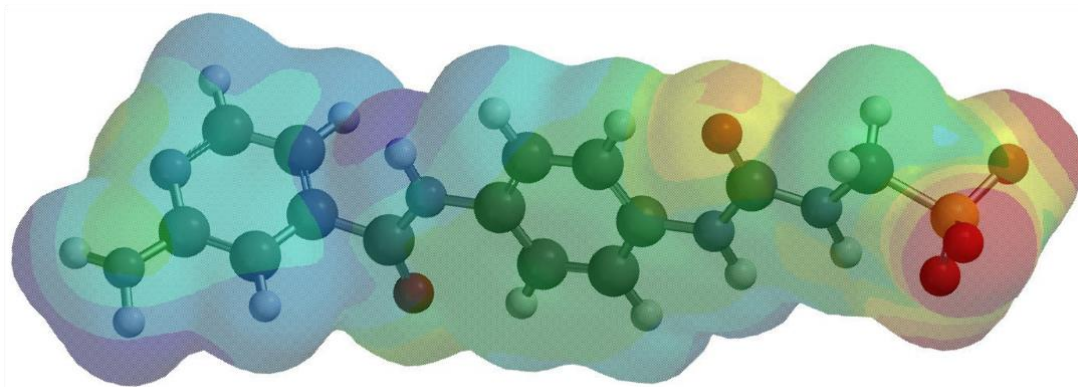


Figure S94 – Electrostatic potential map calculated for the anionic component of **4**.

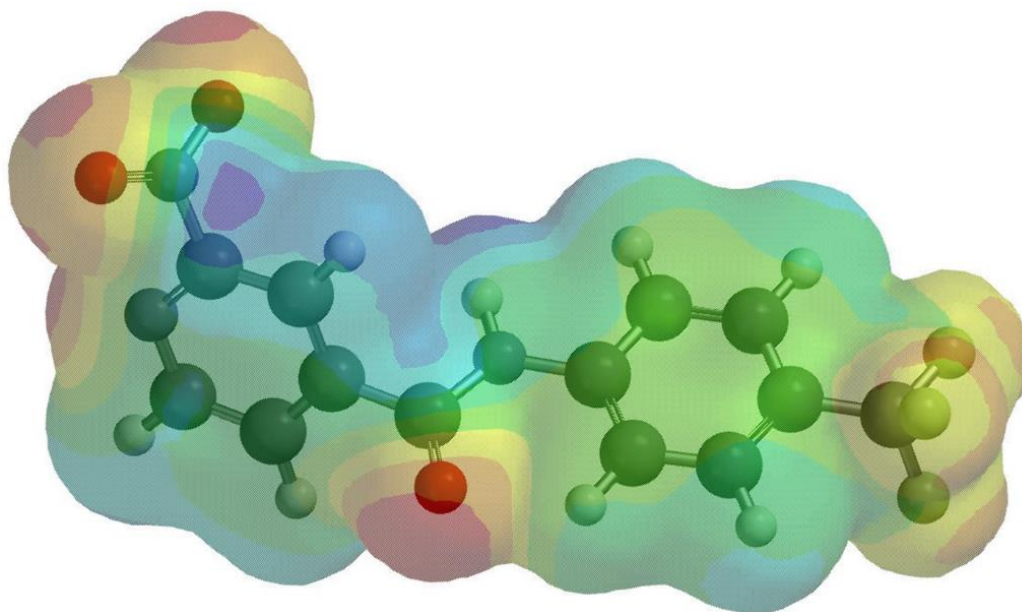


Figure S95 – Electrostatic potential map calculated for compound **5**.

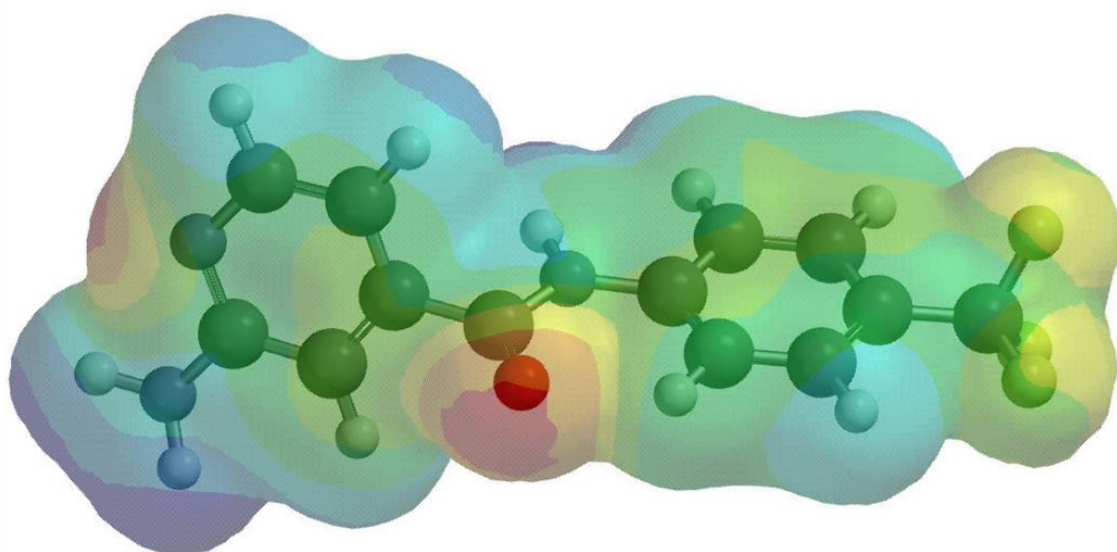


Figure S96 – Electrostatic potential map calculated for compound 6.

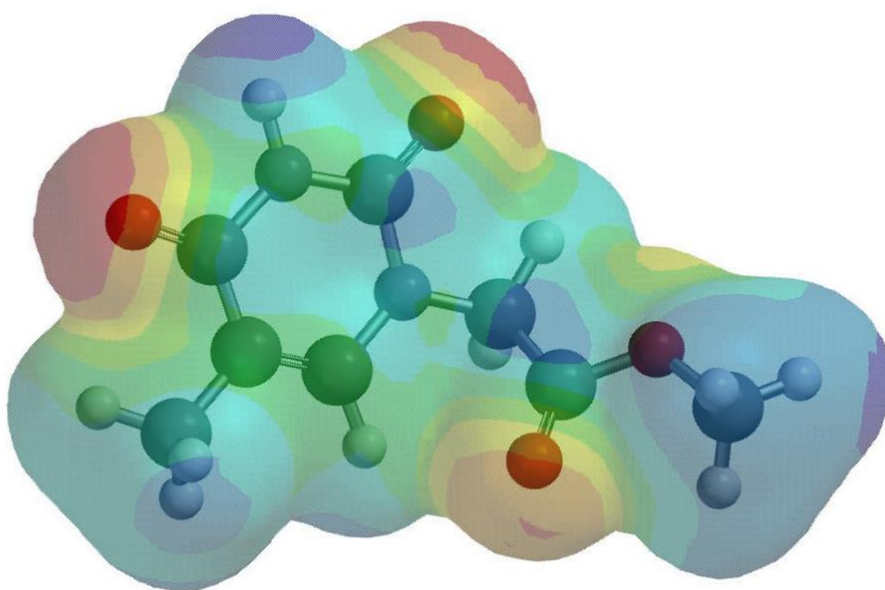


Figure S97 – Electrostatic potential map calculated for compound 7.

Table S19 – Electrostatic potential values calculated for compounds **2-7**.

Compound	E_{\min} (kJ/mol)	E_{\max} (kJ/mol)
Anionic component of 2	35.8994	-716.3030
Anionic component of 3	80.8152	-707.3240
Anionic component of 4	69.9097	-719.4140
5	236.6470	-209.2530
6	200.5310	-271.9090
7	146.2110	-256.9050

References

1. P. Thordarson, K. Sewell and V. Efremova, www.supramolecular.org.
2. G. M. Sheldrick, *Acta Cryst.*, 2015, **A71**, 3-8.
3. G. M. Sheldrick, *Acta Cryst.*, 2015, **C71**, 3-8.
4. O. V. Dolomanov, L. J. Bourhis, R. J. Gildea, J. A. K. Howard and H. Puschmann, *J. Appl. Cryst.*, 2009, **42**, 339-341.
5. C. A. Hunter, *Angew. Chem. Int. Ed.*, 2004, **43**, 5310-5324.
6. J. J. P. Stewart, *J. Mol. Mod.*, 2007, **13**, 1173-1213.
7. J. M. Andrews, *J. Antimicrob. Chemother.*, 2001, **48**, 5-16.
8. T. L. Gumbs, L. J. White, N. J. Wells, H. J. Shepherd and J. R. Hiscock, *Supramol. Chem.*, 2018, **30**, 286-295.
9. L. J. White, S. N. Tyuleva, B. Wilson, H. J. Shepherd, K. K. L. Ng, S. J. Holder, E. R. Clark and J. R. Hiscock, *Chem. Eur. J.*, 2018, **24**, 7761-7773.
10. V. Vendrell-Criado, V. Lhiaubet-Vallet, M. Yamaji, M. C. Cuquerella and M. A. Miranda, *Org. Biomol. Chem.*, 2016, **14**, 4110-4115.